THE PHYSICO-CHEMICAL CHARACTERISATION OF ALGINATE RAFT SYSTEMS

Thesis presented for the degree of
Doctor of Philosophy
in the Faculty of Medicine
of the University of London

October 1995

Fiona Ann Johnson

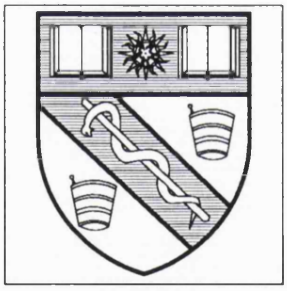

School of Pharmacy
University of London
29/39 Brunswick Square
London. WC1N 1AX

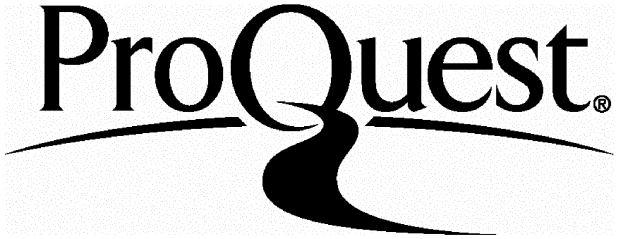

ABSTRACT

Alginate rafts are used in the treatment of reflux oesophagitis and act by forming a buoyant layer on the stomach contents. The aim of this project was to characterise the raft components and investigate the way in which the components affect the properties of the rafts.

The chemical structure of the alginates was investigated using nuclear magnetic resonance (NMR) and circular dichroism (CD). Rheological properties of the solutions were studied both at the concentrations used in the raft forming mixtures and at lower concentrations for the determination of intrinsic viscosity. The properties of gels formed either by the addition of divalent cations or by the action of acid on the solutions were investigated by the use of dynamic mechanical analysis (DMA) techniques. The effect of varying the divalent ion used in gel formation and the differences between alginate samples were studied using DMA. A novel technique for the characterisation of alginate rafts was developed using a texture analyser. The effect of formulation variables on the raft was then studied using the method described.

The results show that the properties of the raft are dependent on the alginate used, the bicarbonate included in the formulation and the presence of additional divalent cations. The strength of the acid in which the raft forms also affects the properties of the raft. It was also shown that the characteristics of the raft are not solely dependent on the properties of the individual components, but the interaction between the components also affects the overall properties of the raft formed.

This work suggests ways in which the performance of alginate rafts may be measured to give an understanding of how the characteristics may be controlled by the variation of the components of the raft forming mixture.

ACKNOWLEDGEMENTS

I would like to take this opportunity to thank all the people who have helped in the completion of this thesis. I am indebted to Dr Duncan Craig for his guidance and boundless enthusiasm throughout the project.

Additionally I would like to thank the many other people at the School of Pharmacy who have helped me practically. In particular, Keith Barnes and Don Hunt in the Pharmaceutics department and Dr Podczeck for her time and help with the image analysis, also, thank you to Dr Drake from Birkbeck College for the circular dichrosim. I am very grateful to Graham Florence for his friendship and assistance throughout. A mention too must go to all the post-graduate students in the Pharmaceutics department who helped to create an enjoyable atmosphere in which to work.

Furthermore, I am very grateful to SERC and SmithKline Beecham for financially supporting the project, with special thanks to Dr J N C Healey, Dr A D Mercer and Dr S Chauhan for their help and encouragement. Particular thanks must go to Stable Microsystems who provided the texture analysis equipment on loan which made the raft characterisation possible.

On a more personal level, I cannot thank my parents enough for their unending patience and support. I am also very appreciative of the special friendship which has developed with Suzanne Boutell during my time at the School and has helped me through some very trying times. Lastly my thanks goes to Stephen Nicholls for his optimism, patience and his emotional support which has been invaluable, especially towards the end of the project.

TABLE OF CONTENTS

LIST OF TABLES

LIST OF FIGURES

CHAPTER 1

CHAPTER 1: INTRODUCTION

1.1 CHARACTERISATION AND PROPERTIES OF ALGINATES

Alginates are polysaccharides originally derived from brown algae. The first extraction of alginate from seaweed was described by E.C.C. Stanford in 1881, who was investigating ways of utilising the abundance of seaweed washed up on beaches. He demonstrated that by a process involving alkaline extraction, a material which he named algin could be separated from the seaweed samples. A variety of uses for this new material were suggested by Stanford (1883) including use in the textile and food industries, where large quantities of alginates are still used as stiffening and gelling agents. The major source of alginate used commercially remains unchanged, being derived from various species of marine algae. However the present day collection of the raw material involves harvesting the algae using large factory ships rather than collecting that which is discarded on the coastline by the actions of tides and the weather.

Alginate comprises about 40% of the dry matter of brown algae; it occurs naturally as a gel with sodium, calcium, strontium, magnesium and barium ions (Haug & Smidsrød, 1967). The function of alginates in the algae is thought to be primarily skeletal, with the gel located in the cell walls and intercellular matrix conferring the strength and flexibility necessary to withstand the force of the water in which the seaweed grows. Nelson and Cretcher (1929) had shown the presence of mannuronic acid residues in alginates while the presence of guluronic acid residues was demonstrated by Fischer and Dörfel (1955). Haug (1964) showed that the chemical composition of the alginate varied between different algae, particularly in the proportion of the two uronic acid residues. Indeed within different parts of the same plant variations in composition may be seen. These differences are in response to the demands in biofunctionality, for example in *Laminaria hyperborea*, which grows in very exposed areas the stipe and holdfast show a very high rigidity, and high guluronic acid content, whereas

the blades of the same plant contain a greater proportion of mannuronic acid and are flexible, streaming with the movement of the water.

Alginate has also been shown to be produced as an exopolymer by certain bacterial species. Linker and Jones (1966) isolated acetylated alginic acid from *Pseudomonas* present in the sputum of cystic fibrosis patients. Alginate was also shown to be produced by *Azotobacter vinelandii* (Lin & Sadoff, 1968). Production from the bacterial source is not generally commercially economical; however, it has been shown by Skjåk-Bræk and Larsen (1985) that it is possible to isolate the enzyme mannuronan 5-C-epimerase from *A. vinelandii* and use this to tailor alginate composition. It is possible that this source may be more widely used in future where the exact composition of the alginate is of primary importance.

1.1.1 Chemical Composition

1.1.1.1 Analysis of Composition

As alluded to previously, not all alginates have the same chemical composition. Early analysis showed that alginic acid was a polymer of an aldehyde sugar (Nelson & Cretcher, 1929). It was thought that the sugar residues present were predominantly D-mannuronic acid (Spoehr, 1947). Analysis by Fischer and Dörfel (1955) showed the presence of L-guluronic acid as well as D-mannuronic acid in the hydrolysis products of alginates. Figure 1.1 shows the structures of mannuronic and guluronic acids which are conformational epimers of each other. Fischer and Dörfel (1955) also showed that the proportions of these two uronic acids varied between alginates extracted from different species of algae. It was not made clear, however, whether the alginate present in a particular seaweed plant was an homogeneous compound, or whether alginates of varying compositions were present. Haug (1959) showed, by fractionation with salt solutions, that alginate extracted from *Laminaria digitata* was heterogeneous, comprising of fractions which differed in solubility and uronic acid composition. The analysis of the uronic acid content of alginates was

Figure 1.1 : The structure of mannuronic and guluronic acids

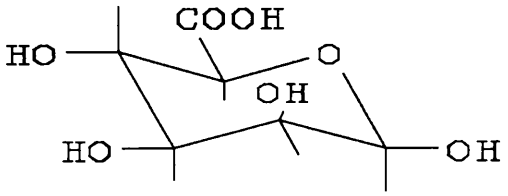

D-mannuronic acid

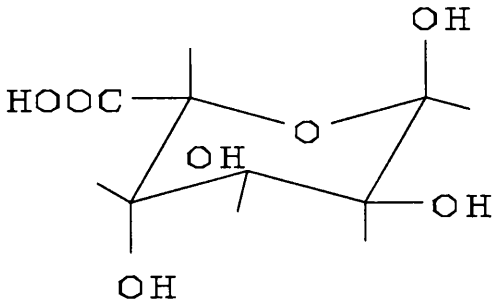

L-guluronic acid

continued by the use of ion exchange columns to separate the uronic acids (Larsen & Haug, 1961). Haug and Larsen (1962) then determined the amounts of each uronic acid present colorimetrically using the orcinol reaction (Brown 1946). The presence of guluronic acid in alginates was confirmed by Drummond et al (1962) who showed that the appearance of guluronic acid in the hydrolysate of alginates could not be due to epimerisation of mannuronic acid during the alkaline extraction process. Hirst et al (1964), Hirst and Rees (1965) and Rees and Samuel (1967) conducted a series of investigations into the structure of alginic acid using mild acid hydrolysis which showed that alginic acid comprises D-mannuronic and L-guluronic acids held linearly by 1,4 glycosidic linkages.

Haug and Smidsrød (1965) used fractionation with calcium and magnesium ions to estimate the proportion of mannuronic and guluronic acid residues present in alginate samples. Acid hydrolysis experiments were also undertaken by Haug et al (1966) and Smidsrød et al (1966) to provide a method of quantitative analysis for alginic acid samples. The relative amounts of each of the uronic acid residues was now estimable, albeit by lengthy chemical analyses. However, the sequence of the components was still unknown. Haug et al (1967) used electrophoresis to examine the hydrolysis products of an alginate and the separated fractions were then analysed by the orcinol reaction. The results suggested that the alginate molecule contains blocks of mannuronic acid residues, blocks of guluronic acid residues and blocks with a predominantly alternating structure.

Nuclear magnetic resonance (NMR) and circular dichroism (CD) are now used for routine analysis of alginate samples. The development of non-destructive methods of analysis of alginates means that the time consuming chemical analyses are no longer favoured for establishing the M/G ratio and block structure.

The CD spectrum of an alginate was found to be dependent on the M/G ratio and to some extent on the block structure (Morris et al, 1975). Circular dichroism had also been shown to be sensitive to the gelation which occurs on addition of calcium to alginate solutions (Morris et al, 1973). Although an undoubtedly useful technique in the study of alginates, routine use in analysis is not widespread due to insufficient availability equipment.

The use of NMR for the analysis of alginate samples was described by Penman and Sanderson (1972). A method for determination of the M/G ratio was demonstrated; however, the method used involved the degradation and fractionation of the alginate sample prior to analysis. Grasdalen et al (1977, 1979) used ^{13}C-NMR and high resolution ^{1}H-NMR to determine the M/G ratio and block structure. ^{13}C-NMR was used to increase the resolution of alginate spectra, although ^{1}H-NMR is more sensitive and thus of more practical use for routine analysis. Although it is no longer necessary to fully hydrolyse and fractionate the samples for NMR, relatively pure samples must be used and generally a partial hydrolysis is required to give good, reproducible results.

1.1.1.2 Sources of alginate

Alginates were first extracted from brown seaweed and this remains the major commercial source to date. As previously mentioned, certain bacteria also produce alginate as an exopolymer, however, this highly acetylated product is not used commercially at present.

There are 265 reported species of marine brown algae (*Phaeophyceae*) of which just three account for the major source of alginate (Glicksman, 1969). The most widely used are *Macrocystis, Laminaria* and *Ascophyllum*, which have different geographical patterns of growth. *Macrocystis pyrifera* is harvested off the west coast of the United States of America and grows in beds several miles long ranging from 50 feet to 1 mile wide and 25-80 feet deep. In northern Europe *Laminaria hyperborea* is harvested along the Norwegian coast and

around the northern coasts of Scotland, as is *Ascophyllum nodosum*, whereas *Laminaria digitata* is predominantly found off the western coasts of Britain and Ireland. Harvesting is carried out mechanically using ships with cutting and loading equipment. The seaweed is cut off about three feet below the surface of the water and the extra light which penetrates after cutting stimulates further growth of the seaweed. This enhanced regrowth means that the beds are ready to be reharvested about four months after the initial cutting. Harvesting plans drawn up between alginate manufacturers, marine biologists and environmental agencies allow the use of these marine resources without their destruction. These sources of *Phaeophyceae* are all naturally occurring, although *Laminaria japonica* is cultivated on rope rafts off the coast of China in large enough quantities to satisfy the local market (Gacesa, 1988).

The source of the alginate is important when considering the composition of the sample. The ratio of D-mannuronic to L-guluronic acid depends on the plant from which the sample was obtained (Smith & Montgomery, 1959). While variation of materials from a natural source is to be expected, differences are not just found between samples from different species, but also it is seen within species and indeed within a single plant. In a report for the Norwegian Institute of Seaweed Research, Haug (1964) presented data for the M/G ratio of alginates from various species. These results were broken down to give the M/G ratio for various parts of the plants (whole plants, old fronds, new fronds, and stipes) together with details of the date and place of harvesting. Seasonal variation was found, especially in *Laminaria sp.* where the alginates extracted contained a higher proportion of mannuronic acid in the summer. This is borne out by the findings that the new fronds contain a higher proportion of mannuronic acid than the old fronds.

1.1.1.3 The effect of composition

The two uronic acid residues present in alginates bestow different properties on the polysaccharide, hence changes in the overall proportions of the

mannuronic and guluronic acids will affect the properties of the alginate. Haug (1959) showed the way in which the ion exchange properties of the alginates were dependent on the mannuronic-guluronic acid ratio. The dissociation of alginic acid was also shown to depend on the composition of the polysaccharide (Haug, 1961). The gel forming ability of alginates is another property which has been shown to depend on the relative proportions of mannuronic and guluronic acids present (Smidsrød & Haug, 1965, 1972). Haug et al (1967) showed that the physical properties of alginates were not only dependent on the M/G ratio, but also differences were seen between samples with different block structures. The selectivity coefficients of different block types for various divalent ions was investigated by Smidsrød and Haug (1968) who showed how gelation of alginates was affected by the composition and block structure. It is, therefore, important when considering the physical properties of alginates, and the way in which they behave, to take into account both the overall proportions of the mannuronic and guluronic acids and also the predominating block structure.

1.1.2 Physical properties

The physical properties of alginates which have caused the most interest are the solubility, the viscosity of the solutions and the gel forming properties. Although they can be considered separately, these three properties are linked by the factors which affect them. These factors include the composition of the alginate, the pH of the surrounding medium and the presence of various ions.

The physical properties of alginates are of particular interest when considering their use in pharmaceutical dosage forms such as the alginate raft. The solubility of the alginate and the viscosity of the solution produced is of interest when considering the properties of the raft forming mixture, and the gelation properties are important when considering the way in which the raft forms within the stomach.

1.1.2.1 Solubility of alginates

Alginic acid is insoluble in cold water and only very slightly soluble in hot water. The sodium, potassium and ammonium salts of alginic acids and the propylene glycol ester are all readily soluble in hot or cold water. In ethanol and water mixtures the solubility of alginate, as with other polysaccharides, is governed both by interactions between polymer segments and those between polymer segments and solvent molecules. When the alginate is in the undissociated form Haug and Smidsrød (1968) showed that the sequence of uronic acid residues was of great importance in the solubility. They suggested that the solubility is determined by forces acting between the alginate molecules; these forces would in turn depend on the steric arrangement of the carboxyl groups, and hence the uronic acid sequence. The forces are probably caused by the formation of hydrogen bonds between carboxyl groups.

The solubility of alginates in water has been shown to be dependent on the composition of the polysaccharide by Haug and Larsen (1963) when they studied the solubility of alginates at low pH. These studies made use of the precipitation of insoluble alginic acid from a solution of sodium alginate by the addition of acid. The dissociation of alginic acid had also been shown to be dependent on the uronic acid composition of the sample by Haug (1961). Values for the dissociation constants of the two uronic acids were calculated and found to be 3.38 for mannuronic acid and 3.65 for guluronic acid. The pK_a values for a variety of alginates with differing compositions were also calculated; these were found to be in good agreement with the values for the acids alone.

The form in which alginate molecules are present in solution was investigated by Smidsrød and Haug (1968) using a light scattering technique. They concluded that alginate molecules in 0.1M salt solution behave as partially free-drained random coils with a very extended form. Further work by Smidsrød et al (1973) showed that the relative extension was a function of block type with

heteropolymeric blocks giving the least extension, homopolymeric G-blocks having the greatest extension and homopolymeric M-blocks being intermediate. The conformation of the molecules, together with the molecular weight, affect the viscosity of alginate solutions. Factors which affect the conformation of the molecules in solution such as the presence of sodium and potassium and the pH of the medium will affect the viscosity of the solutions.

1.1.2.2 Viscosity of alginate solutions

The viscosity of alginate solutions in water depends on the concentration of the alginate, the degree of polymerisation, the temperature, pH, presence of other substances and the composition of the alginate. The composition of the alginate not only determines the viscosity of the solution for a given set of conditions, but it also affects how the viscosity of the solution will change with alterations in those conditions.

The factors which are external to the alginate such as temperature, pH, ionic strength, the nature of the salts present in the solution and the effect of shear rate will be considered first. The effect of the addition of divalent cations to alginate solutions is to cause gelation, although this will be dealt with in Chapter 1.1.2.3.

The method by which the viscosity of alginate solutions is measured has been shown to affect the values obtained for the viscosity. This is due to the effect of the rate and method of shear on the alginate solution, these systems being pseudoplastic; the shear dependence of the apparent viscosity of alginate solutions is more pronounced in more concentrated solutions (Haug, 1958). It is therefore important to either compare results with those obtained under the same conditions of shear or correct the viscosity values to zero rate of shear although this presents difficulties due to the non-linear relationship between the two parameters (Haug, 1964).

The correction of viscosity for concentration is the basis for the calculation of intrinsic viscosity. The intrinsic viscosity of a solution is defined as the specific viscosity divided by the concentration extrapolated to zero concentration. It is a measure of the volume, shape and space occupied by the molecules in the solution. Donnan and Rose (1950) suggested a method for the calculation of intrinsic viscosity as described in Chapter 3.4.1. This method was expanded by Haug and Smidsrød (1962) who proposed that the intrinsic viscosity could be described in two ways. The limit as the concentration tends to zero was considered to be equivalent to $(\eta_r - 1)/C$ or $(\ln \eta_r)/C$ where η_r is the relative viscosity of the solution. By plotting both of these functions against concentration on the same axis two lines are produced which will intersect the viscosity axis at zero concentration. This is discussed in more detail in Chapter 3.4.1.

The effect of increasing temperature on the viscosity of alginate solutions is to decrease the measured viscosity. It is important therefore to note the temperature at which measurements are made. Since it has been shown that there are no discontinuities in the curve relating temperature and viscosity, corrections for temperature can be made by reference to a table of temperature correction factors (McDowell, 1986).

The effect of pH on the viscosity of alginate solutions was investigated by Donnan and Rose (1950) and Haug (1964) who showed that the viscosity is independent of pH within the pH range 5-12. The addition of acid to alginate solutions and the lowering of the pH of the solution below 3.5 causes an alteration in viscosity due to the formation of a precipitous gel of insoluble alginic acid (Haug and Larsen, 1963).

The ionic strength of the solution of an alginate affects the conformation of the molecules. A decrease in the ionic strength of the solution will result in the alginate molecules taking up a more extended form and hence an increase in viscosity. The effect of ionic strength is only seen below a value of about 0.1N,

while above this value the viscosity of alginate solutions can be considered to be independent of ionic strength (Smidsrød et al, 1973). The effect of ionic strength is more pronounced on solutions with a low intrinsic viscosity, therefore the viscosity of solutions of alginate above about 3% can also be considered independent of ionic strength.

It is not only the ionic strength of the solution which affects the viscosity but also the type of ions present. Harkness and Wasserman (1952) investigated the effects of various sodium salts on the viscosity of alginate solutions and found that the flow properties were dependent on the anion present. Haug and Smidsrød (1962) also showed that potassium and sodium salts had different effects on the viscosity of the solutions. However, these effects are only of practical significance in very dilute solutions, with low intrinsic viscosities.

In addition to external factors, the viscosity is also highly dependent on the molecular structure of the alginate. Solutions of different alginates prepared to the same concentration under the same conditions will vary in terms of the composition of the alginate and the degree of polymerisation. The degree of polymerisation is equivalent to the molecular weight and is related to the intrinsic viscosity, as described by Donnan and Rose (1950) and Harkness and Wasserman (1952). The relationship given by these workers between the intrinsic viscosity and the degree of polymerisation serves as a useful guide but is by no means precise, especially for solutions which are anything more than very dilute.

The viscosity of alginate solutions is dependent on the flexibility of the polymer chains, which is in turn dependent on the uronic acid composition. The flexibilities of the different uronic acid blocks was studied by Smidsrød et al (1973), who suggested that alginates having a greater proportion of homopolymeric guluronic acid blocks show the greater viscosity providing other factors such as the degree of polymerisation are the same.

1.1.2.3 Gelation of Alginates

The gel forming ability of the alginates is one of the most widely used properties of these polysaccharides. An alginate gel is basically composed of an insoluble alginate and water, the latter being typically well over 99% in proportion. Alginate gels, in common with other similar gels, are composed of a three dimensional network of long chain molecules (Ross-Murphy, 1991). The molecules are held together at junction zones, typically considered to be guluronic acid blocks in alginates, with the water held in the interstices between the junction zones. The formation of junction zones in an alginate solution may be promoted in one of two ways; either by the presence of certain divalent cations such as calcium, or by the acidification of the solution.

The way in which alginate gels are formed in the presence of acid has not been investigated to the same extent as the gelation caused by divalent cations. The gel formed, as described by Rees (1969), is precipitous in nature, comprising insoluble alginic acid held together by hydrogen bonding. The different pKa values of the two uronic acids means that the guluronic acid residues will tend to be involved in the formation of junction zones at a slightly higher pH than the mannuronic acid residues (Haug and Larsen, 1963). Gel formation commences at a pH of approximately 3.5 and is complete below pH 2.5.

The gelation of alginates with divalent cations, in particular calcium, has been investigated widely with these gels having many practical uses, especially within the food industry. The addition of a divalent metal such as calcium to a solution of sodium alginate causes the formation of cross-links, with the metal ions bridging neighbouring chains to produce an "egg-box" structure as described by Grant et al (1973). The egg-box structure of a calcium-alginate gel is shown schematically in Figure 1.2.

It has previously been shown by Rees (1972) that the different uronic acid blocks have a varying affinity for calcium ions. Homopolymeric guluronic acid

Figure 1.2 : Schematic representation of the "egg-box" structure of a calcium alginate gel

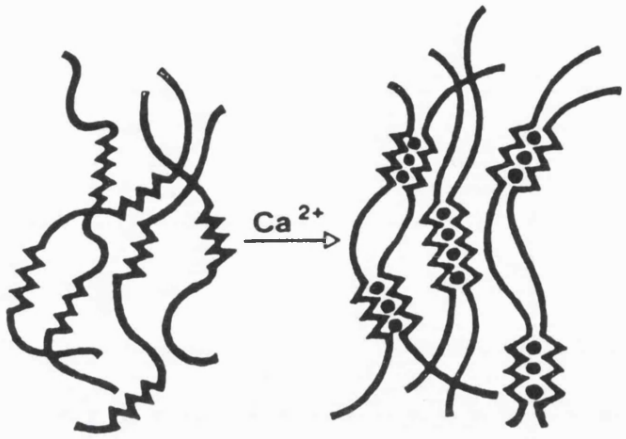

Figure 1.3 : Shematic representation of two different alginate gels

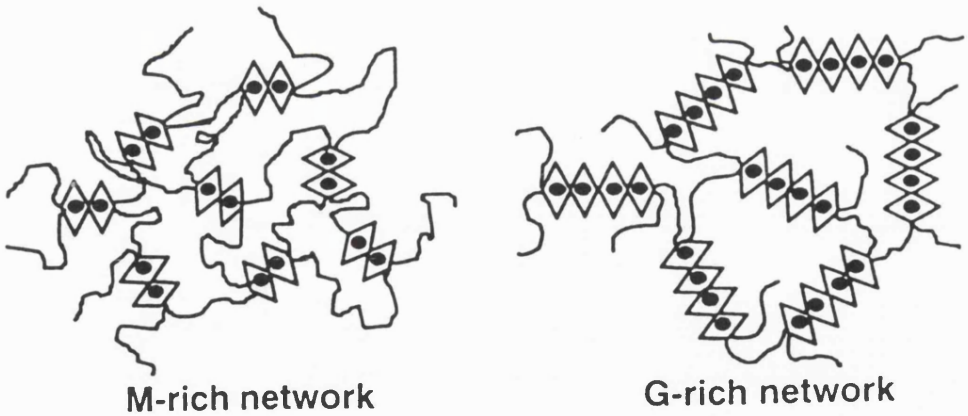

blocks were shown to have the greatest affinity for divalent cations such as calcium, and heteropolymeric blocks the least affinity with homopolymeric mannuronic acid blocks being intermediate. It was therefore concluded that cross-linking in alginate gels occurs predominantly at guluronic acid blocks which form rigid sections, interspersed with more flexible sections of mannuronic acid blocks and heteropolymeric blocks. This accounts for the different properties of gels formed from alginates with different chemical compositions (Smidsrød, 1974). Figure 1.3 shows a schematic representation of two different gels formed from alginates with different chemical compositions.

The ability of different divalent ions to cause gelation of alginate solutions was investigated by Haug and Smidsrød (1965), who showed that the ions could be ranked in order of gel forming ability. The ranking they suggested showed that gel forming ability increased in the order:

Ba>Pb>Cu>Sr>Cd>Ca>Zn>Ni>Co>Mn,Fe

It was also noted that this general ranking did not hold for all alginate samples, although the differences between alginates of differing chemical compositions were minor with the rankings for two ions being transposed. The effect of chemical composition on alginate gels was investigated by Smidsrød and Haug (1972) who showed that polymannuronate did not form a calcium gel with any measurable stiffness, but the modulus of stiffness increases with increasing guluronic acid content. It was also noted that the most rigid gels were transparent whereas the softer gels appeared turbid. This led to the conclusion that long sequences of several chains linked together was characteristic of soft precipitous gels, and that the formation of rigid gels was associated with a hindrance of the formation of large crystalline regions, hence a more homogenous gel is produced.

1.1.3 Uses of alginates

Alginates have found a wide variety of uses in many different industries. The properties of alginates such as low toxicity, solubility and varying viscosity in solution make them highly useful in the food, drink and pharmaceutical industries. The thickening properties and the rheological behaviour of alginates have been used in the textile industry, for "thickening" water used in fire-fighting and in the production of concrete. As well as these major uses for alginates research continues into other potential applications for this unique material.

1.1.3.1 The use of alginates in the textile and paper industries

Alginates are used in very large quantities in the textile industry; indeed about half of the alginate currently produced is consumed by this industry. The major use is as a thickener for the print pastes of dyes used in printing fabrics. The use of alginates in thickening the dyes has three main advantages. Firstly, the print pastes can be prepared with cold water saving preparation costs and time. Secondly, the print pastes produced give very good uniformity of flow characteristics, minimising clogging of the machinery during printing and giving optimal fabric penetration. Thirdly, since the alginate is soluble it is easy to wash out of the fabric after dyeing, giving a soft fabric finish without a "starchy" effect.

In the paper industry alginates are used to give writing paper a smooth surface. The film forming properties also give alginates an anti-stick quality which is utilised in the production of peelable stickers and labels.

1.1.3.2 The use of alginates in the food industry

There are six alginates currently listed as permitted food additives in the Emulsifiers and Stabilisers Directive (74/329/EEC). These have been given serial numbers E400 to E405 which refer to alginic acid, sodium, potassium,

ammonium, calcium and propylene glycol alginate. The gelling properties of alginates are used in foods such as onion rings, bakery fillings, reconstituted fruit, pet food and even pimento strips for cocktail olives. The stabilising effects of alginates are used in many dairy products, fruit drinks, mayonnaise, ice cream and to stabilise beer foam to produce an acceptable head on a glass of beer.

1.1.3.3 Pharmaceutical and medical uses

The use of alginates in the pharmaceutical and biomedical area is expanding with the use of the gelling and stabilising properties being used in conventional dosage systems and in the development of novel uses such as cell encapsulation for cell culture and in controlled release devices. Table 1.1 gives an indication of some of the uses and potential uses for alginates in this area. The largest amounts of alginate in use for pharmaceutical and medical purposes are in the production of anti-refluxants and in the manufacture of dental impression material.

Table 1.1 : The uses of alginates (Gacesa, 1988)

Pharmaceutical	**Medical / Dental**	**Potential uses**
Anti-refluxant	Dental impressions	Drug encapsulation
Suspending agent	Wound dressings	Site release matrices
Tablet disintegrant	Haemostasis	Plasma substitute
Tablet binder	Denture adhesives	Sodium reduction
Modified release	Skin treatments	^{90}Sr removal

This study is based on the use of alginate as an anti-reflux agent, hence this particular application will be described in more detail in Chapter 1.5.

1.2 PECTIN

Pectin, like alginate, is extensively used in the food industry as a gelling and stabilising agent. It was discovered in 1790 by Vauquelin and characterised in 1825 by Braconnot who gave it the name "pectin" and described it as the principal gelling agent of fruit. He showed that pectin gave fruits the ability to form jellies when boiled with sugar. Braconnot (1825) also demonstrated that the correct pH as well as the presence of sugar was essential for the reaction to take place. Pectins, together with celluloses and starches, form the structural components of all green plants, although pectins are generally more concentrated in fruits and vegetables. Pectin is broken down enzymatically in the human digestive system, unlike polysaccharides of algal origin which pass through the human digestive tract unaltered.

1.2.1 The structure of pectin

Pectin is composed of poly (1,4) D-galacturonic acid residues existing as unbranched chains of between 200 and 1000 galacturonic acid units. Figure 1.4 shows a structural comparison of pectic acid and alginic acid. The acid groups exist partly as the free acid and also in the esterified form. The degree of esterification varies widely in the natural product; generally as a fruit matures the degree of esterification decreases. The properties of the pectin, especially the gelation, are dependent largely on the degree of esterification and the molecular weight of the material.

1.2.2 Gelation of pectin

There are two methods by which pectin will undergo gelation, depending on the composition of the pectin. Pectins which have a high degree of esterification require the presence of sugar (60-65%) at a pH of 2.0-3.5 in order to gel. This type of gelation occurs on cooling a boiling mixture of the pectin and sugar; this is the method used in jam making. The other type of gelation does not require

Figure 1.4 : Structural comparison of pectic and alginic acids

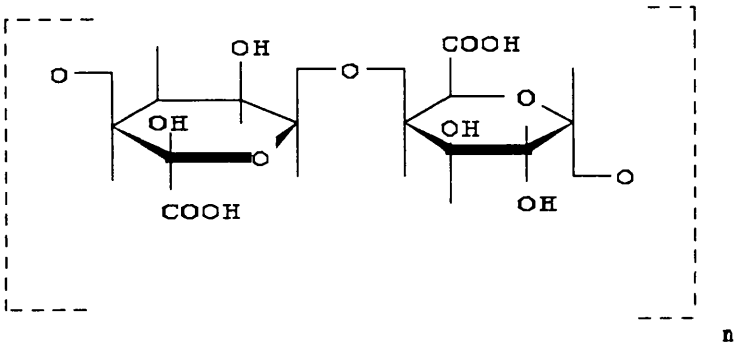

Pectic acid

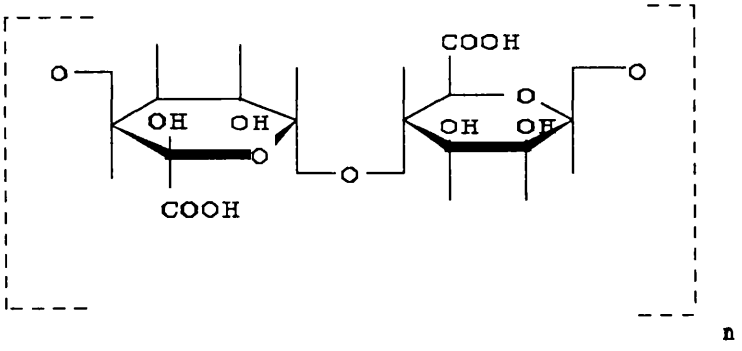

Alginic acid

the presence of sugar; however, it does rely on the addition of a divalent cation such as calcium. The gel formed has an "Egg-box" structure similar to that formed by alginate, with the low ester pectin forming cross-links with the calcium (Durand et al, 1990). The strength of these gels formed by cross-linkage through a polyvalent ion depends on the molecular weight of the pectin as well as on the degree of esterification. The gelation of various grades of low methoxy (low ester) pectin with calcium was investigated by Durand et al (1990). They showed by the calculation of thermodynamic parameters that the formation of cross-links requires only a small change in chain conformation. However, a high enthalpy change is involved due to the cooperative nature of the generation of effective junction zones.

1.2.3 Uses of pectins

Pectin is used as a thickening and stabilising agent in a variety of food products, with the traditional use being in the production of jams and marmalade. It has also been used medicinally in the treatment of infantile diarrhoea. Pectin can be used with alginates in order to form gels with a range of characteristics (Glicksman, 1969). Currently some jams used in baking make use of the combined gelation of a pectin and alginate mixture. This combination could also be applied to alginate raft preparations, although this has not been previously investigated.

1.3 PHYSIOLOGY OF THE STOMACH

The stomach is a J-shaped muscular organ capable of considerable distension. When empty it is only slightly larger in diameter than the large intestine, while when distended it can accommodate two to three pints of material. The main functions of the stomach are mechanical churning of the food and the initial enzymatic hydrolysis.

1.3.1 Anatomy of the stomach

The stomach is connected to the distal end of the oesophagus in the cardiac region of the stomach and to the proximal duodenum by the pyloric sphincter. The stomach is divided into three anatomical regions; the upper part of the stomach which is the cardia, the cardiac sphincter and the fundus; the middle or body of the stomach, and the lower region which consists of the antrum, the pylorus and the pyloric sphincter. Figure 1.5 shows these anatomical features.

The stomach wall is composed of four layers, the serosa, the muscularis mucosa, the submucosa and the mucosa. The serosa is the outer layer of the stomach which is covered by the peritoneum and contains the blood and nervous supply. Under the serosa is the muscularis mucosa which is the muscular layer comprising three layers of smooth muscle as shown in Figure 1.6. The outermost muscle is longitudinal and continuous with the muscle of the oesophagus. The middle layer of muscle is also continuous with that of the oesophagus, but arranged circularly. This muscle is thickened to form the two sphincters as shown in Figure 1.5. The innermost muscle layer is arranged obliquely and is not a complete layer but is concentrated in bands around the cardia and fundus and also the cardia and body of the stomach. The third layer of the stomach wall is the submucosa which is a layer of dense fibrous connective tissue containing lymph and blood vessels. It is an elastic layer which falls into folds or rugae when the stomach is contracted, but will extend when the stomach becomes full. The innermost layer of the stomach wall is the mucosa which is an epithelial layer containing the secretory cells of the stomach. These secretory cells are not uniform over the internal surface of the stomach, but are concentrated in glands and pits with various specific secretory cells being found in different parts of the stomach.

1.3.2 Gastric secretion

The cells of the gastric glands of the stomach produce approximately 2½ to 3

Figure 1.5 : The anatomical features of the stomach

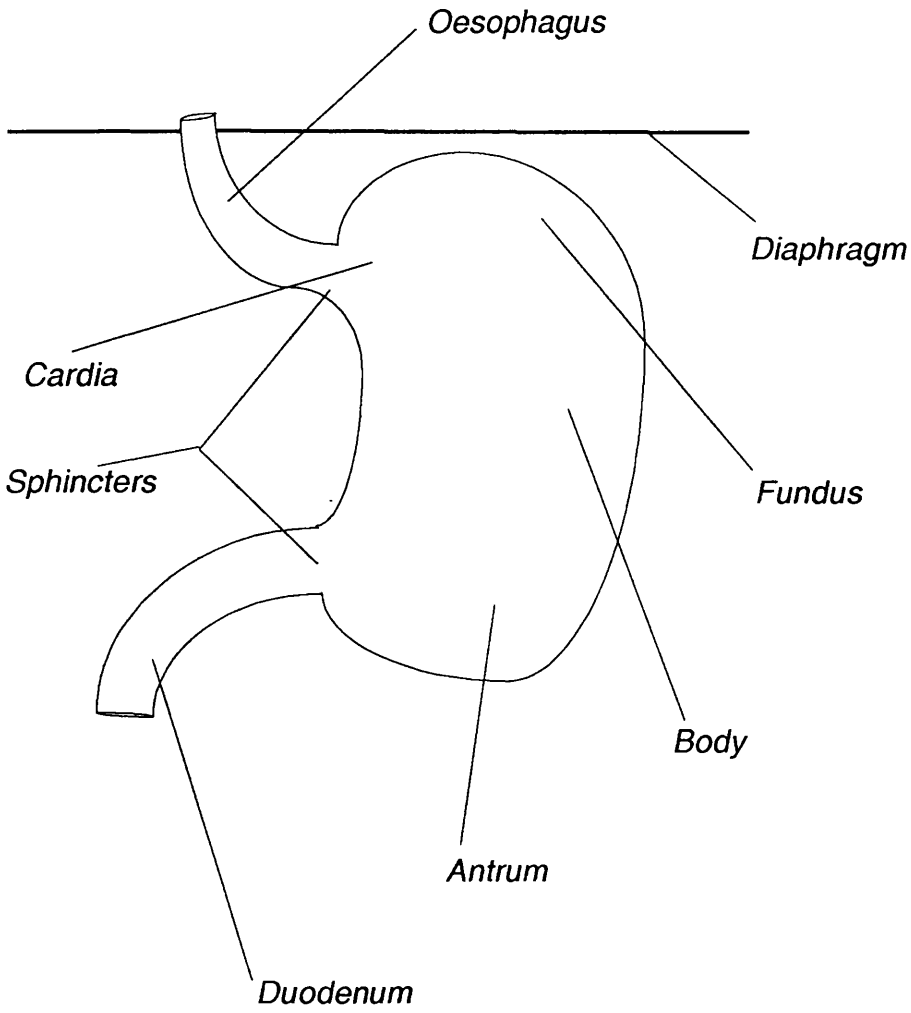

Figure 1.6 : The muscle layers of the stomach

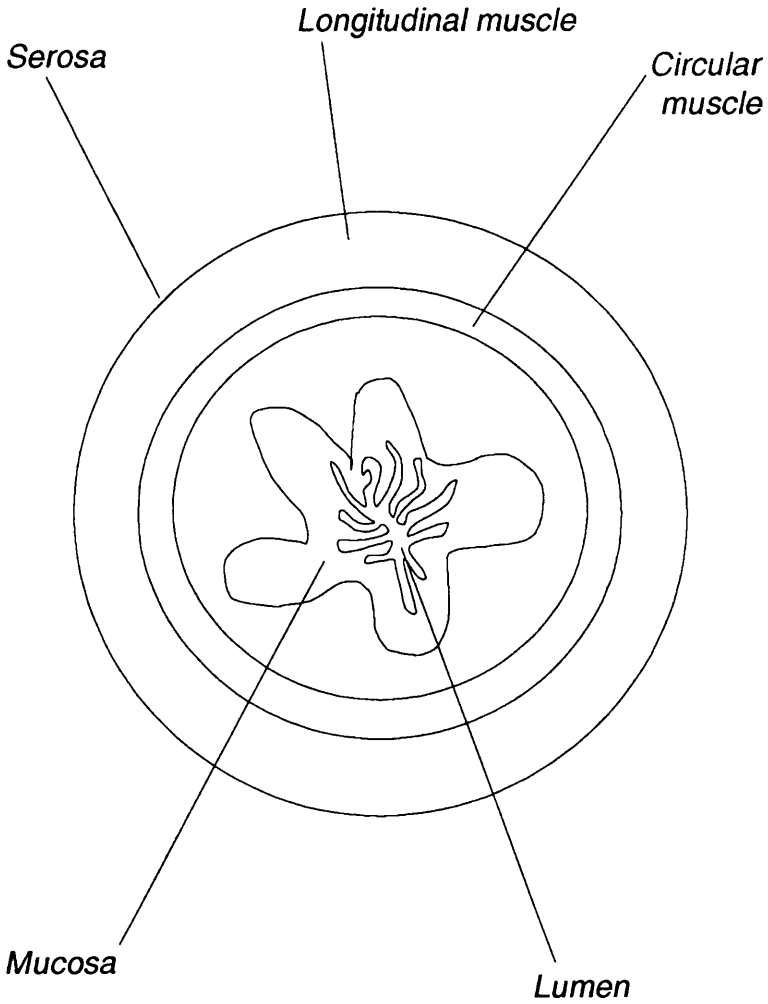

litres of gastric juice daily. The gastric juice contains a variety of substances including mucus, enzymes, hydrochloric acid, cations and anions. Figure 1.7 shows a representation of a gastric gland from the gastric mucosa. These glands are densely packed throughout the stomach, although the type of cells present will depend on the area of the stomach in which the gland is located. The neck cells of all the glands produce the mucus which has a vital protective role for the stomach lining. The glands of the cardiac region produce mainly mucus and have a very few parietal cells. The parietal cells secrete hydrochloric acid which is important in killing ingested bacteria and providing a suitable pH for pepsin to start protein digestion. The gastric glands contained in the fundus of the stomach produce the majority of the hydrochloric acid. Fundic glands also secrete the majority of the digestive enzyme pepsin. Pepsin is converted from inactive pepsinogen, produced by chief cells, in the acid pH of the stomach. The pyloric glands are similar in structure to the cardiac glands and produce mainly mucus.

Gastric secretion is regulated by several methods and take place partly in response to stimuli such as the sight, smell and taste of food. This is the cephalic phase of gastric secretion which is a nervous reflex mediated via the vagal nerve. Gastric influences also affect the secretion in the stomach. There are receptors in the stomach wall which respond to chemical stimuli and also stretch receptors which will result in an increase in secretion due to the presence of food in the stomach. Intestinal influences also regulate the gastric secretion this is achieved via a hormonal system mediated by gastric inhibitory peptide (GIP) and secretin. Some other influences are known to affect gastric secretion these include emotional factors such as stress, stimulants such as caffeine and alcohol and the blood sugar level.

1.3.3 Physiological reflux

Reflux of small amounts of gastric contents into the lower oesophagus occurs normally without causing symptoms, usually after meals when the stomach is

Figure 1.7 : A typical gastric gland

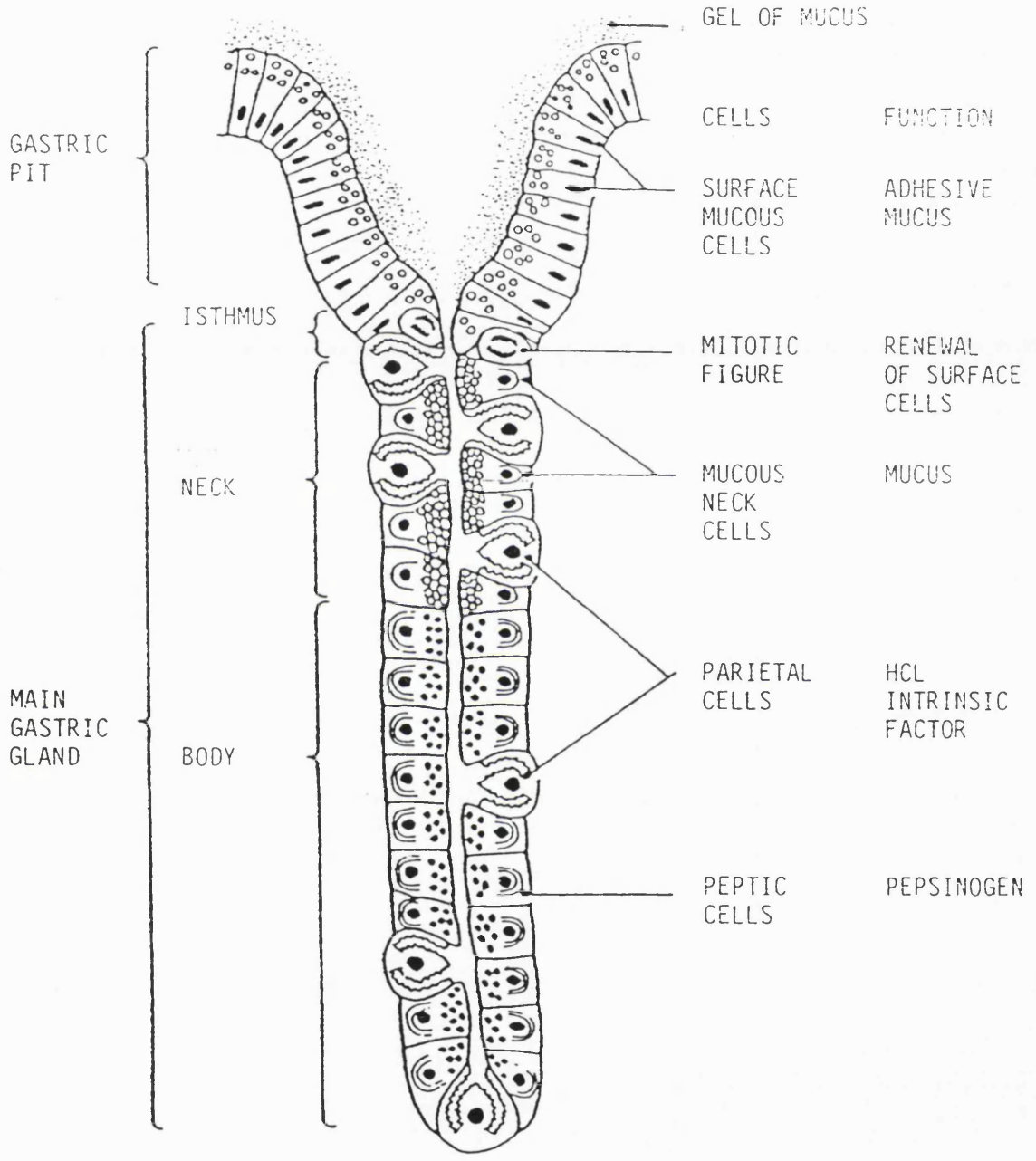

distended. It occurs when the lower oesophageal sphincter relaxes on swallowing without the expected peristaltic wave being produced in the oesophagus. The amount and frequency of reflux is increased after a large meal, but it is often unnoticed or causes only mild heartburn. There are several mechanisms present to prevent the reflux of gastric material into the oesophagus. Firstly, a positive pressure gradient exists between the abdomen and thorax which increases with the contraction of the abdominal muscles, for example during coughing, sneezing and exercise. Secondly, there is the lower oesophageal sphincter which is a zone of thickened circular muscle at the distal end of the oesophagus. There are other anatomical features which are thought to act as a barrier to reflux such as the acute angle between the lower oesophagus and the cardia acting as a valve which is maintained by gastric sling muscles around the fundus and cardia. The resistance of the oesophagus to damage by the refluxed material is also important since, as some reflux is normal, there must be mechanisms in place to prevent the irritant material causing damage to the oesophageal mucosa. The oesophagus is protected by an unstirred layer approximately 30μm thick composed of swallowed saliva and mucus. The epithelium of the lower oesophagus is modified to resist attack by refluxed gastric material, as it is a rapidly regenerating region which produces lipids and mucin to protect the area. The blood supply of the oesophagus is increased by the presence of acid which results in an increase in bicarbonate hence enhancing buffering in the area.

1.4 GASTROESOPHAGEAL REFLUX DISEASE

Gastroesophageal reflux disease or reflux oesophagitis is an inflammation of the oesophagus caused by the reflux of gastric contents. Although some reflux is experienced normally as described in Chapter 1.3.3., reflux oesophagitis occurs when the barriers to reflux are compromised for some reason or the potency of the refluxed material is increased, leading to pain and inflammation of the oesophagus.

1.4.1 Causes of gastroesophageal reflux disease

There are many factors which can contribute to gastroesophageal reflux disease. These include the five factors listed by Dodds et al (1981) which are:

1) efficacy of anti-reflux mechanisms
2) volume of gastric fluid
3) potency of refluxed material
4) efficiency of oesophageal clearance of refluxed material
5) tissue resistance of oesophageal mucosa.

The efficiency of anti-reflux mechanisms can be reduced by abnormal anatomic features such as hiatus hernia, where the stomach protrudes through the diaphragm. The efficiency of the lower oesophageal sphincter may be impaired due to incompetence of the muscle or the neuronal control. Certain drugs are also known to decrease lower oesophageal sphincter pressure such as verapamil, dopamine and adrenoceptor antagonists.

The volume of gastric contents will be important in episodes of reflux since a large gastric volume will result in a greater back pressure which must be combatted by the lower oesophageal sphincter. Gastric volume is not only dependent on the volume and composition of the food ingested, but is also affected by the rate of gastric secretion, the rate of emptying and the frequency and volume of duodenal-gastric reflux.

It is not only the number and frequency of reflux episodes which determines the severity of reflux oesophagitis, but also the potency of the refluxed material. The refluxed material contains not only hydrochloric acid but also the digestive enzyme pepsin, which together are very potent in promoting oesophagitis. Drugs or foods which increase the production of either hydrochloric acid or pepsin will have the effect of increasing the potency of any refluxed material.

Another factor important in determining the potential of a reflux episode to

produce oesophagitis is the efficiency of the oesophageal clearance of refluxed material. When reflux occurs the rate of clearance determines the length of time the noxious refluxed material is in contact with the oesophageal mucosa. Clearance depends on the peristaltic activity of the oesophagus. Salivation promotes swallowing and also aids neutralisation of the refluxed material by dilution. Gravity also aids the clearance of refluxed material, thus oesophageal clearance is impaired in supine subjects. Ageing and degenerative diseases of the nervous and muscular systems can cause a decrease in the peristaltic activity of the oesophagus, and hence increase the likelihood of reflux oesophagitis.

The resistance of the oesophageal epithelium to attack by gastric contents varies between individuals, as some subjects can experience frequent episodes of gastroesophageal reflux without developing oesophagitis. Although the oesophageal mucosa is less resistant to the damaging effects of gastric secretions than other mucosae found in the gastrointestinal tract, it does produce protective mucus. The epithelial cells of the lining of the oesophagus appear to proliferate rapidly to keep pace with the increased desquamation caused by the effect of the refluxed gastric contents. Such protective measures may vary between individuals; for example the volume and composition of mucosal secretions differs between subjects. It is also likely that with increasing age the epithelial turnover may decrease, hence increasing the chances of reflux oesophagitis.

1.4.2 Symptoms and sequelae

The major presenting feature of reflux oesophagitis is burning epigastric or retrosternal pain. This is commonly referred to as heartburn, and is often found to be exacerbated by lifting or bending. It is usually worse at night and is often associated with obesity and pregnancy. Other symptoms which may be present in some individuals include regurgitation, and even respiratory symptoms due to aspiration of acidic oesophageal contents into the lungs.

There is a poor correlation between the presence and severity of symptoms and the presence and severity of reflux oesophagitis. Some patients may be virtually asymptomatic whilst having clinical evidence of oesophagitis while others will suffer from the symptoms of gastroesophageal reflux without the resulting damage to the oesophagus. Mild oesophagitis such as that seen after vomiting or excess alcohol ingestion causes a reddening of the oesophageal mucosa. If reflux continues over a period of time, damage to the mucosa will result in erosion of the epithelium and ulceration. At this stage the damage is reversible, however, if reflux of the noxious stomach contents is not prevented then chronic inflammation will occur. Chronic inflammation of the oesophageal epithelium will cause an increase in the basal germinal layer and fibrosis of the site of ulceration. The presence if areas of fibrosis may lead to the formation of strictures which will inhibit normal oesophageal motility and lead to dysphagia.

1.4.3 Diagnosis

Diagnosis of gastroesophageal reflux disease is often made via a differential diagnosis, ruling out other causes of the symptoms with which the patient presents. There are methods available for the direct diagnosis and assessment of the extent of the disease. However, these are generally reserved for more serious of prolonged cases and may also be used in the clinical study of oesophagitis. These methods for diagnosis and assessment are described by Washington (1991). The methods fall into four general categories, which will be described briefly here.

Firstly the pH of the region can be monitored by means of a pH probe, either over a period of 24 hours or after the administration of 15ml 0.1N HCl to investigate the subject's acid clearance ability. Both of these methods make use of monitoring equipment such as the pH sensitive capsule described by Connell and Waters (1964) and Evans et al (1988).

The second diagnostic technique employed in the assessment of oesophageal reflux is oesophageal manometry. This technique investigates the pressure within the lower oesophageal sphincter in order to determine whether the subject is at a higher risk of reflux than normal. The manometry is carried out using a water filled multi-lumen catheter which is introduced nasogastrically and measures the pressure along the length of the oesophagus. Although manometry has been found not to be a very accurate predictor of reflux oesophagitis, it has been found to be the best method available for the accurate placement of a pH probe.

The third method which may be employed in the investigation of reflux oesophagitis is gamma scintigraphy. A solution labelled with a gamma emitting isotope is ingested by the subject and a gamma detection camera is used to record the intensity and the position of the emitted radiation. Gastroesophageal reflux has been shown by this method both spontaneously and after the ingestion of a labelled meal designed to induce reflux. This method has been shown to be a useful tool in the evaluation of anti-reflux agents (Jenkins et al, 1983).

The final method, and most widely used diagnostic tool, is endoscopy. Endoscopy allows the visualisation of the oesophageal epithelium, hence such signs as ulceration, erosions and strictures may be identified. Biopsies of tissue from the oesophageal mucosa can be taken at the same time which further aids positive diagnoses. As well as having a diagnostic accuracy of 95% the endoscopic technique also gives the opportunity of assessing the extent and severity of the oesophageal damage.

1.4.4 Treatment of gastroesophageal reflux

The treatment of reflux oesophagitis is aimed at decreasing the amount of reflux reaching the oesophagus, decreasing the acidity of the refluxed contents, coating vulnerable tissue or improving clearance mechanisms. The choice of

treatment is highly dependent on the patient, the severity of the disease and the symptoms.

The first line treatment of gastroesophageal reflux disease is suggesting lifestyle changes to the patient which will decrease the number of reflux episodes experienced. These changes include weight loss in obese patients, cessation of smoking, avoidance of large quantities of coffee and alcohol. As well as dietary advice such as the avoidance of highly spiced food, the timing and size of meals can be altered to decrease the number of reflux episodes experienced. Smaller, more frequent meals and not eating close to retiring for the night are generally considered to be essential in reducing reflux.

If lifestyle changes alone do not improve the reflux episodes, antacids are generally the next choice of therapy. However there is little evidence for their effectiveness in reflux oesophagitis. Antacids act by neutralising the gastric acid and although they produce symptomatic relief in some patients, endoscopic evaluation does not show a significant improvement in the appearance of the oesophageal mucosa. Prolonged use of antacids may also promote a rebound increase in acid production on withdrawal of treatment.

Drugs which decrease the production of acid in the stomach are another choice in the treatment of reflux oesophagitis. H_2 antagonists and omeprazole have both been used with effectiveness in this condition. By reducing the amount of acid produced in the stomach the potency of the material refluxed into the oesophagus is reduced. The number of reflux episodes is not affected by the administration of these agents, and whilst healing of the oesophagus occurs during treatment there is a high incidence of recurrence of oesophagitis on cessation of treatment.

Reduction in the number of reflux episodes experienced can be achieved by the administration of drugs which alter the motility of the gastrointestinal tract. Drugs such as metoclopramide, domperidone and cisapride have been shown

to increase gastric peristalsis and increase lower oesophageal sphincter pressure. These agents are particularly useful when used in combination with suppression of acid production.

The final type of therapeutic agents used in the treatment of reflux oesophagitis are the anti-reflux agents such as raft forming products. Sandmark and Zenk (1964) showed that a tablet containing alginic acid and sodium bicarbonate, when chewed, would form a foam which floats on the stomach contents and was effective in relieving the symptoms of oesophagitis in patients with hiatus hernia. The properties and mode of action of these anti-reflux agents is different from that of traditional antacids with which they are often compared. Beckloff et al (1972) described these differences and showed that the floating gel formed is retained longer than the other stomach contents. The mode of action of these preparations was investigated by Malmud et al (1979) using gamma scintigraphy, who found that gastroesophageal reflux was decreased by means of the foaming, floating and viscous properties of the product. Anti-reflux agents will be described in greater detail in Chapter 1.5.

1.5 ALGINATE RAFTS

Alginate rafts are used in the treatment of reflux oesophagitis. They are different from traditional antacids by virtue of the fact that they form a viscous layer on top of the stomach contents. Although raft forming preparations contain sodium bicarbonate in order to produce the gas necessary for buoyancy they do not have a neutralising effect on the bulk of the stomach contents. The method of action makes raft forming products specific to gastroesophageal reflux disease, and they should not be considered interchangeable with standard antacids.

1.5.1 Components of alginate rafts

The two primary components of a raft forming product are the alginate and the

gas producing agent. As described in Chapter 1.1 alginates can vary in their chemical composition and physical properties thus the choice of alginate is important when deciding on the formulation for such product. In order to trap the gas bubbles necessary for buoyancy of the raft the alginate must undergo gelation as described in Chapter 1.1.2.3. Gelation is affected by such variable as the pH of the surrounding medium, the presence of stomach acid causing precipitation of the alginate and the presence of certain ions. It may also be possible to include other polysaccharides into the raft forming mixture, although this has not been explored commercially. The fact that alginate-pectin mixtures have been shown to be useful in the food industry suggests that the addition of pectin to alginate rafts my also have a beneficial effect, although again this has not yet been explored.

The second major component of an anti-reflux agent such as the alginate raft is the gas producing substance. This is a bicarbonate, which on contact with the stomach contents reacts with the acid to form carbon dioxide by the reaction shown in Equation 1.1.

$$NaHCO_3 + HCl \rightleftharpoons NaCl + H_2O + CO_2 \qquad \text{Equation 1.1}$$

The carbon dioxide released is entrapped by the alginate gel which is forming simultaneously; this gives the alginate gel a foam-like appearance and means that the viscous foam rises to the surface of the stomach contents and floats. It is important that the rate of gas formation and the rate of gelation are matched since too much gas formed too quickly will disrupt the raft and not become trapped by the gel. Equally if the gas is produced too slowly, or the gel forms too quickly, the gas will not be able to penetrate the gel and entrapment will again not occur sufficiently to form an adequate raft. Formation of carbon dioxide from bicarbonate depends on many factors. The acid strength and the bicarbonate salt used can be studied *in vitro*, however factors such as the effect of the stomach contents, particulate matter, volume, and other antacids, are more difficult to simulate under laboratory conditions.

The addition of other materials such as other salts to the raft forming mixtures should also be considered here. There are two reasons why other salts may be added to a raft forming system. Firstly, insoluble carbonates such as calcium carbonate may be added in order to aid the gelation of the alginate, as in acid conditions the salt dissociates to release the calcium. This would theoretically be particularly important if pectin were included in the formulation since pectin does not undergo gelation in acid conditions alone, but requires the presence of a divalent ion such as calcium. Although at present calcium carbonate is used in this context, the literature of the gelation of alginates suggests that zinc carbonate may also be a possible candidate for addition to raft forming mixtures, although this has not yet been investigated. The second reason for the addition of salts to a raft forming mixture is to give additional antacid properties to the product. Standard antacids such as aluminium hydroxide or magnesium carbonate have been added; however, there is evidence to suggest that they have the effect of reducing raft strength (Washington et al 1985, 1986). This lowering in raft strength may be a combination of two factors, namely the decrease in gas production due to neutralisation of the acidity of the stomach and the disruption of the gel structure by the aluminium or magnesium ions.

1.5.2 *In vitro* methods of evaluation

Traditional antacids are evaluated by their neutralisation capacity. Tests such as the well established Rossett and Rice test (Rossett and Rice, 1954) are used to evaluate the neutralisation capacity of a known quantity of the antacid against known strengths and volumes of acid. The technique involves adding the antacid to be tested to a known volume of acid and stirring the mixture in a specific fashion. Samples of the solution are taken at predefined intervals and the pH is measured in order to determine the neutralising capability of the antacid. However when used with raft forming antacids this stirring has the effect of disrupting the raft structure. Although a modification to this approach was suggested by Washington et al (1985) the test still measures the

neutralising capacity of the product which does not reflect the way the product acts to combat gastroesophageal reflux. A more appropriate method for the evaluation of raft-forming products was suggested by Washington et al (1986) who developed a piece of apparatus designed to measure the breaking strength of alginate rafts *in vitro*. The apparatus is shown in Figure 1.8. It consists of a horizontal wire probe suspended under the raft from one end of a beam balance.

There is a length of chain attached to the other arm which is controlled by a stepping motor. This increases the load on the probe to raise it through the raft. The deflection of the beam is measured by sensing the transmission of a graded optical neutral density filter attached to the beam. The apparatus gives a measure of the force required to break the raft, this being dependent on the size and shape of the probe which must be standardised. This method is the standard method of assessment for raft forming products of this type. However, the fact that the apparatus has to be individually built from non-standard pieces of equipment means that reproducibility of results between laboratories is difficult, thus comparison of data is not reliable.

It was felt necessary in the present work to find a method for evaluating rafts which uses equipment which may easily be calibrated to be equivalent to the same apparatus used elsewhere. To this end the Stable Microsystems TA.XT2 was used (as described in Chapter 5.3.1) to carry out a similar type of test to that used by Washington et al (1986).

1.5.3 *In vivo* methods of evaluation

The initial *in vivo* studies of Sandmark and Zenk (1964) and Beckloff et al (1972) showed by radiological means that after administration of a tabletted form of a raft forming product, an alginate raft formed on top of the stomach contents and that the raft persisted longer than the rest of the gastric slurry. Malmud et al (1979) used gamma scintigraphy to investigate the mechanism

Figure 1.8 : Raft testing apparatus (Washington et al, 1986)

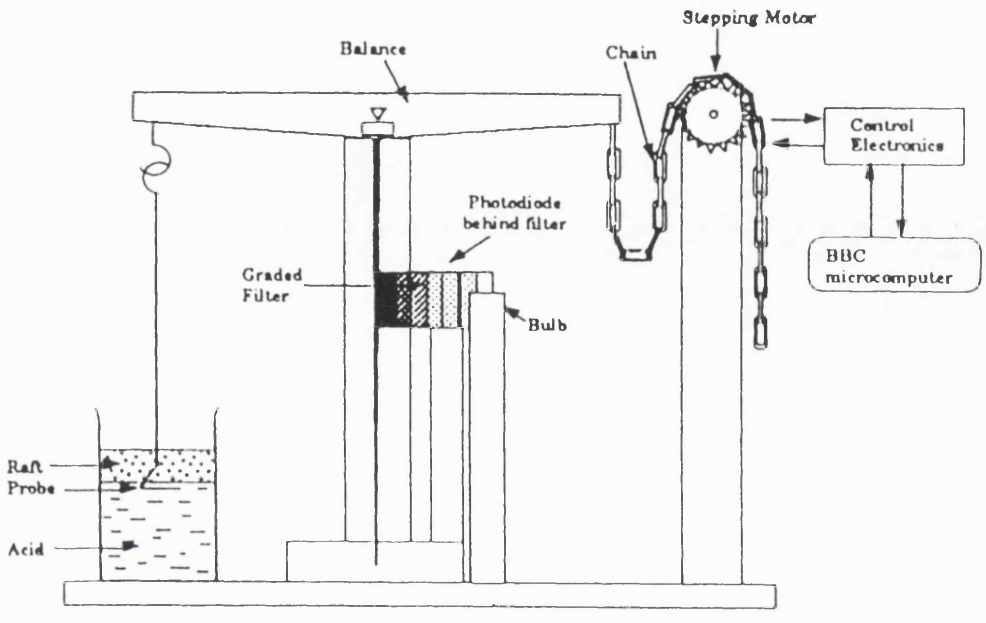

of action of raft forming products. They proposed that the mechanism of action of the rafts was by the formation of a viscous layer on top of the gastric contents which was either preferentially refluxed or acted as a physical barrier to reflux. The use of gamma scintigraphy in the study of alginate rafts was continued by May et al (1984). In these studies the alginate product is labelled with Tc-99m and the test meal is labelled with In-113m. It was shown that the alginate tended to float on the stomach contents and that it only emptied slowly from the stomach. In other investigations a test meal was specifically designed to induce gastric reflux; it comprised scrambled eggs, toast and butter with orange juice and coffee (Washington, 1987). Using this technique of labelling both the meal and the raft it was possible to measure the kinetics of gastric emptying for both the food and the anti-reflux agent, and it allows the calculation of the percentage of the alginate located in the upper (fundal) region of the stomach. It was shown that the raft forming product significantly reduced both the amount of food and the amount of acid refluxed into the oesophagus.

Gamma scintigraphic studies of alginate raft forming products have shown the influence of posture on the gastric emptying of the raft (Bennett et al, 1984), with emptying occurring fastest in patients lying on their left side. The pH dependence of the anti-reflux barrier was investigated by Knight et al (1986), who showed that the stomach contents must be sufficiently acidic before raft formation will occur. Washington et al (1986,1987) showed the way in which formulation variables can affect the residence time and raft forming ability of various raft forming mixtures, concluding that the addition of antacid materials to the alginate interferes with the ability to produce a raft on top of the gastric contents.

Endoscopy has also been used to evaluate the *in vivo* effects of alginate rafts, although the technique is best performed on an empty stomach. Raft formation in a fasted stomach is markedly different because the pH, volume of the contents and the motility of the stomach will be substantially different to that of a fed stomach (Jenkins et al, 1983), thus endoscopy does not give particularly

useful information on the *in vivo* characteristics of the raft.

It is possible to monitor the pH of the lower oesophagus using pH telemetry as described by Washington et al (1985). The data obtained were used to investigate the correlation between the *in vivo* measurements and the measurements made with the modified Rossett and Rice test (1954). This method of pH monitoring was also used by Washington (1990) in an investigation of the barrier action of liquid Gaviscon, an alginate based anti-reflux agent. This study showed that the alginate product reduced the amount of gastric reflux and the effect it has in reducing oesophagitis is not due to the neutralising capacity alone, as with standard antacid products.

1.6 OBJECTIVES

The overall objective in this project was to investigate the way in which each component of the raft affects the raft performance. To achieve this it was necessary to investigate possible strategies for improving the foam, including the choice of the bicarbonate, the use of alternative cations and the inclusion of pectin in the formulation. In order to determine the effect of the individual formulation variables, methods of studying discrete parts of the raft had to be found. These methods involve determination of the alginate composition and the rheological properties of the solutions and gels under various conditions. It was also considered useful to develop a method of establishing the effect of the formulation variables on bubble size as this has not been previously studied. A further objective was to develop a novel method for characterising alginate rafts, with the aim of finding a simple, reliable and reproducible test which would be useful not only in research, but also in the development and quality testing of these systems. In the past the development of alginate raft products has been on a more or less *ad hoc* basis. The systematic approach outlined above should improve the ability to predict what is required for a good raft forming product as well as serving to contribute to the material properties of alginates.

CHAPTER 2

CHAPTER 2: MATERIALS AND METHODS

2.1 MATERIALS

2.1.1 Alginates

The alginate samples used were obtained from Protan Biopolymers A/S (now Pronova Biopolymers A/S), Drammen, Norway. Five different grades of alginate were used in total, although for certain experiments a smaller number were investigated. The five samples were chosen to give a range of characteristics; they show a variety of compositions and viscosities. Within each sample only one batch was used to exclude the problems of interbatch variation which can be a particular problem with materials originating from a natural source such as alginates. Table 2.1 shows the properties of each alginate sample used, as stated in the product specification and certificate of analysis from Pronova for each batch. In the following chapters the alginates used will be referred to by the product name given by Pronova (Protan). In each case this product name refers to the batch detailed in Table 2.1

2.1.2 Bicarbonates

Two bicarbonates were chosen for examination in the raft forming mixtures in order to investigate whether the bicarbonate used affected the properties of the raft formed. The sodium bicarbonate used was obtained from B.D.H., Batch Number: 7097380N. The potassium bicarbonate was also from B.D.H., Batch Number: 71H0733.

2.1.3 Carbonates

Three carbonates were used in total, namely calcium, magnesium and zinc. These were chosen for addition to the raft forming mixtures for a variety of reasons. Calcium was chosen for its gelling properties with alginates and because it is currently used in some commercial raft products. Zinc was

Table 2.1 : The nominal properties of the alginate samples used.

	LFR 5/60	LF 120M	LF 10/40RB	LF 20/200	LF 200DL
Batch No:	803091	SLP 945	SLP 947	SLP 955	802920
Guluronic acid range	65-75%	35-45%	45-55%	65-75%	55-65%
Mannuronic acid range	25-35%	55-65%	45-55%	25-35%	35-45%
Source	*Laminaria hyperborea (stipes)*	*Ascophyllum nodosum*	*Laminaria hyperborea (leaves)*	*Laminaria hyperborea (stipes)*	*Laminaria hyperborea*
Loss on drying (%)	11.6	9.0	11.9	7.1	7.0
Viscosity in 1% w/v solution	530 mPa.s*	85.0 mPa.s	54.8 mPa.s	155 mPa.s	260 mPa.s
pH in 1% solution	7.0	5.6	6.4	7.0	7.7
Particle size	60 mesh (100%)	120 mesh (100%)	40 mesh (100%)	200 mesh (100%)	200 mesh (99.8%)

* 10% solution measured due to low viscosity of 1% solution.

chosen because the literature on the gelation of alginates with divalent cations suggests that although not as potent as calcium, zinc promotes gelation in alginate solutions as described in Chapter 1.1.2.3. Magnesium was also used in some raft experiments as this is also found in some commercially available alginate products, and magnesium carbonate is a constituent of many traditional antacid products. The cations used in the raft forming mixtures were in the form of the carbonate. This was necessary since if a water soluble salt of the ions were used, gelation of the alginate would begin to occur during preparation of the mixture, prior to exposure to the acid. By using the carbonate salt the divalent ions are released by the action of the acid, i.e. at the time gelation is required. The carbonates used were all obtained from B.D.H; the batch numbers used are given below.

Calcium Carbonate	2070240L
Magnesium Carbonate	2853250M
Zinc Carbonate	148 K16256803.

2.1.4 Chlorides

The dialysis solutions used in the preparation of the alginate gels for dynamic mechanical analysis were prepared form the chlorides of calcium and zinc, which are soluble in water. The calcium chloride used was fused granular calcium chloride from B.D.H., batch no: 6346160N. The zinc chloride was also from B.D.H., batch no: 220B 427404.

2.1.5 Pectin

The pectin used was a low methoxy apple pectin. This was chosen because, unlike other pectins, low methoxy content pectins do not require the addition of sugars to promote gelation; they in fact undergo gelation brought about by the presence of calcium. This, and the structural similarity to alginates already discussed in Chapter 1.2 suggested a possible use for its inclusion in the raft forming mixtures. The pectin used was obtained from Sigma, batch number:

60H2610. The calcium content of the batch was assayed by Sigma and found to be 0.48% w/w

2.2 METHODS

2.2.1 Preparation of alginate solutions

Solutions of the alginates were prepared by the addition of the required quantity of sodium alginate powder gently into the vortex created by the action of a magnetic stirrer in the deionised water. The stirring was continued for 20 minutes to allow full dissolution of the powder. All solutions were prepared at 20°C on the day in which they were used due to the possibility of depolymerisation of the alginate in solution and microbial spoilage on storage of solutions.

2.2.2 Pectin solutions

Pectin solutions were prepared by the addition of the required quantity of pectin to boiling deionised water with gentle stirring. The mixture was boiled for 10 minutes until the powder had dissolved completely. After cooling to room temperature the solution was made up to volume with deionised water. The solutions were prepared on the day in which they were to be used.

2.2.3 Alginate/Pectin solutions

Solutions containing both sodium alginate and pectin were prepared by first dissolving the pectin in boiling deionised water, as described above. The required quantity of sodium alginate was added to the pectin solution once it had been cooled to room temperature and made up to volume. The sodium alginate powder was added gently into the vortex created by a magnetic stirrer and the mixture was stirred until all the powder had dissolved. The solutions were prepared on the day in which they were to be used.

2.2.4 Raft forming mixtures

The raft forming mixtures were prepared by dissolving the bicarbonate in the deionised water and then dissolving the sodium alginate as described in Chapter 2.2.1. Where insoluble carbonates were required to be added to the raft forming mixtures these were added to the mixture after the alginate had fully dissolved, thus aiding suspension of the carbonate. In the raft forming mixtures containing both alginate and pectin, the pectin was dissolved first in boiling water as described in Chapter 2.2.2, and cooled before the addition of the bicarbonate and sodium alginate.

2.2.5 Hydrochloric acid dilutions

In all experiments 0.1M HCl was used except in those where the effect of acid strength was being investigated, in which case 0.05M and 0.07M HCl were also used. The required strengths of hydrochloric acid used were prepared by dilution of a 5N stock solution (from B.D.H.) with deionised water in volumetric flasks.

2.2.6 Alginate gels

In order to produce suitably sized homogenous gel samples the alginate gels were formed by dialysis of a 2.5% alginate solution against either 0.1M HCl or a 3% w/v solution of divalent ion chloride. The gels were formed in perspex cylinders with cellulose acetate dialysis membrane over each of the open ends; this is described in more detail in Chapter 4.3.

CHAPTER 3

CHAPTER 3: CHARACTERISATION OF ALGINATES

3.1 INTRODUCTION

In order to be able to relate the *in vitro* performance of an alginate raft to the production and formulation variables it is important to be able to assess the characteristics of the raw material under investigation. One of the major sources of variation is the structure of the alginate being used. The physical properties of alginates have been shown to be affected by the chemical composition (Rees, 1972; Haug et al 1967) as described in Chapter 1.1.1.3. To this end it was important to be able to determine the mannuronic and guluronic acid content of the alginates. This has been achieved using two different techniques, nuclear magnetic resonance (NMR) and circular dichroism (CD). Using these two methods it is possible to establish the chemical composition of the batches used.

It is important when using a material such as alginate, which is subject to wide interbatch variation, to characterise the material by several complimentary methods. The choice of methods should be influenced by the relevance they have to the proposed use of the material. One of the most important properties of alginates is their ability to form viscous solutions in water. This property has been exploited a great deal in the food industry, hence it is desirable to characterise the rheological properties of alginate solutions and establish the factors which affect these properties.

Some of the factors which influence the viscosity of an alginate solution are characteristics of the alginate sample such as the chemical composition, molecular weight and degree of polymerisation, whilst other factors are external conditions such as concentration, temperature, pH and ionic content of the solution (McDowell, 1986). It is important when making measurements of viscosity in alginates that the conditions are standardised as much as possible. The intrinsic viscosity is a useful means of comparing the solutions since the

calculation of the intrinsic viscosity takes into account such factors as the rate of shear and the concentration of the solution. The intrinsic viscosity, together with the viscosities of the solutions measured under known conditions gives a good indication of the variation in the characteristics of the alginates used.

This chapter therefore describes the basic characterisation of the alginate samples used, particularly in terms of the M/G ratio and rheological behaviour. This will allow a more specific understanding of how changing the alginate sample affects subsequent product performance.

3.2 NUCLEAR MAGNETIC RESONANCE

3.2.1 Theory of NMR spectroscopy of alginates

3.2.1.1 The use of NMR in the characterisation of alginates

The standard method for the determination of the block composition of alginates prior to the use of nuclear magnetic resonance (NMR) had been by a series of reactions comprising hydrolysis, fractional precipitation and determination of the uronic acid composition by complete acid hydrolysis (Haug et al, 1966). The hydrolysis method is very reliable but time consuming and thus not suitable for routine characterisation of alginates. Penman and Sanderson (1972) described a method for the determination of block structure using partial acid hydrolysis of the alginate followed by ^{1}H-NMR spectroscopy. They showed that mannuronic and guluronic acid blocks can be differentiated by this technique and thus the relative proportions of the homopolymeric fractions can be calculated, that is fractions containing only one type of uronic acid residue. The ratio of homopolymeric blocks to alternating blocks could therefore be determined experimentally from the yields of the hydrolysis.

Grasdalen et al (1979) extended the use of ^{1}H-NMR for the characterisation of alginates by developing a method using intact or partially depolymerised samples. The results from this NMR spectroscopy gives information on nearest

neighbour (or diad) frequency rather than an analysis of the total block structure. However, the data were shown to correlate well with chemical analyses. ^{13}C-NMR was employed by Grasdalen et al (1981) and found to be useful in estimating block structure due to the ability to give a better estimate of triad frequency (i.e. groups of three uronic acid residues).

For routine characterisation of alginates ^{1}H-NMR has been extensively used in many areas of alginate research. The degree of acetylation of bacterial alginates was investigated using ^{1}H-NMR spectroscopy by Skjåk-Bræk et al (1986[a]), while the enzymatic modification of alginates was studied by Skjåk-Bræk et al (1986[b]) using a combination of ^{1}H-NMR to determine monad, diad, and G centred triad frequencies and ^{13}C-NMR to determine M centred triad frequencies. The Norwegian group has continued to use NMR as a standard method for the characterisation of alginate block structure.

3.2.1.2 Basic principles of NMR

Nuclear magnetic resonance spectroscopy is performed on samples in solution which are placed between the poles of a powerful magnet. The effect of the magnetic field is to produce changes in the energy states of the nuclei in the sample. The different energy states are detected by the absorption of energy of the appropriate wavelength; the relationship between energy and wavelength is given in Equation 3.1.

$$\Delta E = h\nu \qquad \text{Equation 3.1}$$

where : ΔE is the change in energy

h is Planck's constant

ν is the frequency of the light absorbed.

Certain nuclei have only two possible states of magnetic moment, these nuclei include H^{1} and C^{13}. These two states have discrete quantum values of +½ and -½. The α spin state has the value +½; in this state the nuclear

magnetic moment is aligned with the applied field it is therefore the low energy state. In the high energy β spin state (-½) the nuclear magnetic moment is aligned against the applied field. The energy difference between the two spin states is given by Equation 3.2.

$$\nu = \frac{\gamma H}{2\pi} \qquad \text{Equation 3.2}$$

where: ν is the frequency of the light absorbed
H is the magnetic field strength at the nucleus
γ is the magnetogyric ratio of the nucleus.

It would appear that all nuclei of the same atomic exhibit the same response to a given magnetic field. However, it should be remembered that these nuclei are not studied alone but as part of a molecule. When using ^{1}H-NMR with real molecules the protons are surrounded to varying extents by electrons which cause a shielding of the magnetic field. In a magnetic field the electrons move in such a way that their motion induces a magnetic field in opposition to the applied field. Thus the magnetic field at the nucleus will be given by Equation 3.3.

$$H = Ho - H' \qquad \text{Equation 3.3}$$

where: H is the magnetic field at the nucleus
Ho is the applied magnetic field
H' is the induced magnetic field.

The reduction in magnetic field at the nucleus is known as diamagnetic shielding. The magnitude of the shielding depends on the amount of electrons in the vicinity of the nucleus under consideration and also the presence of any electronegative or electropositive groups or elements. Electronegative groups will tend to reduce the shielding effect on a nucleus and therefore cause the peak to shift downfield. Since the various protons in a molecule will be affected to different degrees by diamagnetic shielding the peaks corresponding to the

nuclei will appear at different places in the spectrum. Increasing the applied magnetic field will cause larger opposing fields to be set up, hence greater shielding will be seen leading to better resolution. Since the energy of the transitions is related to the magnetic field strength, the results gained from machines using different field strengths can not be compared directly. The measurements taken are therefore compared with those of a calibrant, tetramethylsilane (TMS) and converted to the standard units, parts per million (ppm or δ). The relative amounts of each proton present can be calculated from the area of the peak, or from the relative heights of the integrals if these are given.

3.2.1.3 NMR spectroscopy of alginates

The method used in the present work and the analysis of the spectra is similar to that proposed by Grasdalen et al (1979). Figure 3.1 is reproduced from Grasdalen et al (1979) and shows typical NMR spectra for three fractions of an alginate. The spectrum for a guluronic acid fraction is shown in Figure 3.1(a), that for a mannuronic acid fraction is shown in Figure 3.1(b) whilst Figure 3.1(c) shows a typical spectrum from an alternating M-G fraction. These peak assignments were proposed by Penman and Sanderson (1972) and confirmed by Grasdalen et al (1979). It is also possible to detect peaks due to two or three linked residues as shown in Figure 3.2 where the peak assignments have been added to the spectrum. The assignments given are for both the proton at position 1 on the sugar residue and that at position 5 (see Figure 3.3) and are distinguished by the number after the peak assignment.

3.2.2 Method

The method used for the preparation of samples and the measurement of NMR spectra was that used by SmithKline Beecham for in-house evaluation of raw materials. The preparation of the sample used is of great importance in NMR. At the concentrations convenient for ^{1}H-NMR analysis, alginate solutions are

Figure 3.1 : Typical NMR spectra for three fractions of an alginate

(a) 90% L-guluronate

(b) 85% D-mannuronate

(c) ~60% L-guluronate

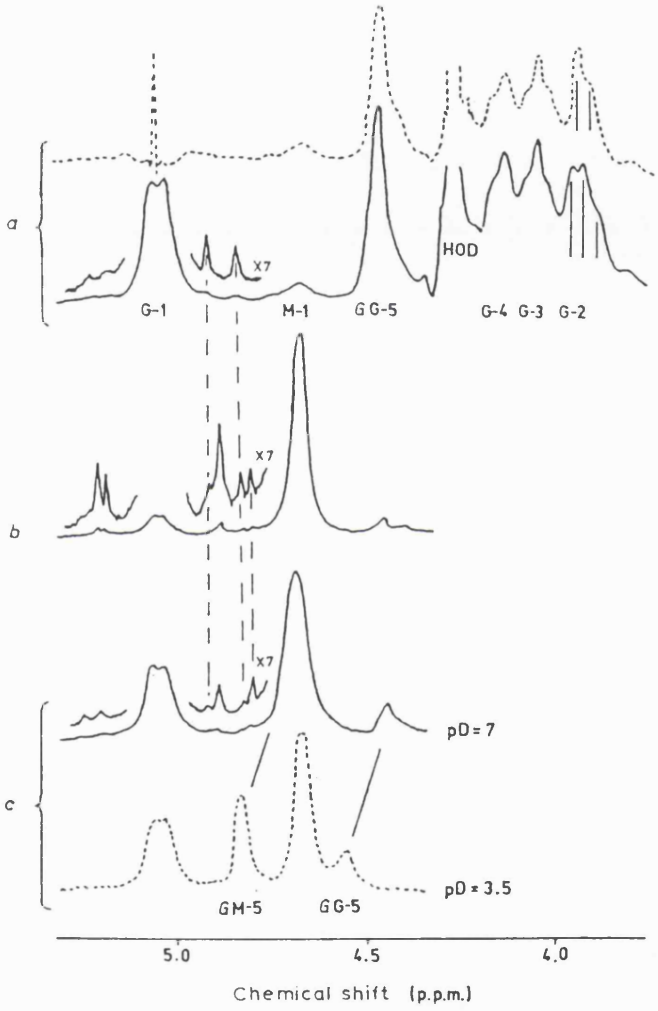

Figure 3.2 : Peak assignments for an NMR spectrum of an alginate

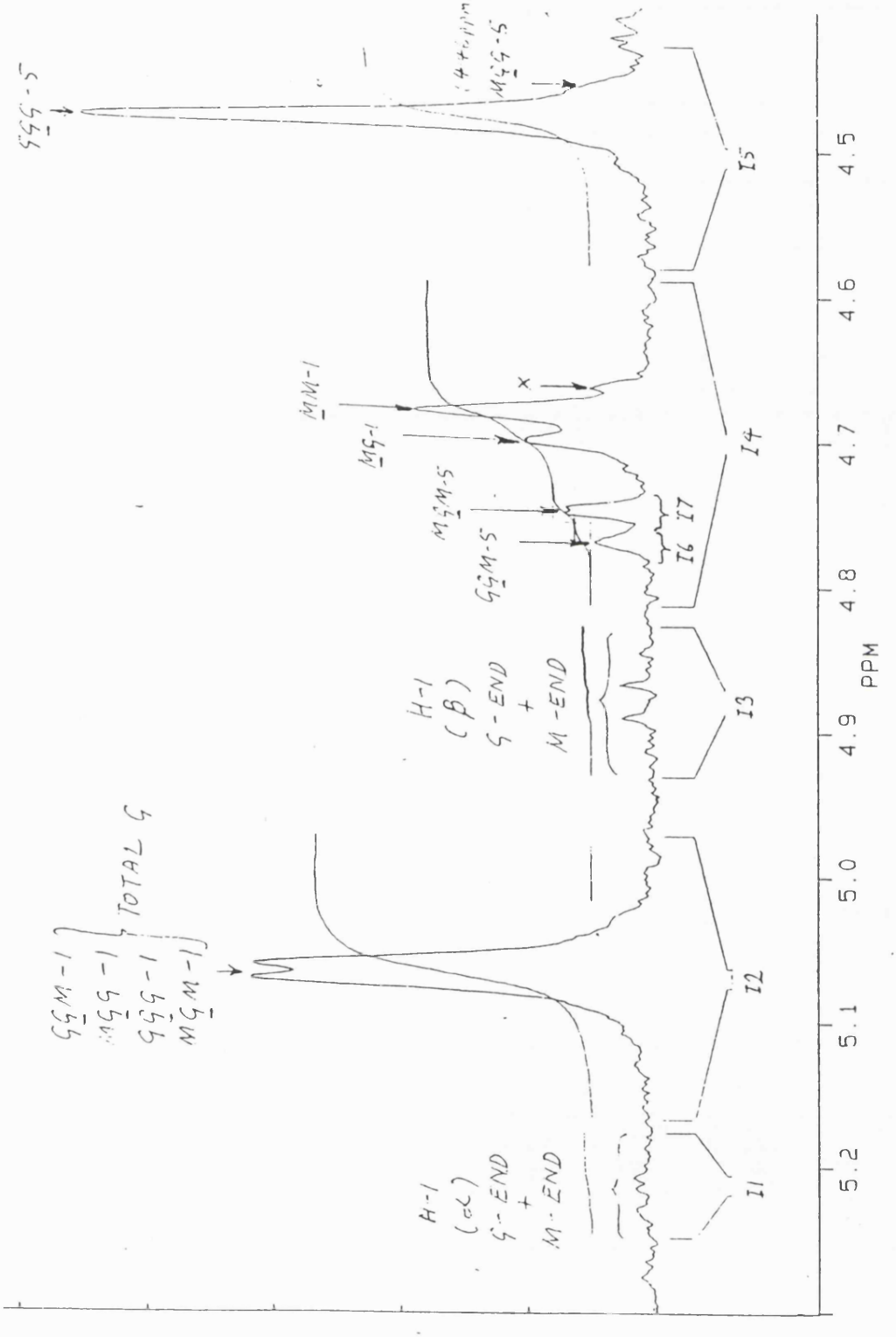

Figure 3.3 : Diagram of mannuronic and guluronic acids showing numbering of carbon atoms

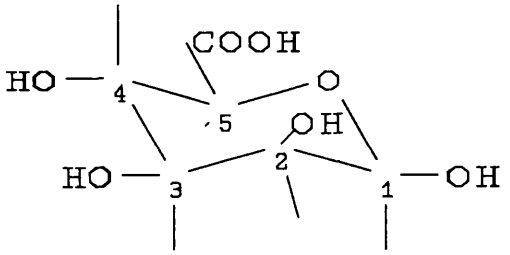

D-mannuronic acid

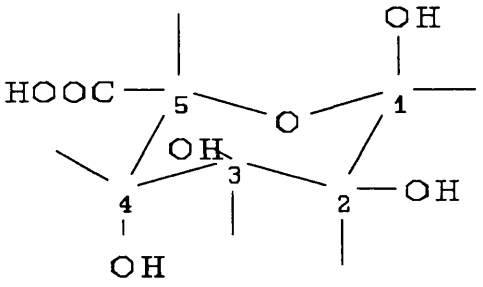

L-guluronic acid

fairly viscous which will cause line broadening of the NMR spectrum. In order to reduce the viscosity it is necessary to perform a mild partial hydrolysis on the alginate samples before analysis.

The sodium alginate sample (200mg) was weighed into a 250ml round bottomed, two necked flask. This was shaken vigorously with 100ml distilled water for two minutes to partially dissolve the sodium alginate. A pre-calibrated pH meter was used to measure the pH of the mixture. The pH was adjusted to 5.2 by the dropwise addition of either 1M sodium hydroxide or 1M hydrochloric acid and the suspension was again shaken for two minutes to dissolve the remaining sodium alginate. The solution temperature was then raised to boiling point, and the solution was refluxed under nitrogen for 15 minutes. After cooling to room temperature the pH of the solution was adjusted to 3.6 with 0.05M sulphuric acid and the solution was refluxed under nitrogen for a further 25 minutes. After cooling to room temperature the solution was divided into two aliquots, transferred to stoppered round-bottomed flasks and freeze-dried overnight.

The freeze-dried solid was then prepared for analysis. The contents of one of the round bottomed flasks, containing approximately 100mg freeze-dried solid, was dissolved in 5.0ml deuterium oxide (99.8%D or better) containing 0.5% w/w trimethylsilyl-3-propionic acid d_4-2,2,3,3, sodium salt (TSP) by warming gently as necessary. 120µl saturated disodium EDTA (0.3M) solution was added to complex any di- and trivalent cations present and the solution pH was adjusted to 4.2 using approximately 1% w/w sodium deuteroxide solution.

A dummy sample tube containing 0.50ml D_2O and TSP was placed in the magnet, the probe temperature was set to 90°C and allowed to stabilise for 40 minutes. After tuning for optimum resolution the NMR tube containing 0.50ml of the alginate solution was placed in the probe and 20 minutes allowed for the solution temperature to stabilise. After retuning the proton spectrum was recorded. The baseline was corrected and the spectrum integrated at 400MHz,

at 90°C using 300 pulses, a pulse angle of 28°, a spectral width of 12ppm, and zero pulse delay.

3.2.3 Results

The results for the fraction of guluronic acid present in the samples and the average G block length have been calculated from the NMR spectra recorded as described. The spectra for the alginate samples are shown in Figure 3.4 with the integrals of the peaks. The size of the integrals is used to determine the relative amounts of each of the fractions. The numerical data presented in Table 3.1 are the average values obtained from two separate hydrolyses for each of the five samples under investigation. For each of the samples the fraction of guluronic acid and mannuronic acid residues are given, F(G) and F(M). Also shown are the relative amounts of the individual diads and triads, i.e. fractions comprising two or three uronic acid residues. The average G block length for chain lengths greater than one unit (NG>1) is also given. This is a measure of whether the guluronic acid residues in the alginate occur in blocks or are more isolated. The values obtained for the guluronic acid content of the alginates are in good agreement with the nominal values given by Protan (shown in Table 2.1). It is interesting to note that the alginates LFR 5/60 and LF 20/200 have similar values of F(G) which are 67.2 and 67.0 respectively whilst the values of NG>1 seem to vary more, suggesting that in LFR 5/60 the guluronic acid residues are more concentrated into blocks than in the LF 20/200.

3.3 CIRCULAR DICHROISM

3.3.1 Theory of circular dichroism

Circular dichroism (CD) was shown to be a useful technique in the study of alginates by Morris et al (1973). It was demonstrated that the technique could be used to estimate the chemical composition of the alginates and to study the effect of calcium on the sol $\rightarrow$ gel transition of the alginate.

Figure 3.4(a) : NMR spectrum of LFR 5/60

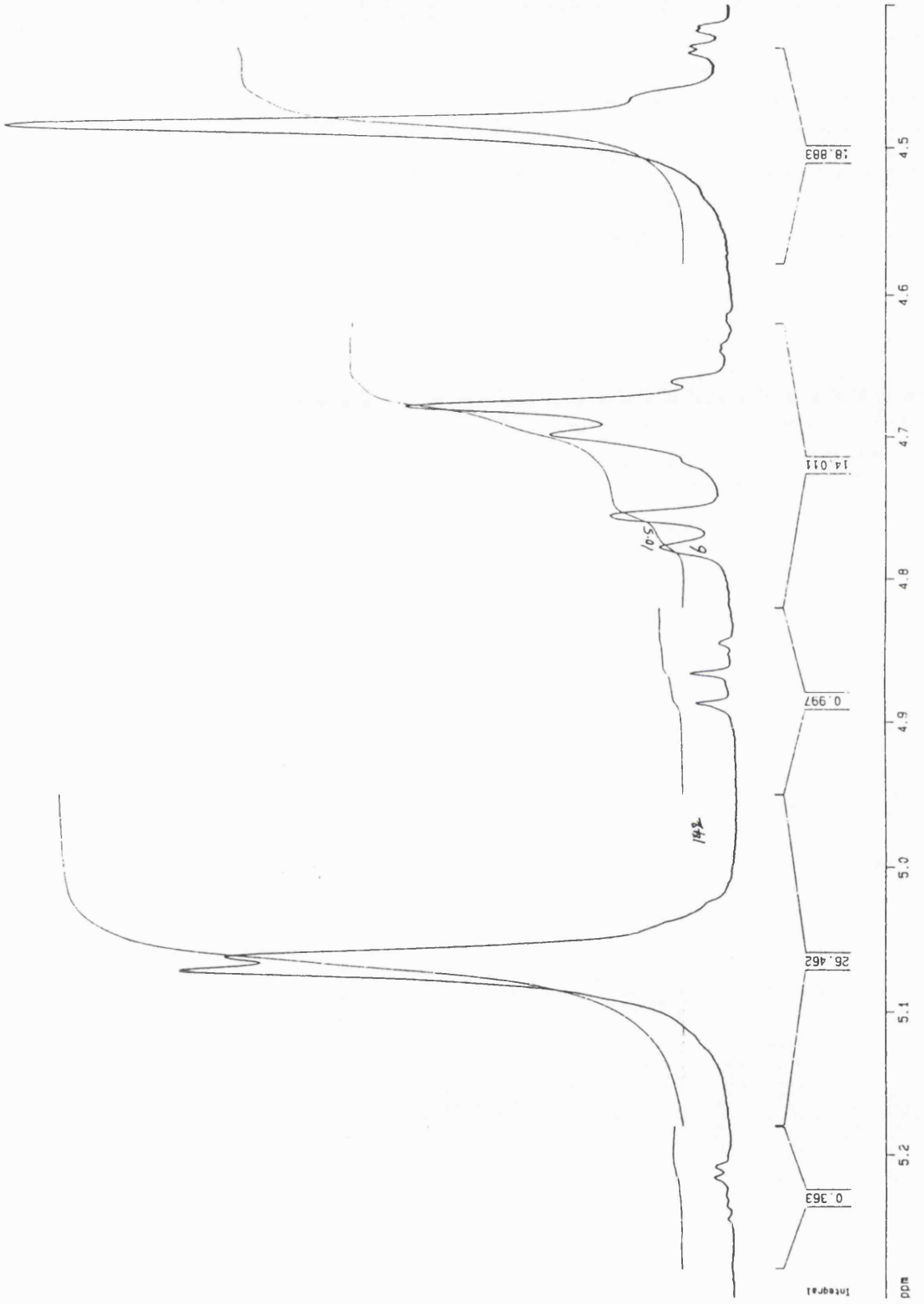

Figure 3.4(b) : NMR spectrum of LF 120M

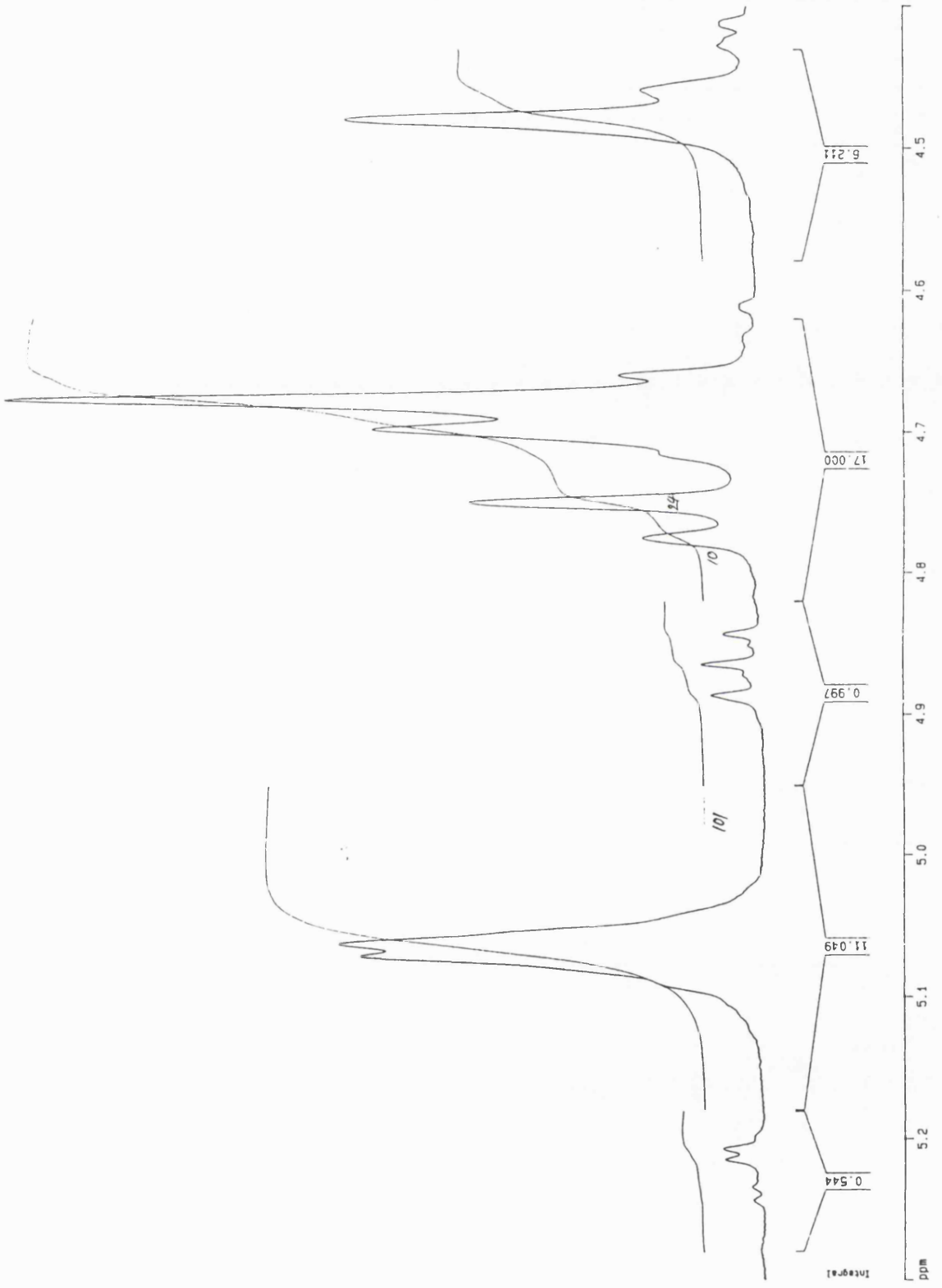

Figure 3.4(c) : NMR spectrum of LF 10/40RB

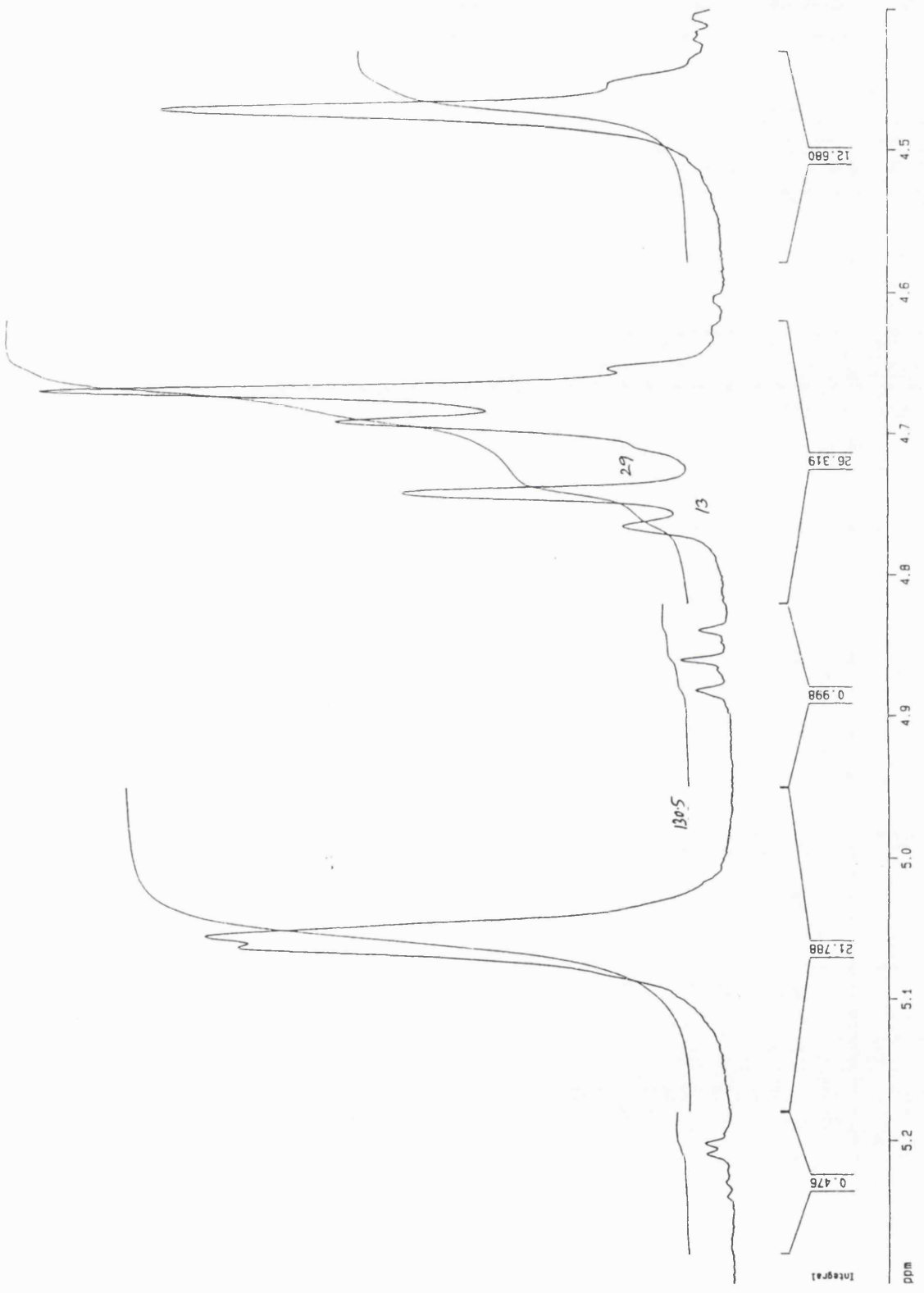

Figure 3.4(d) : NMR spectrum of LF 20/200

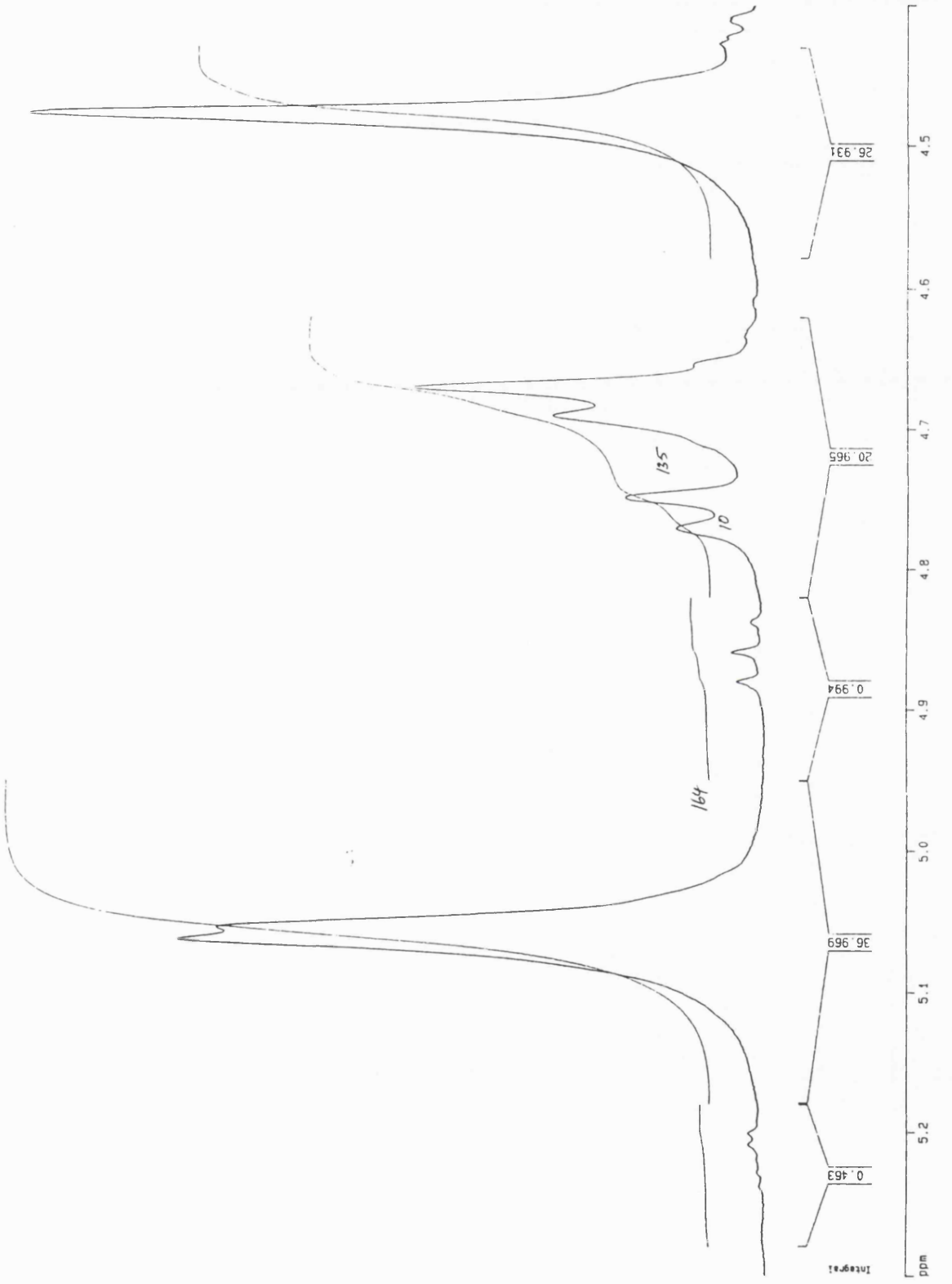

Figure 3.4(e) : NMR spectrum of LF 200DL

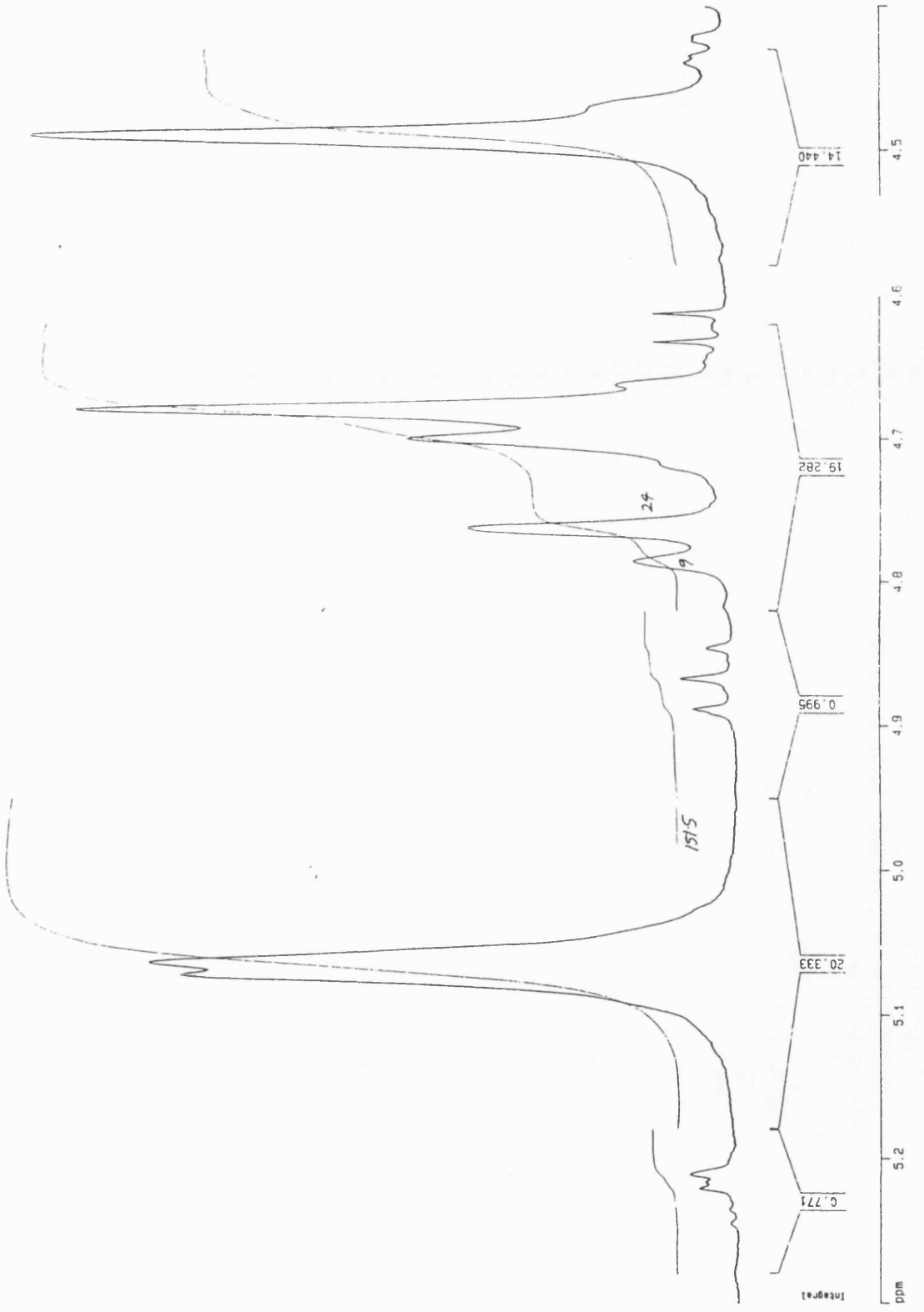

Table 3.1 : Average composition values as determined by NMR.

Alginate	F(G)	F(M)	F(GG)	F(MM)	F(GM)	F(GGG)	F(GGM)	F(MGM)	NG>1
LFR 5/60	0.672	0.328	0.582	0.238	0.090	0.546	0.035	0.055	17.5
LF 120M	0.424	0.576	0.266	0.419	0.158	0.221	0.046	0.112	6.9
LF10/40RB	0.509	0.491	0.334	0.315	0.175	0.282	0.053	0.122	7.4
LF 20/200	0.670	0.330	0.562	0.223	0.108	0.517	0.045	0.063	13.6
LF 200DL	0.551	0.449	0.419	0.318	0.131	0.384	0.036	0.096	12.7

Circular dichroism is an optical technique which measures the absorption of polarised light as a function of wavelength. For the technique to be applicable to a particular system there must be a chiral molecule present which has a UV absorption in the range 190-750nm. Alginates, as previously described, are copolymers of D-mannuronic and L-guluronic acid residues. These two residues have a different configurations at C(4) and C(5) which results in the differences in molar absorptivity ε_L and ε_R between the two components. Since ε_L and ε_R are not equal the vector sum of the two components will no longer be linear, but rather will follow an ellipse. The difference in the ε's is related to the molecular elipticity θ of the material as shown in Equation 3.4.

$$[\theta]=3300.(\varepsilon_L-\varepsilon_R) \qquad \text{Equation 3.4}$$

where: θ is the molecular elipticity

ε_L and ε_R are the molar absorptivity terms for the two directions

The optical activity of organic molecules is dependent on the wavelength at which it is measured and generally increases towards the shorter wavelengths, hence this variation allows the measurement of absorption spectra for suitable materials.

Morris et al (1975) showed that all D-uronic acid glycosides give a positive band at 212nm as their principal spectral feature and that L-uronic acid glycosides give a corresponding negative band. This difference in sign is due to the configuration of the C(5) carbon atom of the sugar affecting the position of the oxygen atom in the ring relative to the chromophore (the carboxyl group in this case). The position of the hydroxy group on the carbon atom at position C(4) on the ring is also close enough to the carboxyl group to interact with it directly.

The two uronic acid monomers which are present in sodium alginate have opposite configurations at both the C(4) and C(5) positions which makes them particularly amenable to study by circular dichroism. The difference in configuration at C(5) results in the bands in the n $\rightarrow\pi^*$ region of the spectrum

being of opposite sign. The opposite configuration of the monomers at C(4) causes the principal bands of the spectrum to be offset, thus the positive and negative bands are clearly separated. These two configuration differences result in the n $\rightarrow\pi^*$ transitions occurring at around 212nm and 200nm giving a trough and a peak respectively. The relative proportions of guluronic and mannuronic acid residues can be calculated from the ratio of the peak height and trough depth (P/T ratio). Morris et al (1975) showed the way in which the P/T ratio is related to alginate composition, Figure 3.5 shows the way in which P/T varies with the percentage of mannuronic acid residues in the sample.

3.3.2 Method

Sodium alginate solutions (3mg/ml) were prepared in deionised water as described in Chapter 2.2.1. The solutions were adjusted to pH 7 by the careful addition of 1M sodium hydroxide. After thoroughly cleaning and drying the cell (pathlength 0.5mm) the alginate solution was introduced using a pasteur pipette, taking care to avoid allowing air bubbles to enter the cell. The CD spectra were obtained using a JASCO J600 spectropolarimeter equipped with a thermostatted cell holder, which maintained the sample temperature at 25°C. The wavelength region between 185nm and 260nm was scanned as this was the region of interest identified by Morris et al (1975) and the UV maximum found with the samples occurred at 210-206nm. The values for the peak/trough ratio were calculated from the spectra and from these values the relative amounts of mannuronic and guluronic acid residues were calculated with reference to the calibration graph prepared by Morris et al (1975) and is shown in Figure 3.5

3.3.3 Results

The CD spectra for the five alginates are shown in Figure 3.6. By measuring the peaks and troughs for each sample the P/T ratios were calculated for each alginate as shown in Table 3.2. From these P/T ratios the percentage of

Figure 3.5 : Graph of peak/trough ratio against % mannuronic acid

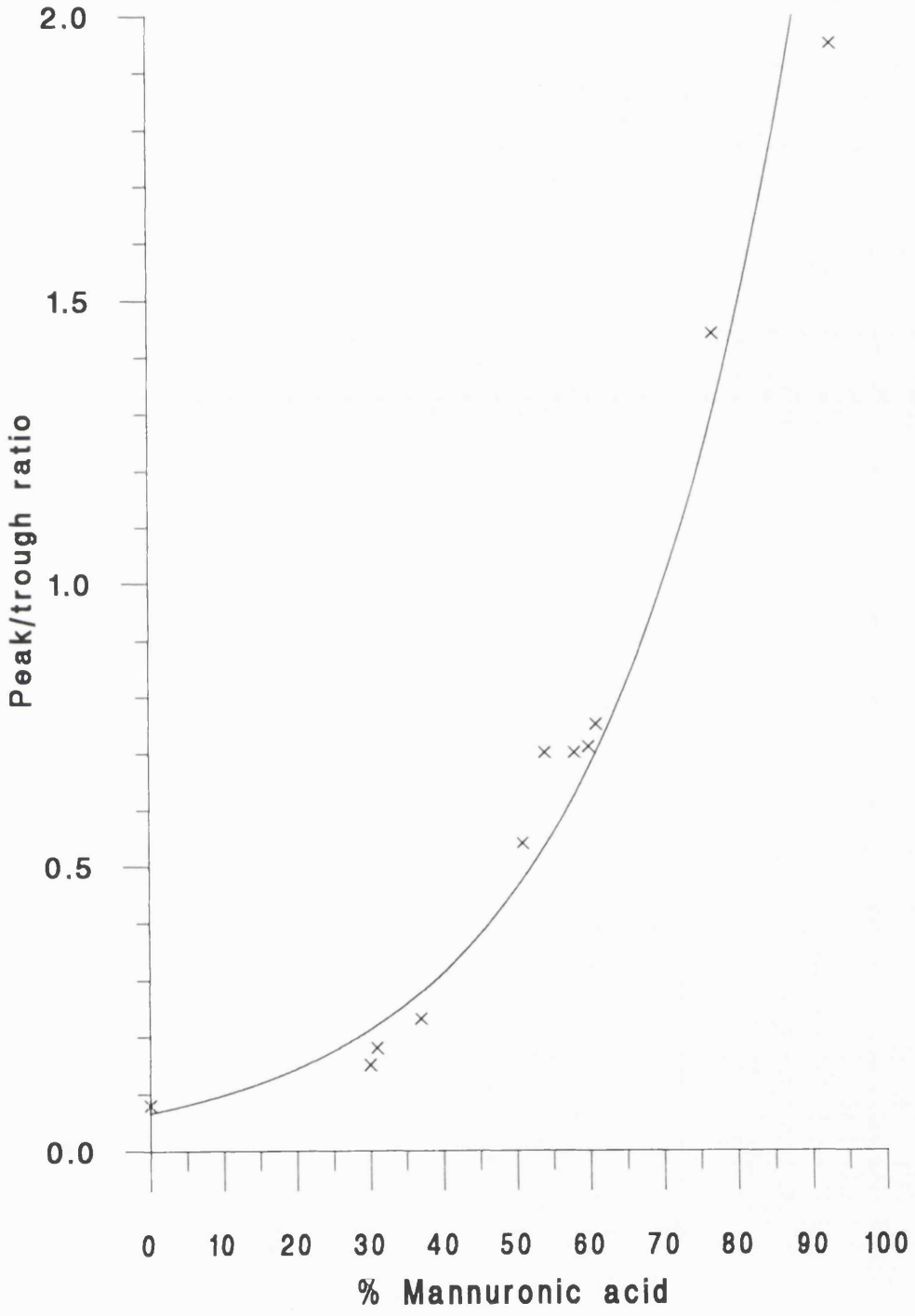

Figure 3.6 : CD spectra for the alginate samples

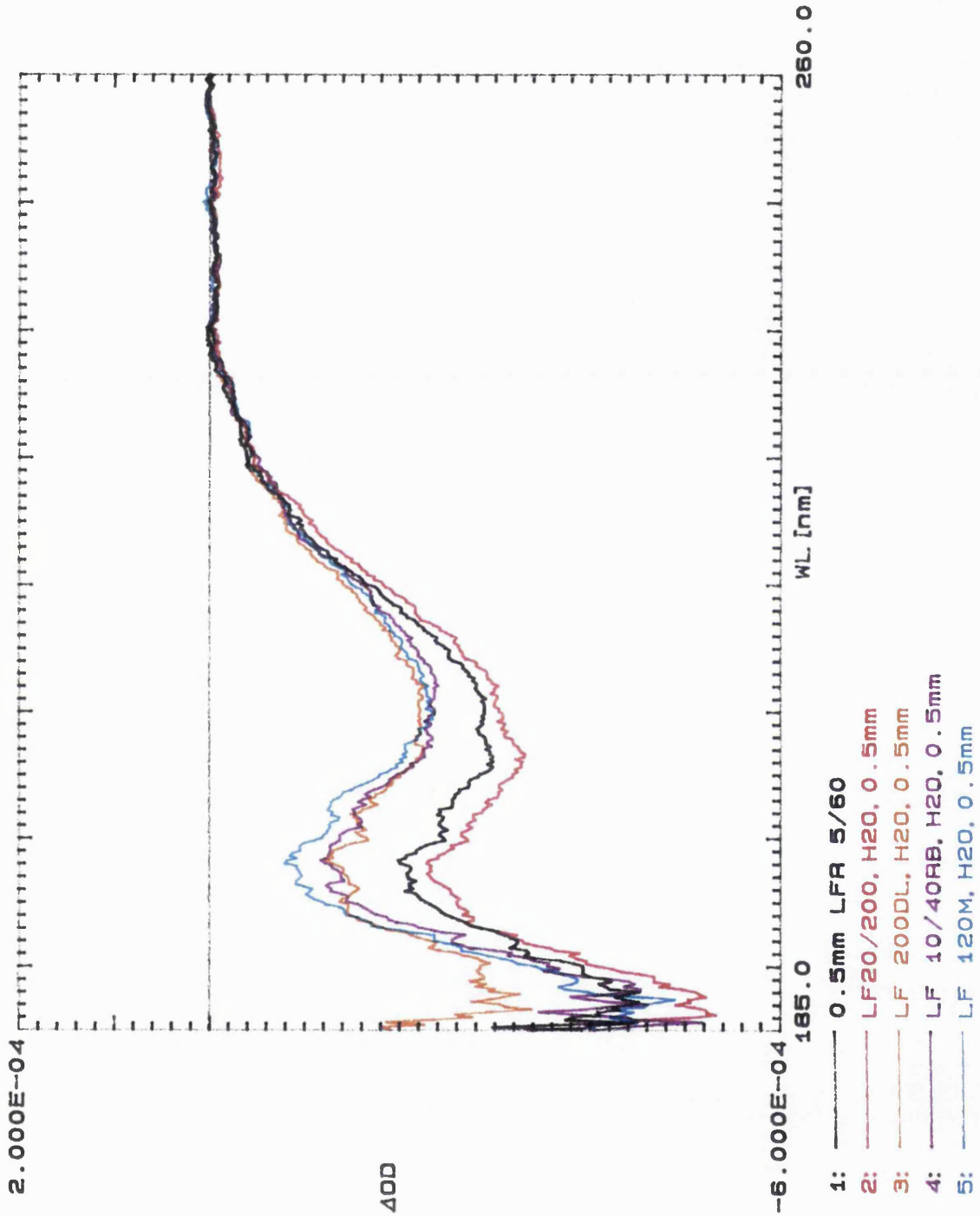

guluronic acid residues present could be found by reference to the graph in Figure 3.5. In order to provide a more accurate measure of the percentage of mannuronic acid present the data given by Morris et al (1975) were plotted and the equation of the curve was used in the calculation of the relative uronic acid contents from the P/T ratios.

The values for guluronic acid content calculated from the CD results are lower than the values found using NMR. The variation was not constant and could possibly have been due to the variation in the viscosity of the solutions affecting the clarity of the solutions. The CD values were in broad agreement with the nominal values given by Protan, although they were generally towards the lower limits quoted.

Table 3.2 : Composition values as determined by CD

Alginate sample	P/T Ratio	% G
LFR 5/60	0.32	59.2
LF 120M	0.62	42.1
LF 10/40RB	0.5	47.7
LF 20/200	0.27	63.6
LF 200DL	0.42	52.2

3.3.4 Discussion

The values obtained for the relative proportions of mannuronic and guluronic acids in the samples investigated are given in Table 3.3 along with the ranges given by the supplier of the raw material. There is good agreement between the two experimental methods used (NMR and CD) in the ranking of the alginates by guluronic acid content. The values obtained by CD are

consistently lower than those found using NMR. The values for %G found using NMR are well within the range given by the manufacturer for the samples, although the values given by CD are towards the lower end or just outside the range given by Protan. Both experimental methods used appear to give a good indication of the guluronic acid content of alginates; whilst NMR has the advantage of giving a wider range of information about the block structure, CD does not require hydrolysis of the sample and is therefore a more straightforward procedure.

Table 3.3 : Comparison of %G values obtained by NMR and CD

Alginate	Nominal range (From Protan)	%G NMR	%G CD
LFR 5/60	65-75	67.2	59.2
LF 120M	35-45	42.2	42.1
LF 10/40RB	45-55	50.9	47.7
LF 20/200	65-75	67.0	63.6
LF 200DL	55-65	55.1	52.2

3.4 RHEOLOGY OF ALGINATE SOLUTIONS

3.4.1 Theory of the rheology of alginates

3.4.1.1 Introduction

The viscosity of alginate solutions is of great importance in many of the practical uses of these polysaccharides as described in Chapter 1.1.2.2. An understanding of the rheological properties are not only important when considering the final use of the product but also in many instances when considering the processing of the material. It is necessary when deciding on

a method for the measurement of the rheological properties of alginates to choose a technique which will allow the investigation of the solution over the concentration range used in the product of interest. This is important because there is no simple relationship between the concentration of an alginate solution and its viscosity. In the present work the rheological properties of the 2.5% solutions were investigated, as this is the concentration to be used in all further work. A range of more dilute solutions were also studied to enable the estimation of the intrinsic viscosity for each of the alginate samples used.

3.4.1.2 General rheology

The viscosity of a fluid is described as its resistance to flow; it was defined quantitatively by Newton who showed that the rate of flow was proportional to the applied stress. The constant of proportionality was termed the coefficient of dynamic viscosity, η, more usually referred to as the viscosity. Fluids which obey this relationship are termed Newtonian fluids and those which deviate from this ideal are known as non-Newtonian. Newton's law can be expressed by Equation 3.5.

$$\eta = \frac{\tau}{D} \qquad \text{Equation 3.5}$$

where: η is the viscosity
τ is the shear stress
D is the rate of shear.

When dealing with a solution it is useful to express the viscosity as the viscosity ratio or relative viscosity as given in Equation 3.6.

$$\eta_r = \frac{\eta}{\eta_o} \qquad \text{Equation 3.6}$$

where: η_r is the relative viscosity
η_o is the viscosity of the solvent.

The specific viscosity (η_{sp}) of a solution is then given by Equation 3.7.

$$\eta_{sp} = \eta_r - 1 \qquad \text{Equation 3.7}$$

When considering a solution such as that formed by dissolving sodium alginate in water, the equation derived by Einstein for colloidal dispersions may be used to relate the viscosity of the solution to the volume fraction of the solute, as given in Equation 3.8.

$$\eta = \eta_o (1 + 2.5\phi) \qquad \text{Equation 3.8}$$

where: ϕ is the volume fraction.

This equation may be rearranged and given in terms of the specific viscosity, by substitution of the terms in Equations 3.6 and 3.7 to give Equation 3.9.

$$\frac{\eta_{sp}}{\phi} = 2.5 \qquad \text{Equation 3.9}$$

Since the volume fraction of the solute is directly related to the concentration the specific viscosity divided by the concentration will be constant. This is termed the viscosity number or reduced viscosity. If the reduced viscosity is determined at a number of concentration it may be plotted against concentration to produce a linear relationship. The intercept of the extrapolation of this line on the y-axis will give the limiting viscosity number or intrinsic viscosity, [η].

The Mark-Houwink equation relates the intrinsic viscosity of polymers to their approximate molecular mass as shown in Equation 3.10.

$$[\eta] = K.M^{\alpha} \qquad \text{Equation 3.10}$$

where: M is the molecular mass

K and α are both constants which relate to the specific polymer-solvent system.

Thus by calculation of the intrinsic viscosity an estimate can be made of the molecular mass of a polymer.

3.4.1.3 The application of rheological measurements to alginates

It has been shown by Donnan and Rose (1950) that the viscosity of alginate solutions is independent of pH within the pH range 6-8. The pH of alginate solutions used falls within this range and were therefore considered to be unaffected by slight differences in pH. The ionic content of the external solution is known to be of importance, since certain divalent cations cause large changes in viscosity by gelation (Smidsrød & Haug, 1965; Haug & Smidsrød, 1965). As discussed in Chapter 1.1.2.2 it has been shown that the anions present in the solution can affect the viscosity (Harkness & Wassermann, 1952). It was therefore necessary to measure the viscosity of not only the alginate solutions alone, but also the solutions containing sodium and potassium bicarbonates as used in the raft forming mixtures. This was performed in order to determine the effect that the addition of the bicarbonates had on the alginate solutions at the concentrations which were to be used in the measurement of the raft characteristics.

In the past viscosity measurements of alginate solutions have been made using a variety of techniques and equipment. The measurements made by Donnan and Rose (1950) were made using an Ostwald viscometer, as were the measurements made by Harkness and Wassermann (1952) in their determinations of intrinsic viscosities of a range of alginate samples. In his investigation of the viscosity of alginate solutions Haug (1958) used both a Wagner-Russell viscometer and a Höppler viscometer to determine the way in which the viscosity of alginate solutions varies with concentration and temperature. The standard method for the determination of the viscosity of alginate solutions used by the raw material manufacturers employs a Brookfield rotational viscometer, although other similar viscometers are also used. The viscosity of an alginate is dependent on the rate of shear, hence the values obtained for the viscosity by various techniques will not necessarily be consistent; the values should therefore be extrapolated to zero rate of shear for comparative purposes.

As well as measuring the alginate solutions at the concentration to be used in other work, measurements were also made of more dilute solutions. This enables the estimation of the intrinsic viscosity of the sample, which is related to the volume and shape occupied by the molecules in the solution. The intrinsic viscosity is not only affected by the molecular weight of the alginate but it is also influenced by the flexibility of the polymer chains. The flexibility of the chains is determined by the chemical composition (i.e. the block structure) since parts of the chains containing predominantly G blocks are less flexible than those containing predominantly M blocks which are in turn stiffer than areas of roughly alternating M and G (Smidsrød et al, 1973). Donnan and Rose (1950) gave an approximate relationship between the intrinsic viscosity of alginates and the degree of polymerisation based on the Mark-Houwink relationship given in Equation 3.10. This relationship, given in Equation 3.11, should only be regarded as an approximation of the degree of polymerisation as the equation does not take into account the M/G ratio or block structure of the alginate.

$$\frac{D.P.}{[\eta]} = 58 \qquad \text{Equation 3.11}$$

where: $D.P.$ is the degree of polymerisation.

This enables the calculation of the approximate mean degree of polymerisation for each of the alginate samples. Since the degree of polymerisation is related to the molecular weight of a polymer it is possible to give an estimate of the molecular weight of the alginate samples. This is achieved by multiplying the degree of polymerisation by 193, the molecular mass of a single uronic acid unit. The measurement of molecular mass of alginates is difficult and imprecise, hence this method is a useful working tool.

The method chosen for the measurement of viscosity of the alginate solutions in the present work was using a Carri-med CSL500 controlled stress rheometer. The machine configuration used was a cone and plate measuring system set up to measure flow curves. The cone and plate measuring system consists of

a flat metal plate with a wide angle cone above it. The cone is attached directly to the air bearing of the rheometer, which is programmed to carry out a steady increase in the stress applied to the sample via the torque exerted on it from the cone. The angular velocity produced is recorded by the computer and from this the viscosity can be calculated by the use of Equation 3.12 below:

$$\eta = \frac{3\omega T}{2\pi r^3 \alpha} \qquad \text{Equation 3.12}$$

where: η is the viscosity

ω is the angular velocity

T is the applied torque

r is the radius of the cone

α is the radius between the cone and plate.

The intrinsic viscosity of a polymer solution can be determined as described in Chapter 3.4.1.2. This relationship was used by Donnan and Rose (1950) and Haug and Smidsrød (1962) and developed for use with alginates. The intrinsic viscosity has been defined by Equation 3.13, and by plotting either of the terms against concentration it is possible to extrapolate the line to zero and estimate the intrinsic viscosity of the solution.

$$[\eta] \equiv \lim_{c \to 0} \left(\frac{\eta_r - 1}{C}\right) \equiv \lim_{c \to 0} \left(\frac{\ln \eta_r}{C}\right) \qquad \text{Equation 3.13}$$

where: $[\eta]$ is the intrinsic viscosity

η_r is the viscosity of the solution relative to the solvent

C is the concentration in g/100ml.

The viscosity values for the 2.5% solutions can also be used by direct comparison with other solutions to investigate the effect that the addition of bicarbonates and pectin have on the alginate solutions.

3.4.2 Method

Flow rheology measurements were made on the alginate solutions using a Carrimed CSL500 controlled stress rheometer (version 5.0). The alginate solutions were prepared as described in Chapter 2.2.1. In order to be able to estimate the intrinsic viscosities of the alginates a range of concentrations was used from 2.5% w/v (the same concentration used in the raft forming mixtures) to 0.5% w/v. The effect of the addition of sodium or potassium bicarbonate was investigated at an alginate concentration of 2.5% w/v. These solutions were prepared by dissolving the bicarbonate in the deionised water before the addition of the required quantity of alginate.

The rheometer was used with a cone and plate measuring geometry; the cone had a diameter of 4.0cm and a cone angle of 2°. The temperature of the plates was maintained at 20°C using the Peltier temperature control system housed in the rheometer. This was done to minimise any evaporation from the sample which may occur during the course of the experiment. A sample of approximately 0.6ml was placed on the bottom plate using a syringe. After raising the ram the edges of the sample were examined to ensure that the sample was correctly loaded (see Figure 3.7). Incorrect loading of the sample could lead to inaccuracies in measurement due to edge effects. Each solution was measured at least three times with the plates being cleaned and fresh sample loaded each time. For each of the 2.5% w/v samples, including those with pectin and bicarbonates, the strain was measured as the sample was subjected to a stress increasing from $0Nm^{-2}$ to $15Nm^{-2}$ in 2 minutes. The sample was then held at $15Nm^{-2}$ for 30 seconds before the stress was decreased at the same rate. This was carried out at least three times, using a fresh sample for each run. The measurements made for the calculation of intrinsic viscosity were only made during the ascent portion of the run, i.e. as the stress increased from $0Nm^{-2}$ to $15Nm^{-2}$. A curve fit of the rheogram was performed by the software to compare it with known mathematical models of flow rheology.

Figure 3.7 : Diagram of a cone and plate

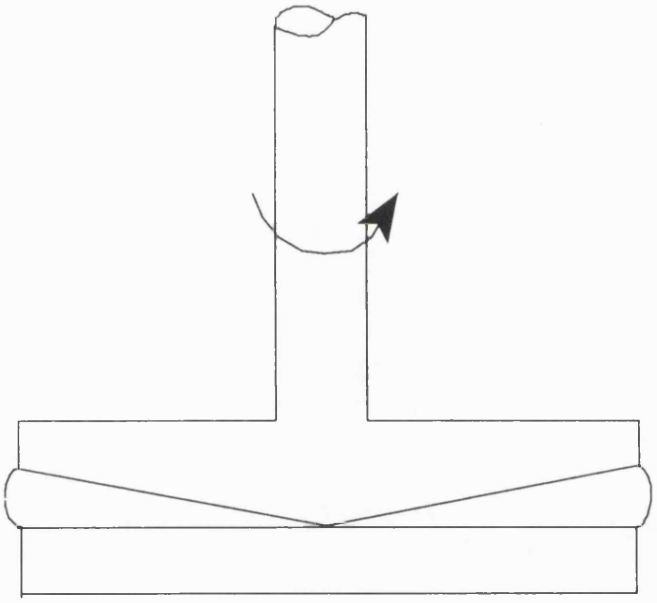

3.4.3 Results

The flow curves for the alginates investigated here, under the conditions given in the method used, show little deviation from Newtonian flow. The curve fit used to calculate the viscosity from the flow curves was therefore the Newtonian model.

3.4.3.1 Intrinsic viscosity

The mean values for the viscosity, the relative viscosity and the specific viscosity of each solution used are given in Table 3.4 along with the parameters to be plotted as described in Chapter 3.4.1.2. The values of η_{sp}/C and ln η_r/C given in Table 3.4 were plotted against concentration as shown in Figure 3.8. The intrinsic viscosity for each of the samples was calculated from the intercepts of the graphs shown in Figure 3.8.

Table 3.4(a) : Mean viscosity values for LFR 5/60 used in calculation of intrinsic viscosity

Concentration (g/100ml)	η (Nm^2)	η_r	η_{sp}	η_{sp}/C (100ml/g)	ln η_r/C (100ml/g)
2.5	0.01341	3.283	2.283	0.9134	0.4755
2.0	0.01082	2.649	1.649	0.8247	0.4871
1.5	0.00749	1.836	0.836	0.5571	0.4051
1.0	0.00563	1.380	0.380	0.380	0.3221
0.5	0.00474	1.161	0.161	0.322	0.2986

Figure 3.8 : Graph used for the calculation of intrinsic viscosity

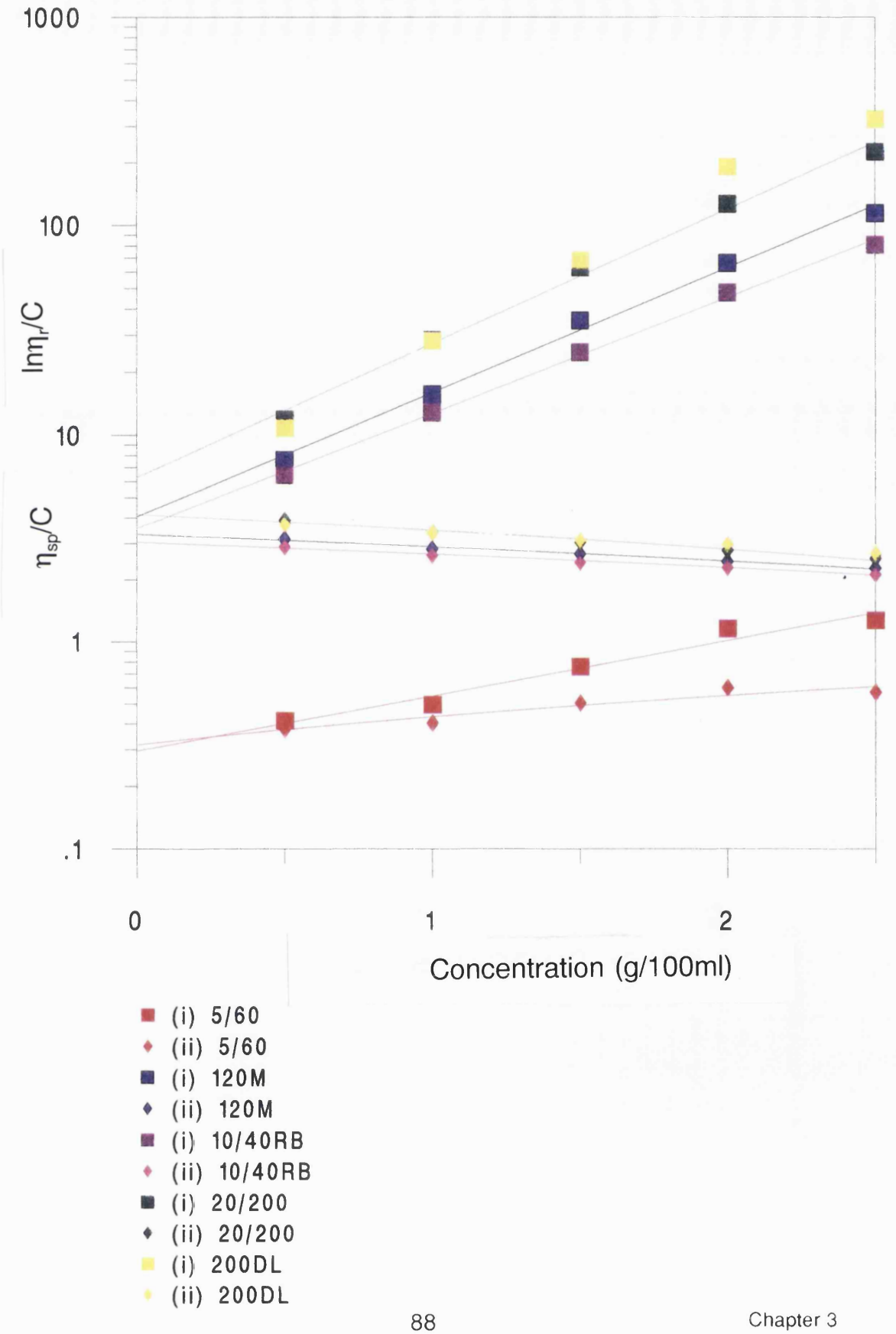

Table 3.4(b) : Mean viscosity values for LF 120M used in calculation of intrinsic viscosity

Concentration (g/100ml)	η (Nm^2)	η_r	η_{sp}	η_{sp}/C (100ml/g)	$\ln \eta_r/C$ (100ml/g)
2.5	0.8709	213.2	212.2	84.90	2.145
2.0	0.4002	97.99	96.99	48.49	2.292
1.5	0.1606	39.32	38.39	25.55	2.448
1.0	0.0507	12.42	11.42	11.42	2.519
0.5	0.0153	3.744	2.744	5.488	2.640

Table 3.4(c) : Mean viscosity values for LF 10/40RB used in calculation of intrinsic viscosity

Concentration (g/100ml)	η (Nm^2)	η_r	η_{sp}	η_{sp}/C (100ml/g)	$\ln \eta_r/C$ (100ml/g)
2.5	0.6080	148.9	147.9	59.15	2.001
2.0	0.2881	70.54	69.54	34.77	2.128
1.5	0.1145	28.04	27.04	18.02	2.222
1.0	0.0420	10.03	9.280	9.280	2.305
0.5	0.0135	3.309	2.309	4.617	2.393

Table 3.4(d) : Mean viscosity values for LF 20/200 used in calculation of intrinsic viscosity

Concentration (g/100ml)	η (Nm^2)	η_r	η_{sp}	η_{sp}/C (100ml/g)	$\ln \eta_r/C$ (100ml/g)
2.5	1.660	406.5	405.5	162.2	2.403
2.0	0.7542	184.7	183.7	91.84	2.609
1.5	0.2840	69.54	68.54	45.69	2.828
1.0	0.0886	21.70	20.70	20.70	3.077
0.5	0.0219	5.357	4.357	8.715	3.357

Table 3.4(e) : Mean viscosity values for LF 200DL used in calculation of intrinsic viscosity

Concentration (g/100ml)	η (Nm^2)	η_r	η_{sp}	η_{sp}/C (100ml/g)	$\ln \eta_r/C$ (100ml/g)
2.5	2.432	595.5	594.5	237.8	2.556
2.0	1.162	284.5	283.5	141.8	2.825
1.5	0.318	77.89	76.89	51.26	2.904
1.0	0.0912	22.33	21.33	21.33	3.106
0.5	0.0206	5.056	4.056	8.113	3.241

Table 3.5 shows the intrinsic viscosity of each of the alginate samples along with the degree of polymerisation for each sample calculated from the intrinsic viscosities and an estimation of the molecular weight of each alginate as described in Chapter 3.4.1.3.

Table 3.5 : Intrinsic viscosity of alginate samples

Alginate	%G (from NMR)	$[\eta]$ (100ml/g)	Mean D.P. (approx)	Mol. wt. (approx)
LFR 5/60	67.2	0.238	14	2,700
LF 120M	42.4	2.836	165	32,000
LF 10/40RB	50.9	2.515	145	28,000
LF 20/200	67.0	4.079	240	46,000
LF 200DL	55.1	3.561	205	39,000

3.4.3.2 The effect of the addition of sodium/potassium bicarbonates

Table 3.6 shows the viscosities of 2.5% alginate solutions alone and with the addition of sodium bicarbonate or potassium bicarbonate. The viscosities quoted are the means of three samples calculated from the up curves of the rheograms as shown in Figure 3.9. The stress on each sample increased from 0 to 15Nm^{-2} over the period of two minutes.

3.4.3.3 The effect of the inclusion of pectin

Figure 3.10 shows a rheogram of the effect of the addition of sodium and potassium bicarbonate to a 2.5% solution of LFR 5/60. The effect of the inclusion of pectin in the solution is shown in Table 3.7 which gives the viscosities of the solutions of the LFR 5/60 with and without pectin. The

Figure 3.9 : Rheograms showing the effect of the alginate used

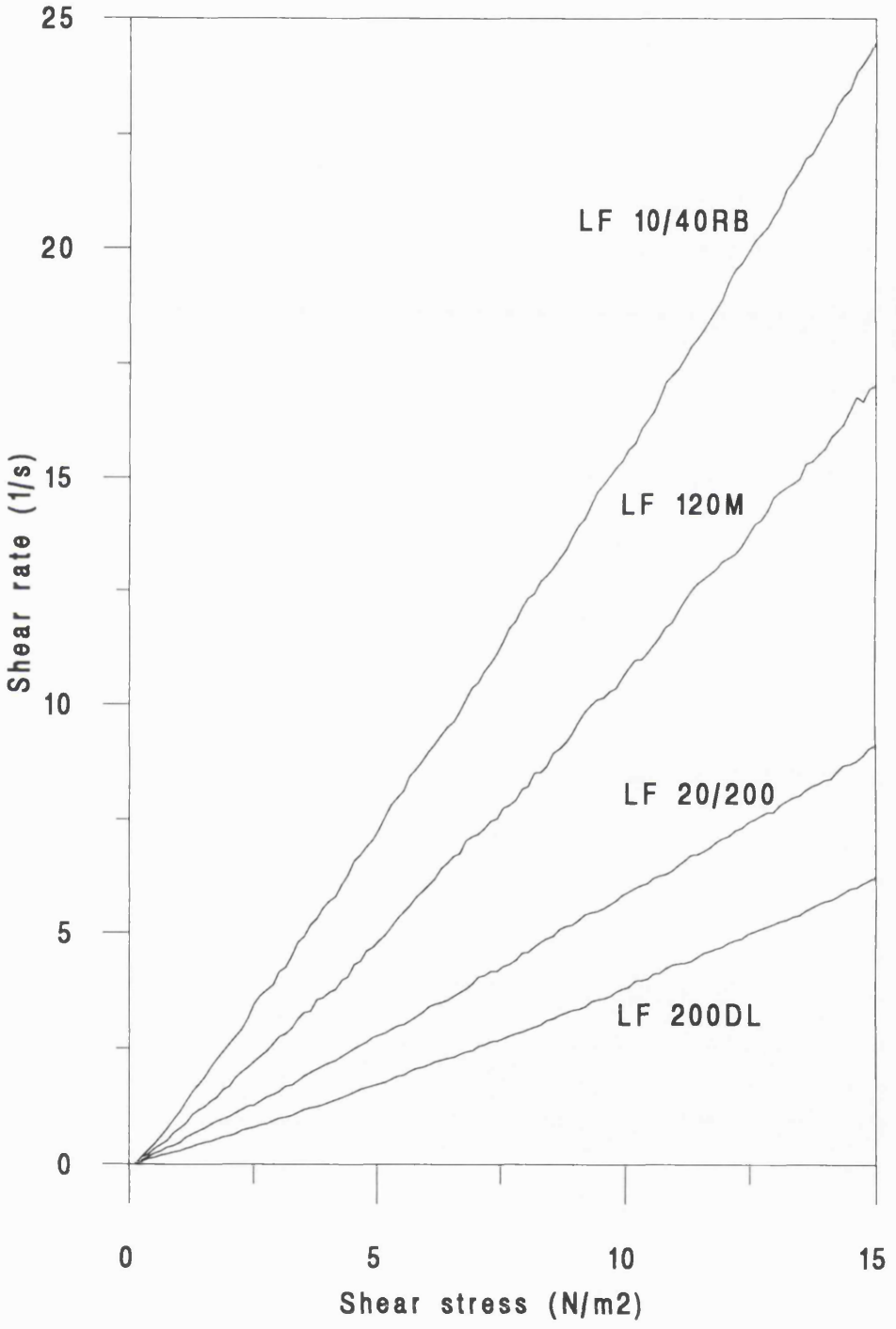

Figure 3.10 : Rheograms of LFR 5/60 solutions with added bicarbonates

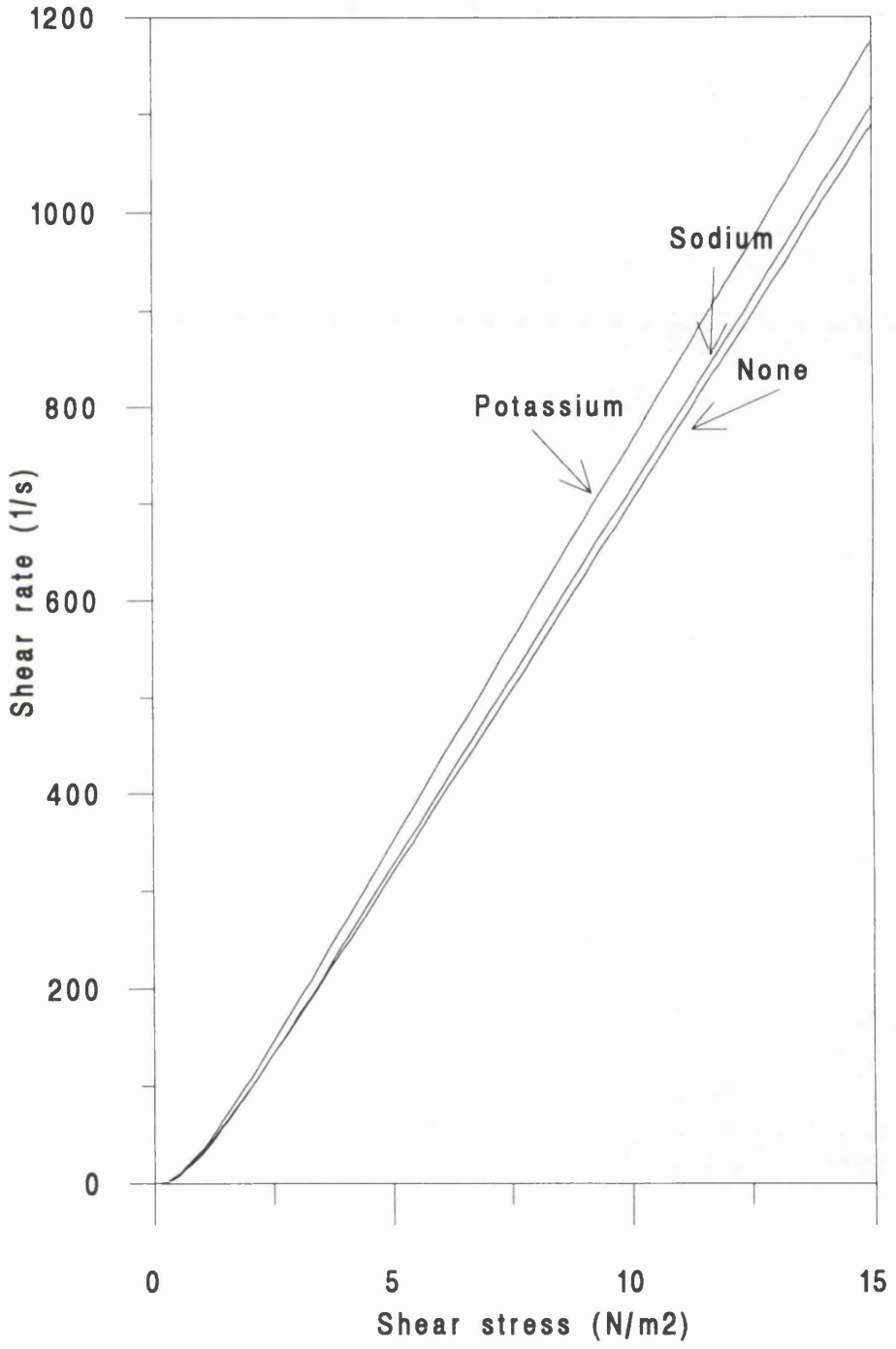

Figure 3.11 : Rheograms of LFR 5/60 and pectin mixtures with added bicarbonates

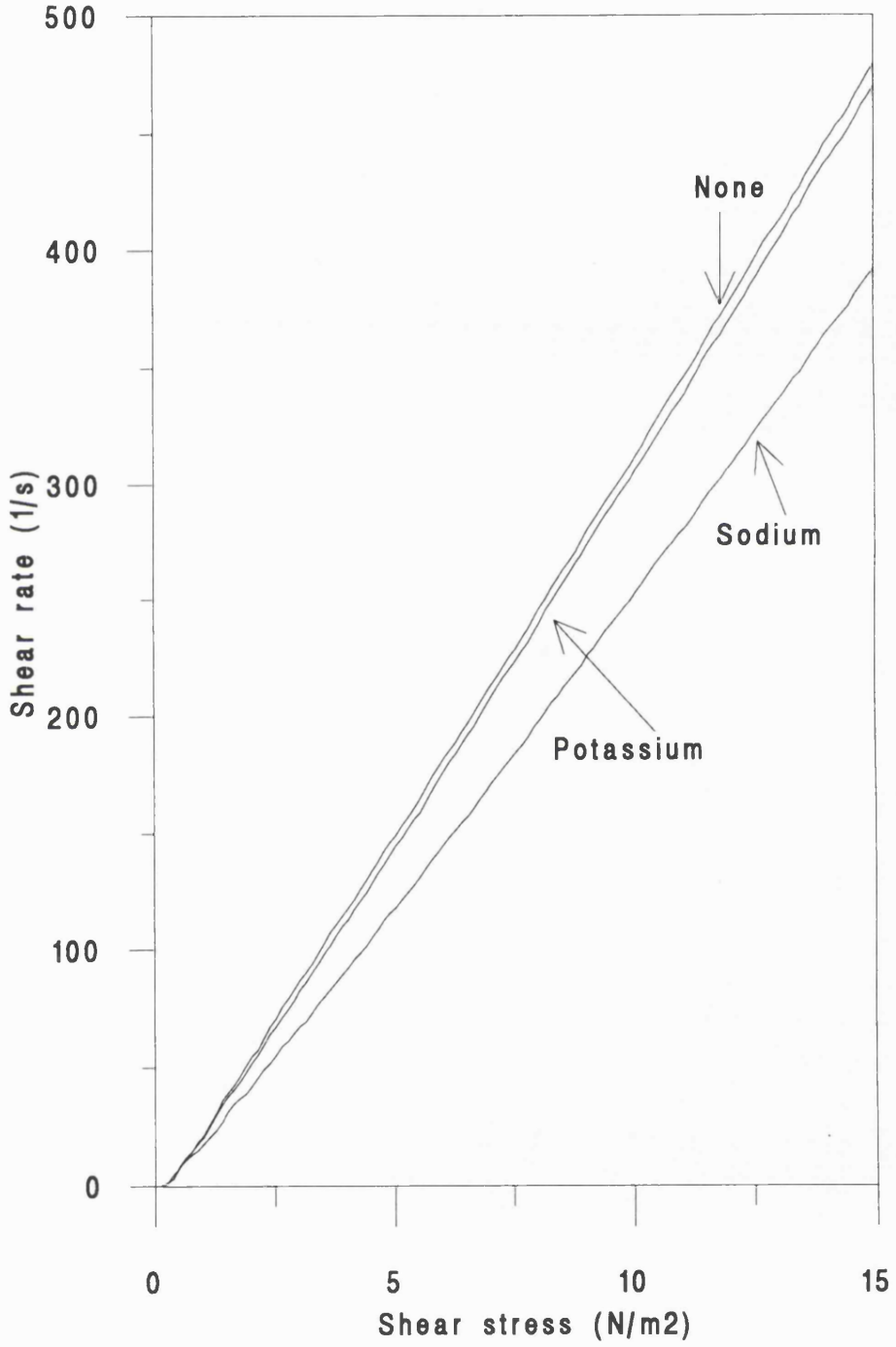

rheograms for the solutions containing pectin both with and without bicarbonates are given in Figure 3.11.

Table 3.6 : Viscosity of 2.5% alginate solutions.

	Viscosity (Pa.s) ± s.d		
Alginate	No bicarbonate	$NaHCO_3$	$KHCO_3$
LFR 5/60	$0.01351 \pm 2.8\times10^{-4}$	$0.01306 \pm 1.8\times10^{-4}$	$0.01221 \pm 7.5\times10^{-5}$
LF 120M	$0.8709 \pm 7.0\times10^{-3}$	$1.069 \pm 6.9\times10^{-3}$	0.9426 ± 0.012
LF 10/40RB	$0.6080 \pm 4.5\times10^{-3}$	1.108 ± 0.042	0.4914 ± 0.013
LF 20/200	1.660 ± 0.022	1.902 ± 0.043	1.889 ± 0.022
LF 200DL	2.432 ± 0.052	2.663 ± 0.073	2.205 ± 0.062

Table 3.7 : The effect of pectin on the viscosity of LFR 5/60 solutions.

	Viscosity (Pa.s)		
Solution	No bicarbonate	$NaHCO_3$	$KHCO_3$
LFR 5/60	$0.01351 \pm 2.8\times10^{-4}$	$0.01306 \pm 1.8\times10^{-4}$	$0.01221 \pm 7.5\times10^{-5}$
LFR 5/60 + pectin	$0.03119 \pm 2.5\times10^{-4}$	$0.03717 \pm 5.7\times10^{-4}$	$0.03155 \pm 1.1\times10^{-3}$

3.4.4 Discussion

The intrinsic viscosities calculated show that viscosity of alginate solutions can not be simply linked to the chemical composition of the polysaccharide as both the molecular weight and the block structure of the alginate have an effect. The alginate LFR 5/60 has a very low D.P. and hence a lower molecular weight than the other samples. This may be explained by the fact that commercial

grades of alginates can be altered by processing to change the degree of polymerisation. This means that the product is more easily soluble and has a low viscosity in water.

The viscosity values of the 2.5% solutions with the bicarbonates give useful indications of the behaviour of the raft forming mixtures before the introduction of acid. There seems to be no real pattern to the behaviour of the solutions with potassium bicarbonate added, although sodium bicarbonate does increase the viscosity of all the solutions slightly with the exception of LFR 5/60. The alginate most affected by the addition of either sodium or potassium bicarbonate is the LF 10/40RB solution. From the NMR results given in Chapter 3.2.3 the alginate LF 10/40RB seems to have the greatest proportion of alternating mannuronic and guluronic acid residues hence this may be of relevance to the effect of the bicarbonates on the viscosity of the solution.

The results of the inclusion of pectin in the LFR 5/60 solutions showed that pectin increases the viscosity both in the presence and absence of a bicarbonate. The increase in viscosity is greatest in the solution with sodium bicarbonate and smallest in the solution containing no added ions.

Clearly there are a number of parameters that must be considered when characterising alginates, including M/G ratio, block structure, molecular weight and degree of polymerisation. The structural and rheological information outlined here will be useful in the explanation of the behaviour of the raft forming systems particularly in the gelation and bubble formation stages of raft formation.

CHAPTER 4

CHAPTER 4: CHARACTERISATION OF ALGINATES GELS

4.1 INTRODUCTION

The property of alginates most exploited in both the food and pharmaceutical industries is the ability to form gels. There are two conditions under which alginates undergo gelation; the first is the presence of divalent cations and the second is the acidification of the surrounding media. Both these conditions are of relevance to the formation of alginate rafts which rely on a low pH in the stomach to promote the formation of a precipitous gel, while formation may also be aided by the presence of divalent ions in the formulation.

In solution the flexibility of alginate molecules and hence the rheological properties are affected by the M/G ratio and the block structure of the alginate; the blocks may be ranked, MG<MM<GG, in order of increasing inflexibility. Light scattering studies (Smidsrød et al, 1973) showed that the relative dimensions of the blocks were in the same rank order. This was explained by hindrance of rotation around the glycosidic linkages. This and other factors affecting the viscosity of alginate solutions are discussed in Chapter 1.1.2.2. In the presence of certain cations the composition and block structure of the alginate has a greater importance in determining the properties of the gel formed than the molecular size.

4.1.1 Gelation of alginates induced by acid

The gelation of alginates by the action of acid has been less well documented than the gelation with cations. However, Haug and Larsen (1963) showed the important effect of the intrinsic viscosity of the solution on the solubility at a low pH. The effect was that alginates with lower intrinsic viscosities gave a smaller volume of gelatinous precipitate when the pH was decreased than those with higher intrinsic viscosities. It was also noted that the gelation was affected by the composition of the alginate. This was attributed to the differences in the

dissociation constants of mannuronic and guluronic acids. Haug (1961) calculated dissociation constants for various samples of alginic acid and for mannuronic and guluronic acids concluding that the composition of an alginate determines the overall dissociation constant. The values for the dissociation constants obtained for mannuronic and guluronic acid were found to be 3.38 and 3.65 respectively.

4.1.2 Gelation of alginates induced by cations

Haug (1959) showed that there are differences in the ion exchange properties between alginates from various sources and that this can be explained by variations in the relative amounts of mannuronic and guluronic acid residues present in the molecule. The dependence of the ion exchange properties of alginates on the uronic acid composition of the molecules was further investigated by Smidsrød and Haug (1968). To describe the affinity the two different uronic acid residues have for various cations they ascribed selectivity coefficients to the two monomers present, and calculated these parameters for a number of ion exchange reactions. They also showed differences in selectivity between alginate samples of different uronic acid composition.

The gelation of alginates with cations is not only affected by the composition of the alginate but also by the ions present and the concentrations of ions and alginate in the mixture. Smidsrød and Haug (1965) showed that the affinity of alginates for calcium increases with an increasing proportion of guluronic acid residues in the alginate. The amount of sodium ions present was also shown to affect the gelation of alginates with calcium. Sodium was initially present in the solution from the use of sodium alginate in the preparation and the amount was altered during the course of the experiments. Less calcium was required to give a gel of maximum viscosity at low sodium concentrations, whereas at higher sodium concentrations the amount of calcium required was increased. This is attributed to the displacement of the ion exchange equilibrium between the soluble sodium alginate and calcium alginate gel in an unfavourable

direction for gelation.

The effects of different divalent ions on the properties of alginate solutions was investigated by Haug and Smidsrød (1965) who showed a rank order of the concentrations of the ions needed to bring about gelation. The concentration of the ion required depended on the affinity of that metal for the alginate and the gel forming ability of the ion. Since it has been shown that the affinity of alginates for divalent ions is to some extent dependent on the uronic acid composition of the alginate (Smidsrød and Haug, 1968) it is reasonable to expect that the gelation properties will be affected by the composition of the alginate. The rank order of divalent ions given by Haug and Smidsrød (1965) therefore holds for most samples, although they noted that for some alginate samples there were small changes in the order of the ions. The rank order which was given for the concentration of the metallic ion required to bring about gel formation was: Ba<Pb<Cu<Sr<Cd<Ca<Zn<Ni<Co<Mn<Mg.

Kohn et al (1968) investigated the binding of calcium to some polyuronides and monouronates. They showed that calcium ions did not bind to the monouronates, indicating that the binding of calcium, and probably other divalent ions, is a property of the polymeric nature of alginates. The binding of calcium to polyguluronate and polygalacturonate (derived from pectin) was much stronger than binding to polymannuronate. The differences observed between alginates of different compositions may be caused by differences in the steric arrangement of the groups active in binding in the polymer chain. The properties of poly(1,4 hexuronate) gels with different chemical compositions were investigated by Smidsrød and Haug (1972). These gels included alginates from various sources and pectin. It was shown that the mechanical properties of alginate gels formed by the presence of divalent ions are affected by both the overall chemical composition of the alginate (the M/G ratio) and to some extent by the sequence of the uronic acid residues in the chain. The guluronate residues were again shown to be responsible for gel formation in alginates, and the gelation of poly(L-guluronate) was shown to resemble that

of calcium pectate. It was shown by Smidsrød (1974) that the modulus of rigidity for GG blocks, MM blocks and pectic acid with four divalent ions showed a clear correlation with the ability of the polyuronate to bind those ions.

Smidsrød (1974) described some of the physical properties of alginate gels in terms of their molecular structure. The gels investigated were formed by dialysis of sodium alginate solutions against solutions of divalent cations. It was suggested that the blocks comprising solely of guluronic acid residues, which have a higher affinity for ions such as calcium than other blocks, are associated with a form of regular packing of the polysaccharide chains in the gel form. This regular packing was described by Grant et al (1973) as an egg-box model.

4.1.3 Mechanical properties of gels

The method used for the determination of the mechanical properties of the alginate gels by the workers at the Norwegian Institute of Seaweed Research was described by Smidsrød et al (1972). It involved the formation of gel cylinders by dialysis of sodium alginate solution against aqueous solutions of the ions under investigation. These cylinders were sectioned and the mechanical properties determined by compression at a constant rate in an Instron TTK Universal Testing Machine. In certain cases the testing was carried out with the sample submerged in the ionic solution in order to minimise evaporation of water from the gel samples. This method involved the application of a linear stress to the sample and the measurement of the deformation caused by the compression. It was concluded that this method was only fairly accurate and that it did not give a description of all the mechanical properties of the gels which were of interest. It would therefore be of considerable interest to use a more sophisticated rheological technique for the measurement of alginate gels.

Investigations of similar gel systems have been carried out using dynamic

mechanical analysis. For example Watase and Nishinari (1993) investigated the rheological properties of pectin-water gels under various conditions. Dynamic mechanical analysis has been widely exploited as a technique for materials characterisation in the polymer sciences, and has been shown to have a range of applications to pharmaceutical systems (Craig & Johnson, 1995). Polysaccharides such as dextran, pullulan and amylose have been investigated in combination with thermogravimetric analysis by Scandola et al (1991) to establish patterns of water loss by the samples and the effect this has on the mechanical properties of the system. Water loss can be an undesirable feature of many rheological investigations of high water content gels. Bao and Bagga (1993) reported how water loss from hydrogels could be overcome by fitting an internal liquid bath to the dynamic mechanical analyser. In the present work an internal water bath was specially designed for a Perkin Elmer DMA 7 in order to investigate the mechanical properties of high water content alginate gels of varying compositions.

4.2 THEORY OF DMA

Dynamic mechanical testing has been shown to be useful in the characterisation of viscoelastic materials, particularly in the areas of plastics and polymer research. There is a variety of equipment available for the measurement of dynamic mechanical properties which can be distinguished from standard rheological techniques by the fact that the sample is subjected to an oscillating force. The response of the sample may be measured as a function of the magnitude and frequency of the applied force; the behaviour of the sample can also be measured with respect to time and temperature.

When a perfectly elastic solid is subjected to an applied force the behaviour is described by Hooke's law. This law says that the resultant strain produced is directly proportional to the applied stress, where the constant of proportionality is Young's modulus as shown in Equation 4.1.

$$E = \frac{stress}{strain}$$ Equation 4.1

where: E is Young's modulus.

This is often thought of as being analogous to a loaded spring where the extension produced in the spring is directly proportional to the applied weight on the spring. The assumption made with a perfectly elastic solid is that the response to the stress is instantaneous, hence the behaviour of the sample is not dependent on time.

When considering the response of a perfectly Newtonian liquid to an applied stress the liquid will flow rather than deform instantaneously as described in Chapter 3.4.1.2. This time dependence of the response means that the rate of strain is proportional to the applied stress. In this case the proportionality constant is the viscosity of the liquid.

4.2.1 Stress scans

The majority of materials do not behave either as perfectly elastic solids or as perfectly Newtonian liquids, but deviate from this behaviour in a number of ways. A sample may exhibit stress anomalies where there is a non-linear relationship between stress and strain, or rate of strain. The sample may also show the dependence of stress on both the strain and rate of strain; these are time anomalies. Materials which deform with time and show both solid and liquid characteristics are known as viscoelastic. When an increasing stress is applied to a viscoelastic material the sample will show time anomalies but not stress anomalies up to a specific value of stress, the linear viscoelastic limit. Below this limit, in the linear viscoelastic region, the proportionality between stress and strain is constant, although the strain may vary with time. Studying the behaviour of materials within the linear viscoelastic region means the interpretation of results is simplified and more useful comparative data may be

obtained than by working outside the linear region.

It is important when studying viscoelastic materials either with static or dynamic methods to ensure that the stress applied does not exceed the linear viscoelastic limit for the sample. This can be done by subjecting the sample to a linearly increasing stress and recording the strain produced. This is the stress scan which can be used to determine appropriate values of stress to be used in other experiments.

4.2.2 Creep-recovery

The time dependence of samples is often investigated by creep recovery testing. This method, as described by Ferry (1961), involves applying an instantaneous stress to the sample and holding the sample under this stress for a predetermined period of time before the stress is removed. The response of the sample to this stress and the recovery phase is measured and from this the compliance of the sample can be calculated. The compliance at any time during the test is the measured strain divided by the applied stress. Figure 4.1 shows a typical compliance-time curve for a polymer. It can be divided into six principal regions as shown.

The first region of interest is that denoted J_o in Figure 4.1, which is a region of instantaneous compliance. In this area bonds between the molecules are stretched elastically and if the stress were removed in this region the sample would recover completely. The instantaneous compliance can be described mathematically be Equation 4.2.

$$J_o = \frac{\varepsilon_o(t)}{\sigma} \qquad \text{Equation 4.2}$$

where: J_o is the instantaneous compliance
$\varepsilon_o(t)$ is the instantaneous strain
σ is the applied stress.

Figure 4.1 : A typical creep compliance-time curve

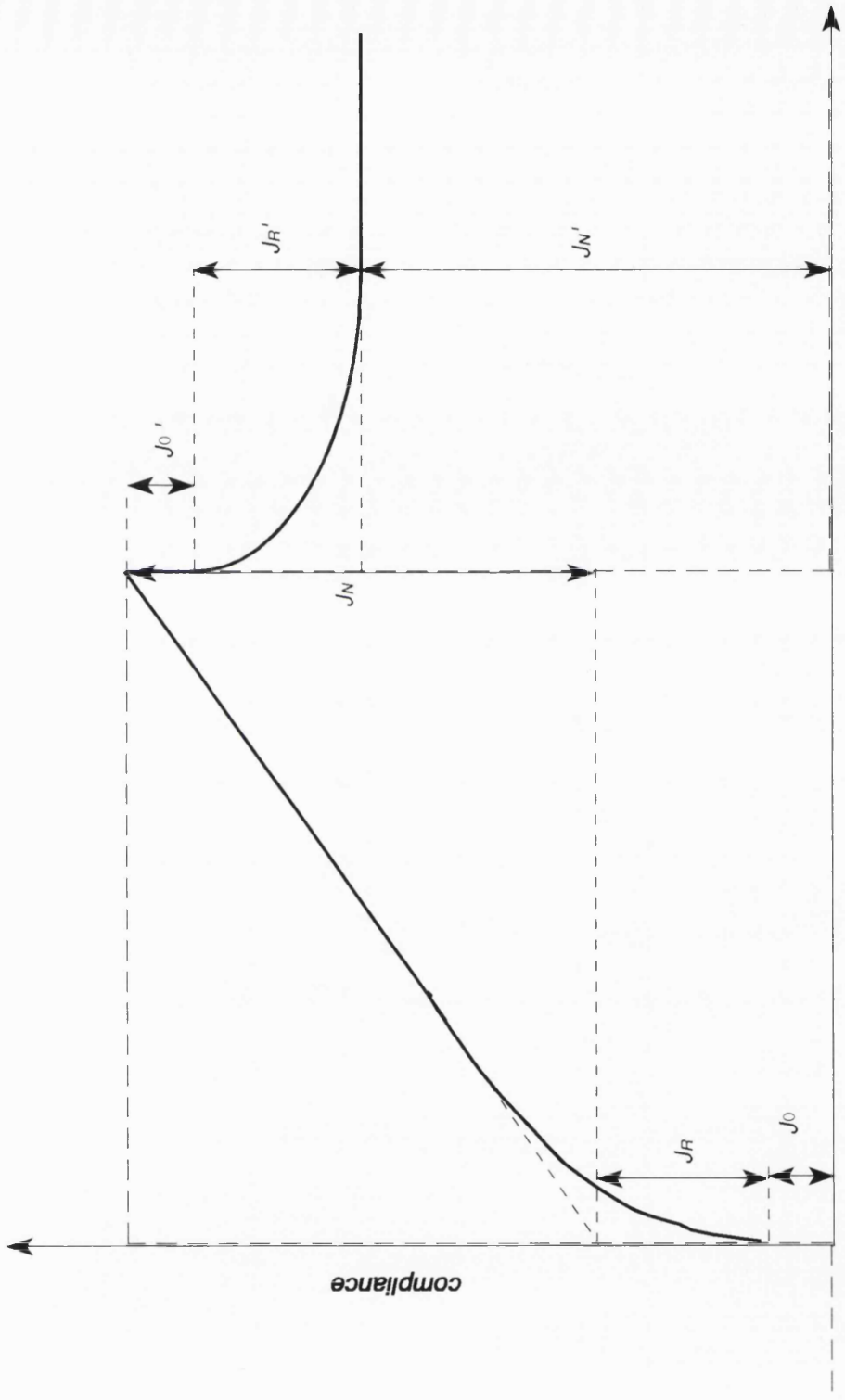

The second section of interest in the creep compliance curve is the time dependent retarded elastic region, with a compliance J_R. In this region the bonds between the molecules are breaking and reforming. However not all the bonds break and reform at the same rate, the weaker bonds breaking at lower values of t than the stronger ones. The simplest mathematical expression for the compliance in this region is given in Equation 4.3, in terms of the mean compliance and mean retardation time for the bonds involved. An expanded form of this relationship may be used which is based on the distribution of bond strengths, rather than the mean values.

$$J_R = J_m \left[1 - \exp\left(\frac{-t}{\tau_m}\right)\right] \qquad \text{Equation 4.3}$$

where: J_R is the retarded creep compliance

J_m is the mean compliance of the bonds

τ_m is the mean retardation time.

The third region of note in Figure 4.1 is the linear region of Newtonian compliance, J_N. At this stage of the test the time taken for the bonds to reform is longer than the period of the experiment, thus the alginate molecules tend to flow past one another. The Newtonian compliance is related to the viscosity as shown in Equation 4.4.

$$J_N = \frac{t}{\eta_N} \qquad \text{Equation 4.4}$$

where: J_N is the Newtonian compliance

η_N is the Newtonian viscosity.

When the stress is removed from the sample the recovery follows a similar pattern to the creep compliance. There is an instantaneous elastic recovery, the region marked J_o' in Figure 4.1. This is followed by the retarded elastic recovery, where the compliance is denoted by J_R', and should be equivalent to

the retarded creep compliance. The final portion of Figure 4.1 is shown as J_N' which is equivalent to the Newtonian compliance as shown in Equation 4.4. This region represents the structure which is not recovered due to the bonds which were broken in the region of Newtonian creep compliance.

4.2.3 Frequency scans

The behaviour of a sample under the conditions of creep recovery can be considered as a single oscillation in a dynamic test with a very low frequency, square wave form stress loading pattern. It is more usual in dynamic mechanical measurement techniques to use a sinusoidal wave form of a particular frequency to stress the sample. The strain at any time on the sample varies with time according to Equation 4.5.

$$\varepsilon = \varepsilon_o \cos \omega t \qquad \text{Equation 4.5}$$

where: ε is the strain
ε_o is the maximum amplitude of the strain
ω is the angular frequency and
t is the time.

If the sample subjected to this type of varying strain was a perfectly elastic solid obeying Hooke's law, the stress would vary in a similar manner, as shown in Equation 4.6.

$$\sigma = \sigma_o \cos \omega t \qquad \text{Equation 4.6}$$

where: σ is the stress
σ_o is the maximum amplitude of the stress

For viscoelastic materials, however, the strain is not produced instantaneously when a stress is applied to the sample, as shown in Figure 4.2. The damping of the system means that the stress cycle will lead the strain cycle by a phase angle, δ, thus the stress for a viscoelastic material will be given by Equation 4.7

$$\sigma = \sigma_o \cos(\omega t + \delta) \qquad \text{Equation 4.7}$$

where: δ is the phase angle.

Equation 4.7 can be expanded to give Equation 4.8 which includes two components, one of which is in phase with the strain and the other which is out of phase.

$$\sigma = \sigma_o \cos\delta \cos\omega t - \sigma_o \sin\delta \sin\omega t \qquad \text{Equation 4.8}$$

The component of the stress which is in phase with the strain has a magnitude $\sigma_o\cos\delta$. The other component of the stress leads the strain by 90° and has a magnitude of $\sigma_o\sin\delta$. The in phase component describes the instantaneous deformation of the sample that is the solid response, whereas the out of phase component shows the relationship between the stress and the rate of strain which is the liquid response of the sample. By resolving the stress into these two components it is possible to define two moduli, E', in phase with the strain and E'', out of phase with the strain which are described by Equations 4.9 and 4.10.

$$E' = \frac{\sigma_o}{\varepsilon_o}\cos\delta \qquad \text{Equation 4.9}$$

$$E'' = \frac{\sigma_o}{\varepsilon_o}\sin\delta \qquad \text{Equation 4.10}$$

where: E' is the storage modulus

E'' is the loss modulus

Substitution of the moduli into Equation 4.8 gives an expression for the stress in terms of the moduli as shown in Equation 4.11.

Figure 4.2 : Variation in stress and strain of a sample subjected to an oscillating signal with time

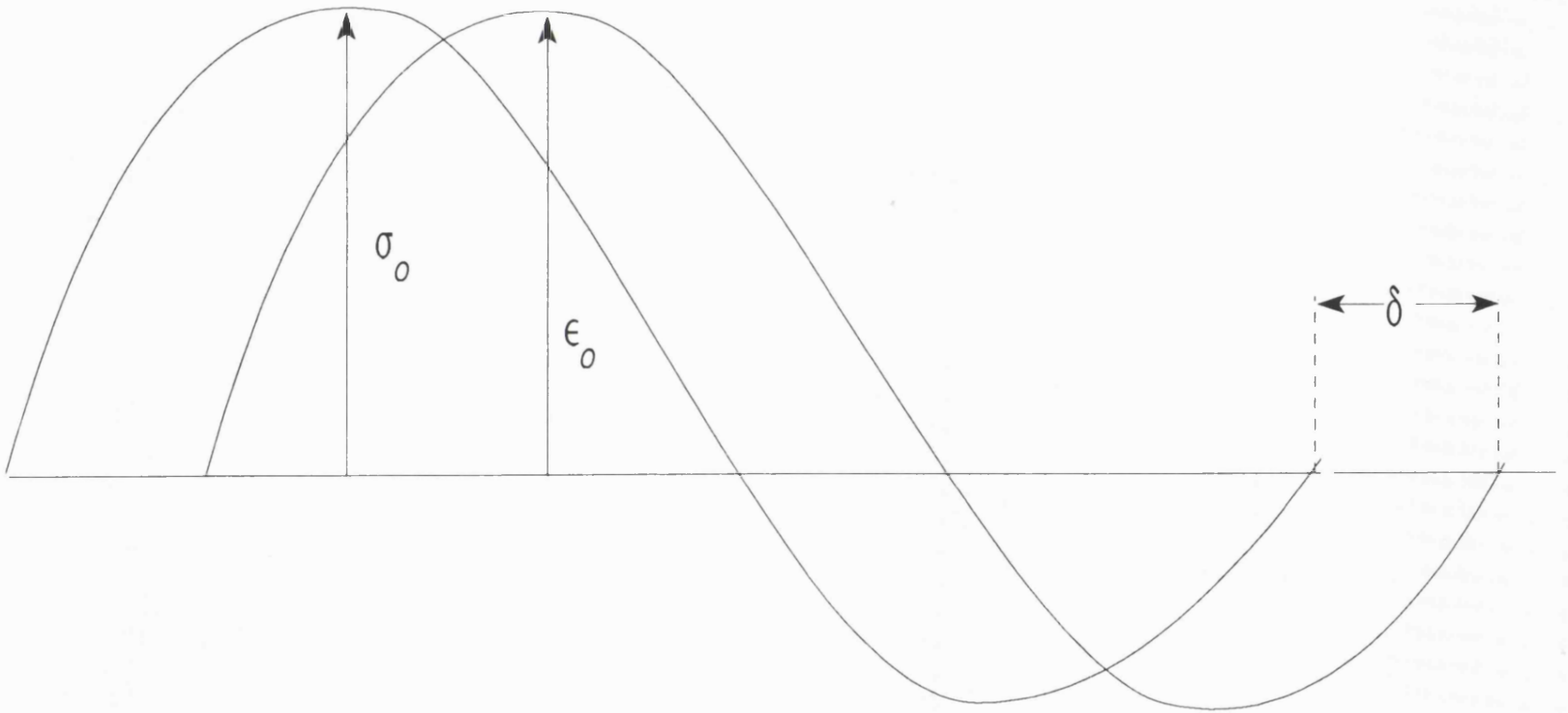

$$\sigma = \varepsilon_o E' \cos \omega t - \varepsilon_o E'' \sin \omega t \qquad \text{Equation 4.11}$$

The phase angle, δ, can also be expressed in terms of the moduli as shown in Equation 4.12.

$$\tan \delta = \frac{E''}{E'} \qquad \text{Equation 4.12}$$

It is also useful to express the moduli in terms of complex notation where i=√-1, as shown in Equation 4.13. The real part of the modulus, E', is also known as the storage modulus because it represents the energy stored within the system with each cycle. It shows the solid, or elastic behaviour of the system. The imaginary part of the modulus, E'', also known as the loss modulus represents the energy dissipated in each cycle, it describes the liquid or viscous behaviour of the system.

$$E^* = E' + iE'' \qquad \text{Equation 4.13}$$

where: E^* is the complex modulus and
i is √-1.

If the dynamic measurements are made within the linear viscoelastic region of the material the moduli will be dependent on the temperature and frequency at which the measurements are made. It is therefore usual to either keep the frequency constant and measure the response of the sample over a range of temperatures or to keep the sample at a constant temperature and record the response of the sample over a range of frequencies.

The temperature dependence of the mechanical properties of viscoelastic materials can give information on the structure and properties of polymers at a molecular level. In general polymers show a decrease in the storage modulus with increasing temperature. The storage modulus will show areas of

different gradient which are associated with peaks in the tan δ (phase angle) values. These tan δ peaks are due to molecular transitions which cause an increase in the freedom of the molecules, hence the decrease in elasticity and the increase in viscosity of the sample. The transitions of a material occur at characteristic temperatures and may be used as an identification profile. The glass transition temperature is often used for identification and purity determination purposes.

The way in which the mechanical properties vary with the frequency of the applied load can also be used to gain an insight into the structure of polymers. This method of analysis is particularly useful in the study of high water content gels where increases in temperature tend to cause drying of the gel and hence changes in the mechanical properties, as described by Scandola et al (1991). In general, the storage modulus is high at high frequencies when the sample is behaving in a glassy manner, and low at lower frequencies when the behaviour is more rubbery (Ferry, 1961). Between these two extremes E' can alter at different rates. Tan δ and the loss modulus are generally low at both high and low frequencies but show a maximum at an intermediate frequency, in the same region as the rapid change in E'. The maximum in tan δ corresponds to a maximum in the damping of the sample which occurs when the applied frequency is equal to the natural frequency for chain rotation. The frequency at which transitions occur is dependent on temperature, although at a fixed temperature these transitions may be expressed in terms of the frequency at which they occur.

4.2.4 Perkin Elmer DMA 7

The dynamic mechanical analyser used in the present work was the Perkin Elmer DMA 7. It is capable of characterising a range of materials and has a number of options for mounting samples. For the gel samples used in this investigation the parallel plate geometry was found to be most suitable and the gels could be prepared to match the size of one of the pairs of plates available.

Figure 4.3 : Schematic representation of the Perkin Elmer DMA 7

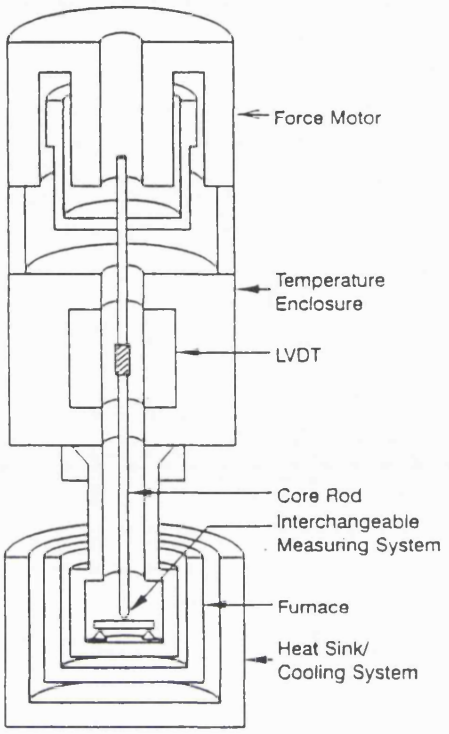

Figure 4.4 : Diagram of the liquid bath

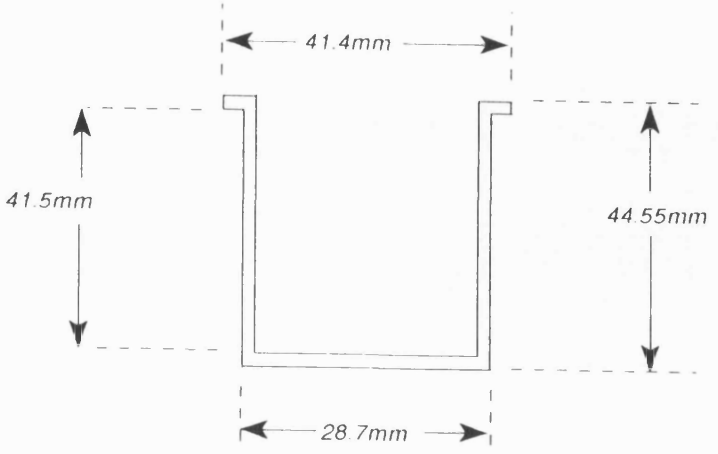

The force is applied to the sample via the core rod and probe assembly by force motor as shown schematically in Figure 4.3. The LVDT measuring system is housed below the force motor in a temperature enclosure, it is a vertically mounted, temperature controlled displacement detector. The sample is mounted between the plates, the top one of which is attached directly to the core rod. The furnace assembly is then raised to enclose the sample holder. The furnace and cooling system together allow accurate control of the sample environment. As a modification to the original equipment a liquid bath was designed to fit inside the furnace, as shown in Figure 4.4. This allowed the measurement of samples under a liquid medium, hence overcoming the problems of water loss during measurement.

The advantage of using the DMA 7 for the rheological investigations on the alginate gels were twofold. Firstly the measuring system and the sample size could be matched easily. This could have been a problem with equipment needing larger sample sizes as the production of large amounts of homologous alginate gels is difficult. The second advantage in using the DMA 7 is that the same equipment can be used for the three tests carried out, that is the stress scan, creep-recovery and frequency scan. This means that the sample conditions can be kept constant.

Rheological information available about alginate gels is basically limited to tests such as the linear compression studies carried out by Smidsrød et al (1972). The use of dynamic mechanical analysis with alginate gels should provide more information on the rheological properties of these systems than the limited data gained from the linear compression tests. A novel approach using a combination of three dynamic tests, stress scan, creep-recovery and frequency scan, was chosen for the present work.

4.3 METHOD

The alginate, pectin and the alginate and pectin solutions were prepared as described in sections 2.2.1 and 2.2.3. The gel samples were prepared by a similar method to that described by Smidsrød et al (1972), that is by dialysis of 2.5%w/v alginate solutions against either 0.1M HCl, 3%w/v calcium chloride solution or 3%w/v zinc chloride solution. Perspex cylinders, 20mm in length with an internal diameter of 15mm, were used as formers for the gelation process. A cellulose acetate dialysis membrane was held in place over the ends of the cylinder with elastic bands, as shown in Figure 4.5. Care was taken when attaching the second dialysis membrane not to allow the inclusion of air bubbles into the cylinder which would affect the mechanical properties of the gel.

Each cylinder was then placed in a glass jar containing 50ml of the dialysis solution. The gels were left to form for 48 hours, with the dialysis solution being changed every 12 hours. Once formed the gels were sectioned using a sharp scalpel, care being taken to ensure that the section was cut parallel to the end of the gel cylinder. The gel discs of approximately 0.5cm were used as this gave a good sample size for use in the dynamic mechanical analyser. Only the two end sections from the gel cylinder were used to allow for any inhomogeneity in the gel cylinders as described by Skjåk-Bræk et al (1989). The samples were placed between the parallel plates of the DMA as shown in Figure 4.6. The samples were measured under compression, with the dynamic stress on the sample being produced by the force motor and transmitted via the core rod to the measuring system housed within the furnace. The furnace and cooling system were not used for temperature cycling in these experiments but are still necessary for the maintenance of a constant reproducible temperature of 20°C. A stainless steel liquid bath, made to the specifications given in Figure 4.4, was fitted into the furnace and the probe assembly was lowered into the bath which contained 12ml deionised water.

Figure 4.5 : Formation of alginate gels by dialysis

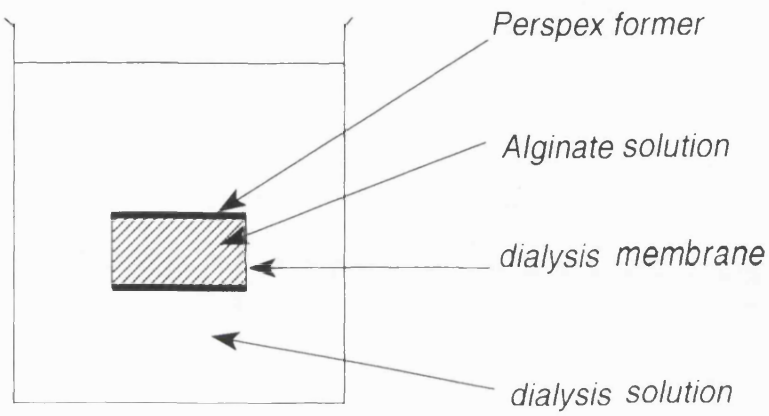

Figure 4.6 : Correct sample loading between parallel plates

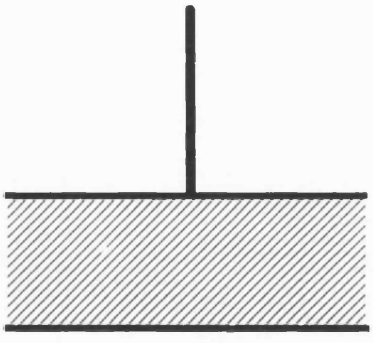

4.3.1 Stress Scans

The stress scan mode of the DMA was chosen and the parameters given in Table 4.1 were entered into the method page. The zero measurement was read into the computer with the probe assembly in the liquid bath, this means that the effect of the buoyancy of the water is taken into account in the measurements. After the plates had been zeroed the sample was placed between the parallel plates and the height of the sample was measured by the DMA and automatically read into the software.

Table 4.1 : DMA settings for stress scan experiments

Parameter	Value used
Sample diameter	10mm
Static force	1mN
Frequency	1Hz
Hold for	0 min
Initial force	1.0mN
Force rate	50mN/min
Final force	100.0mN

Each sample was discarded after being measured, and measurements were repeated with fresh samples. At least three measurements were made for each sample. The range of force used was chosen to exceed the viscoelastic limit for all the samples. The sample diameter is dictated by the size of the plates used and the values of the static and initial forces were chosen in order to maintain contact between the plates and the sample at all times.

4.3.2 Creep-recovery

The creep-recovery mode of the DMA was chosen and the parameters given in Table 4.2 were entered into the method page. The zero and sample height were measured as described in Chapter 4.3.1. Each sample was discarded after being measured, and measurements were repeated with fresh samples. At least three measurements were made for each sample. The creep force was chosen to be below the viscoelastic limit of the gels as determined by the stress scan experiments. This is important as creep-recovery experiments should be carried out within the linear viscoelastic region.

Table 4.2 : DMA settings for creep-recovery experiments.

Parameter	Value used
Sample diameter	10mm
Creep ramp	Off
Hold for	1.0 min
Creep force	5.0mN
For	5.0 min
Recovery force	0.0mN
For	5.0 min
Temp	20°C
Time	11 min

4.3.3 Frequency Scans

The frequency scan mode of the DMA was chosen and the parameters given in Table 4.3 were entered into the method page. The zero and sample height were measured as described in Chapter 4.3.1. Each sample was discarded

after being measured, and measurements were repeated with fresh samples. At least three measurements were made for each sample. The dynamic force was chosen to be within the linear viscoelastic region and the static force applied to the sample should be about 120% of the dynamic force in order to ensure the plates remain in contact with the sample. The frequency range was chosen to be outside the resonant frequency of the system.

Table 4.3 : DMA settings for frequency scan experiments.

Parameter	Value used
Sample diameter	10mm
Static force	6.0mN
Dynamic force	5.0mN
Initial frequency	10.00Hz
Final frequency	0.10Hz

4.4 RESULTS

4.4.1 Stress scan results

The behaviour of the samples was measured with an increasing force. The results are most usefully considered in terms of the way the strain produced in the sample varies with the force applied. In the case of viscoelastic materials the strain is seen to vary linearly with force up to a certain force value, the linear viscoelastic limit. It is important that this force is not exceeded in other experiments since the equations used in the calculation of results are only valid within the viscoelastic region. The values for the viscoelastic limit for the samples were calculated from the force against strain curves given in Figure 4.7. Tangents to the curves were used to determine the point at which the curve ceased to be linear. The mean force values ± standard deviation for the

Figure 4.7(a) : Stress scans for LFR 5/60 gels

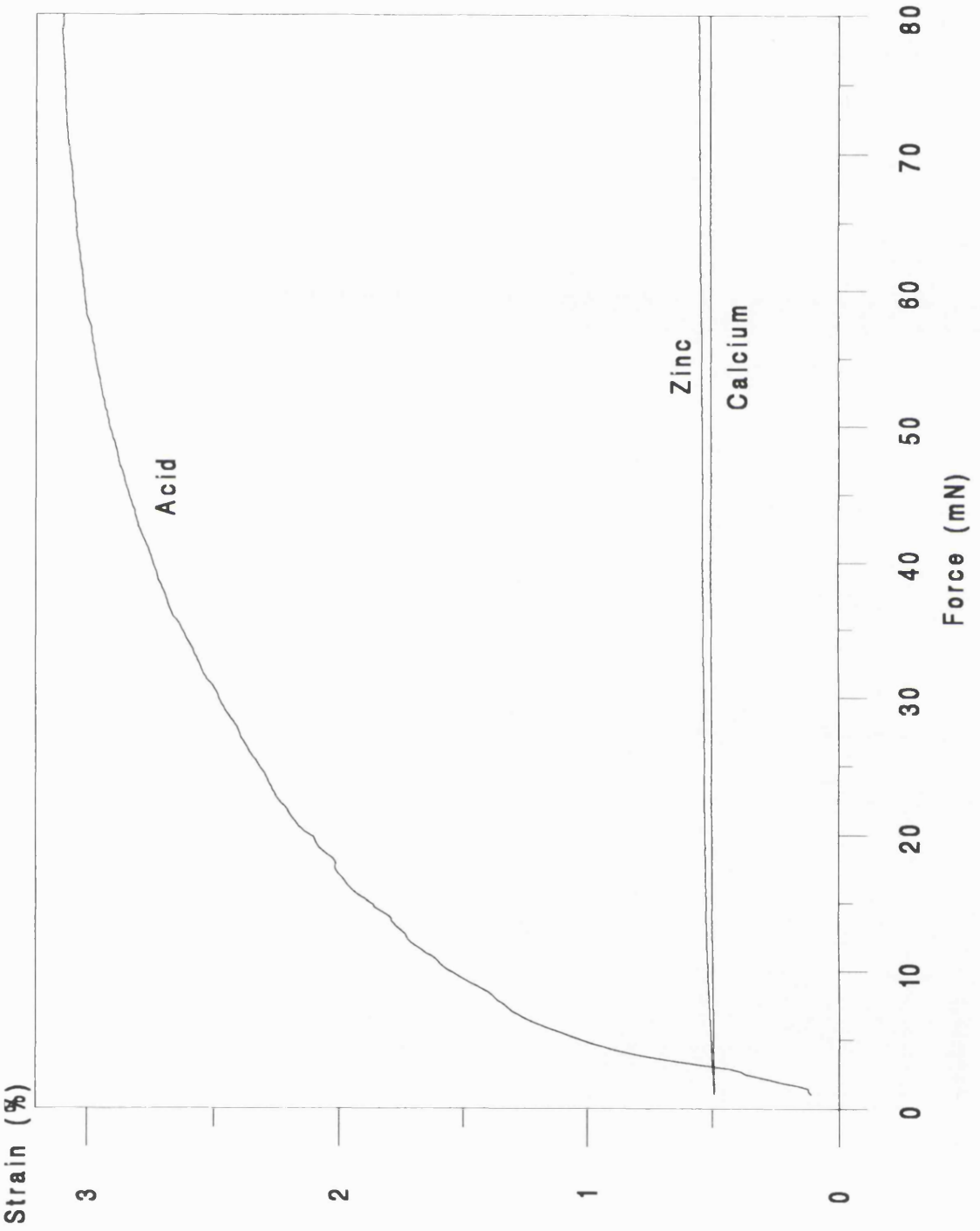

Figure 4.7(b) : Stress scans for LF 120M gels

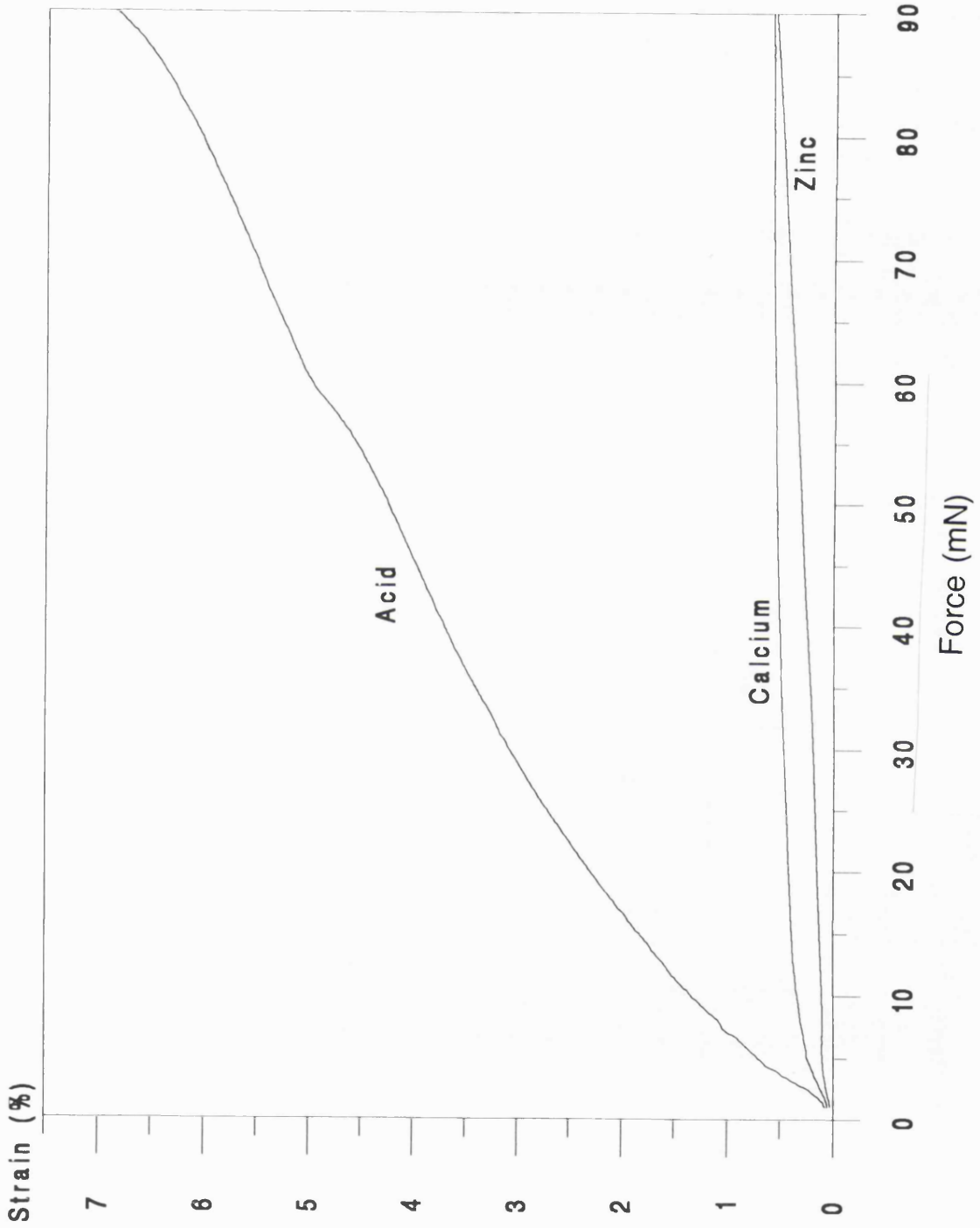

Figure 4.7(c) : Stress scans for LF 10/40RB gels

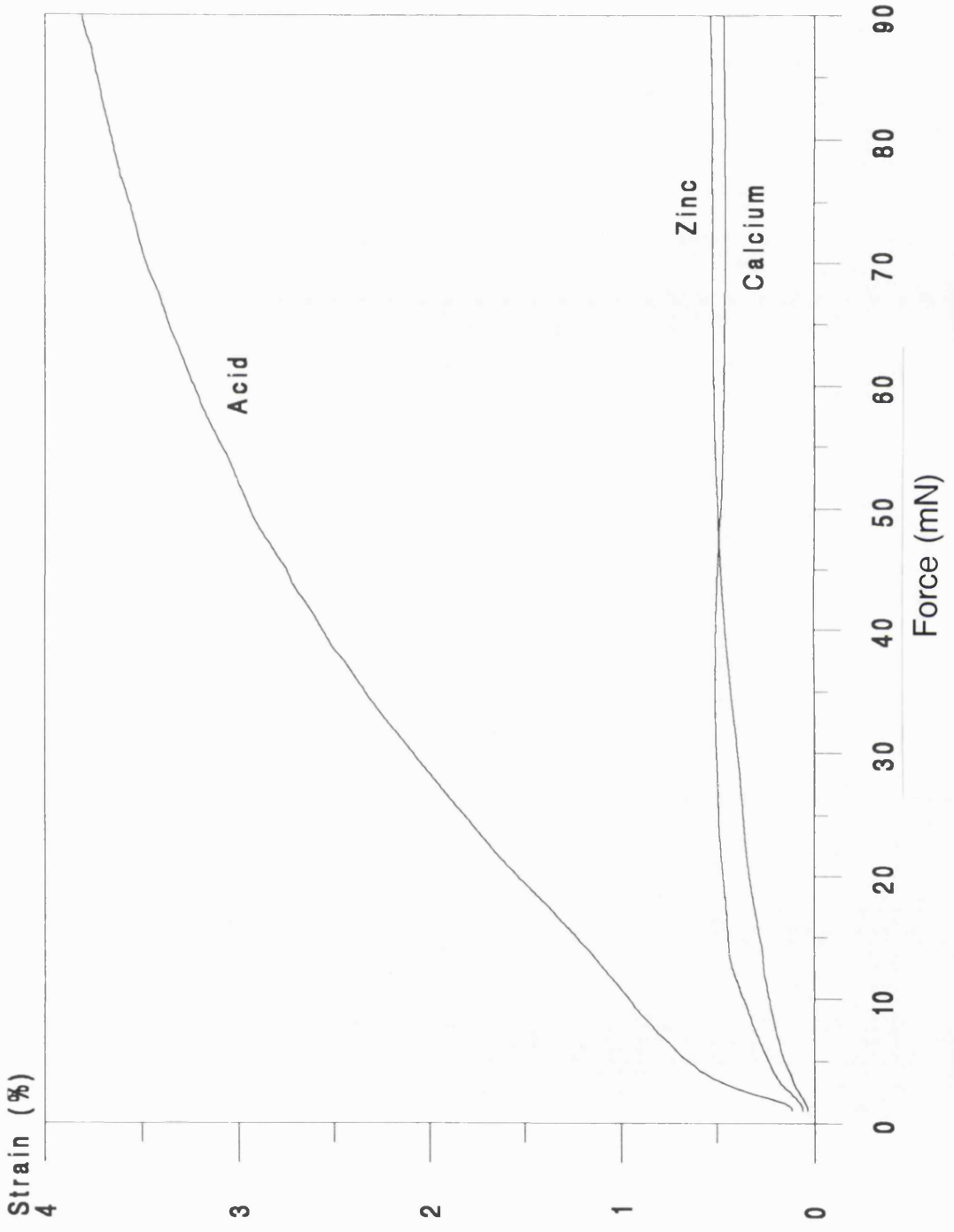

Figure 4.7(d) : Stress scans for LFR 5/60 + pectin gels

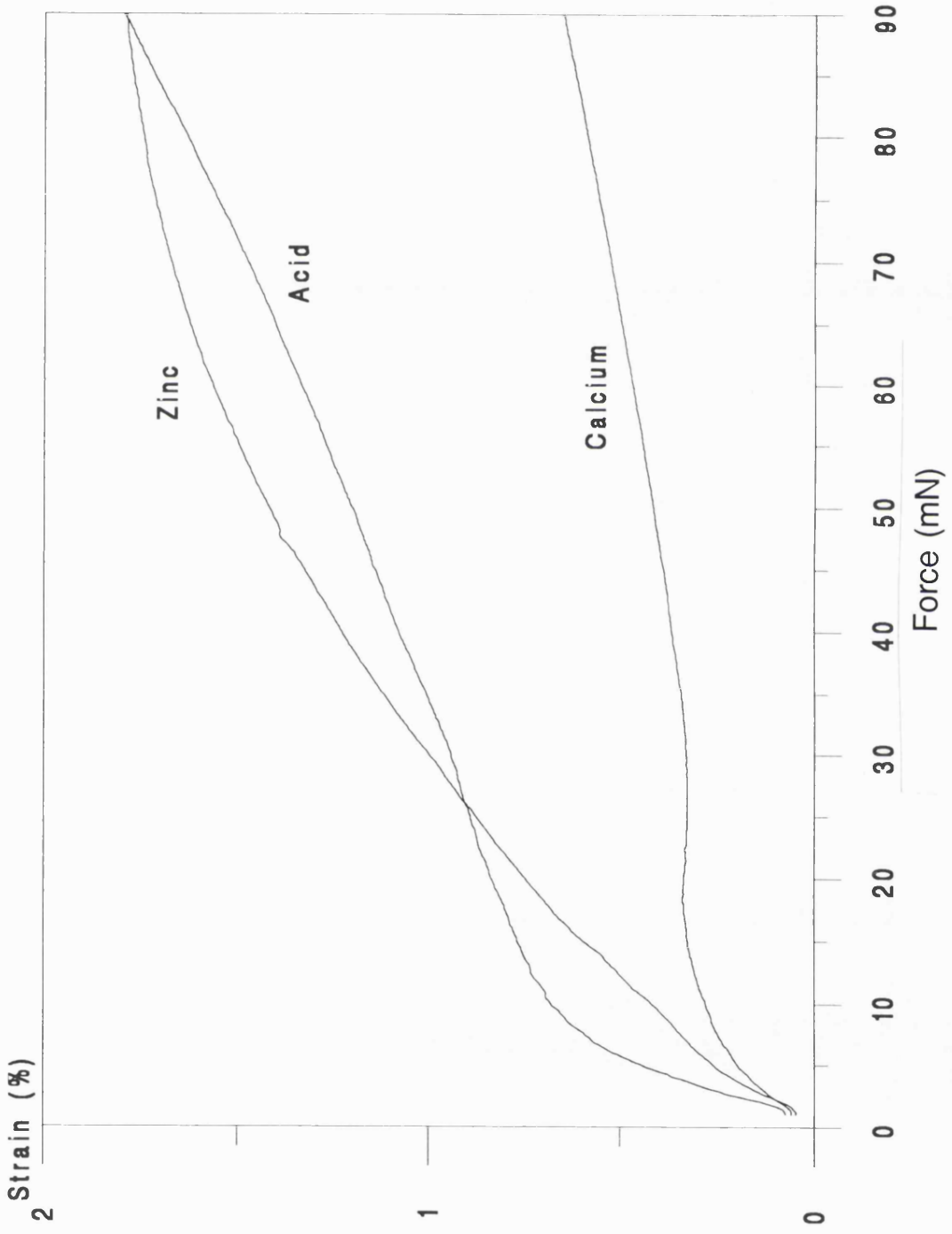

viscoelastic limit obtained for the calcium gels are shown in Table 4.4. Mean values for the strain at two points on the curve are also given, the lower force at which the strain is recorded is within the linear viscoelastic region, and the higher force is outside that range.

Measurements were also made of the same alginate and pectin samples using zinc as the gelating ion. The results from these experiments are given in Table 4.5 in the same way as the calcium gels.

Gels were also measured which were not formed by the action of a cation but by dialysis against 0.1M HCl. These results are shown in Table 4.6 in the same format as the previous results. Results are not given for the pectin sample because pectin does not form a gel in acid conditions without the presence of cations.

The results show that the viscoelastic limit varies depending on the alginate and/or pectin used as well as the on the method by which the gel is prepared. The viscoelastic limit was found to be greater than 5mN, which was the magnitude of the force chosen for use in both the creep-recovery and the frequency scan experiments. The primary reason for carrying out the stress scan experiments was to determine the viscoelastic limit, however the results also give some information about the nature of the gels formed.

From the graphs of force against strain given in Figure 4.7 it can be seen that in all cases the alginate gels formed in acid showed much greater deformation than those formed by the action of a cation. The difference between the gels formed with calcium and zinc showed very little difference suggesting a similar mechanism of gelation. The gels formed by a mixture of alginate and pectin showed the acid and zinc gels to be similar with the calcium gel producing much less deformation.

Table 4.4 : Stress scan results for calcium gels

Sample	%G (NMR)	Mean viscoelastic limit (mN) ± s.d.	Strain (%) ± s.d.at 3mN	Strain (%) ± s.d. at 60mN
LFR 5/60	67.2	5.085 ± 0.80	0.066 ± 0.01	0.224 ± 0.02
LF 120M	42.4	12.73 ± 0.35	$0.152 \pm 4.0 \times 10^{-3}$	0.552 ± 0.01
LF 10/40RB	50.9	12.20 ± 1.7	0.160 ± 0.02	0.463 ± 0.07
LFR 5/60 + Pectin	-	8.17 ± 2.11	0.167 ± 0.04	0.536 ± 0.05
Pectin	-	9.804 ± 2.87	0.634 ± 0.18	4.394 ± 0.89

Table 4.5 : Stress scan results for zinc gels

Sample	%G (NMR)	Mean viscoelastic limit (mN) ± s.d.	Strain (%) ± s.d. at 3mN	Strain (%) ± s.d.at 60mN
LFR 5/60	67.2	5.386 ± 1.0	0.236 ± 0.04	0.397 ± 0.01
LF 120M	42.4	6.095 ± 1.4	0.068 ± 0.01	0.369 ± 0.03
LF 10/40RB	50.9	10.83 ± 2.7	0.094 ± 0.01	0.472 ± 0.06
LFR 5/60 + Pectin	-	6.761 ± 1.7	0.296 ± 0.12	$1.56 \pm 8.6 \times 10^{-3}$
Pectin	-	8.082 ± 2.0	0.238 ± 0.10	1.630 ± 0.05

Table 4.6 : Stress scan results for acid gels

Sample	%G (NMR)	Mean viscoelastic limit (mN) ± s.d.	Strain (%) ± s.d. at 3mN	Strain (%) ± s.d.at 60mN
LFR 5/60	67.2	20.49 ± 6.7	0.586 ±0.07	2.974 ± 0.25
LF 120M	42.4	18.55 ± 0.61	0.307 ±0.03	4.637 ± 0.27
LF 10/40RB	50.9	6.074 ± 1.3	0.425 ± 0.02	3.177 ± 0.07
LFR 5/60 + Pectin	-	11.05 ± 3.19	0.209 ± 0.04	1.324 ± 0.03

Comparison of the strain values obtained from the various gels gives an indication of the rigidity of the gels. The values of strain obtained above the viscoelastic limit are less reliable than those taken at 3mN. When comparing the strain recorded at 3mN for the various gels it should be noted that a lower strain indicates a higher rigidity of the gel.

The stain values at 3mN given in Tables 4.4, 4.5 and 4.6 show that in the gels formed by the action of calcium, the LFR 5/60 produced the gel with the greatest resistance to deformation. The gels formed by LF 120M and LF 10/40RB showed similar deformation which was greater than that for LFR 5/60. The calcium and pectin gel showed the greatest strain at 3mN, with the LFR 5/60 and pectin mixture gel being intermediate between the individual components.

The zinc gels showed the least deformation with LF 120M, followed by LF 10/40RB. The deformation of the zinc and LFR 5/60 gel was greater than the other two alginates and similar to that of the pectin and zinc gel. The gel formed by the mixture of LFR 5/60 and pectin showed a strain at 3mN higher than that of either of the individual components.

The rank order for the acid gels of the alginates is the same as with zinc in that LFR 5/60 shows the greatest deformation and LF 120M the least. However, in the gels formed by the action of acid the pectin and LFR 5/60 mixture showed the least deformation of all the gels investigated. It seems, therefore that the rank order of the deformation of the alginate gels depends on the method of formation of the gels.

4.4.2 Creep-recovery results

The variation of strain produced in the sample was recorded during the course of the creep experiment. By measuring the way in which the strain is affected by the instantaneous application of the force and the removal of that force it is

possible to produce a creep-recovery curve. The creep-recovery curves for the three alginates investigated are shown in Figure 4.8. The parameters described in Chapter 4.2.2 and shown in Figure 4.1 were calculated from the compliance data for the calcium gels and are shown in Table 4.7. The same parameters have been calculated for the gels formed by dialysis against zinc ions and are shown in Table 4.8. The compliance values for the acidic gels are given in Table 4.9; no values for pectin alone are given since pectin does not form a gel with acid but requires either divalent cations or sugar for gelation.

From the creep-recovery curves given in Figure 4.8 a comparison can be made of the three different formation mechanisms with each of the alginates. LFR 5/60 gels with calcium as the gelating agent show the least deformation of all the LFR 5/60 gels. The acid gels show very little viscous behaviour, but the greatest recovery of the LFR 5/60 gels. Those gels formed with zinc initially demonstrate lower deformation than the acid gels, but with time the deformation of the zinc gels becomes greater and shows less recovery. The calcium and zinc gels show both elastic and viscous characteristics, whilst the gels formed by the action of acid demonstrate a mainly elastic nature. Calcium forms the most rigid of the gels with those formed with acid and zinc having a similar rigidity.

The LF 120M gels show less marked differences; again the calcium gels show the greatest deformation with the zinc and acid gels being similar. In the same way as with the LFR 5/60 gels, the LF 120M and acid gel shows mainly elastic behaviour, while the ionic gels have a greater viscous component.

There is a difference with the LF 10/40RB in that the zinc gels show a greater rigidity that the calcium gels, however, as before the acid gels show the least viscous behaviour and the greatest recovery. In general although the rank order may change between the alginates the acid gels show the greatest overall deformation, the most elastic behaviour and the greatest degree of

Figure 4.8(a) : Creep-recovery curves for LFR 5/60 gels

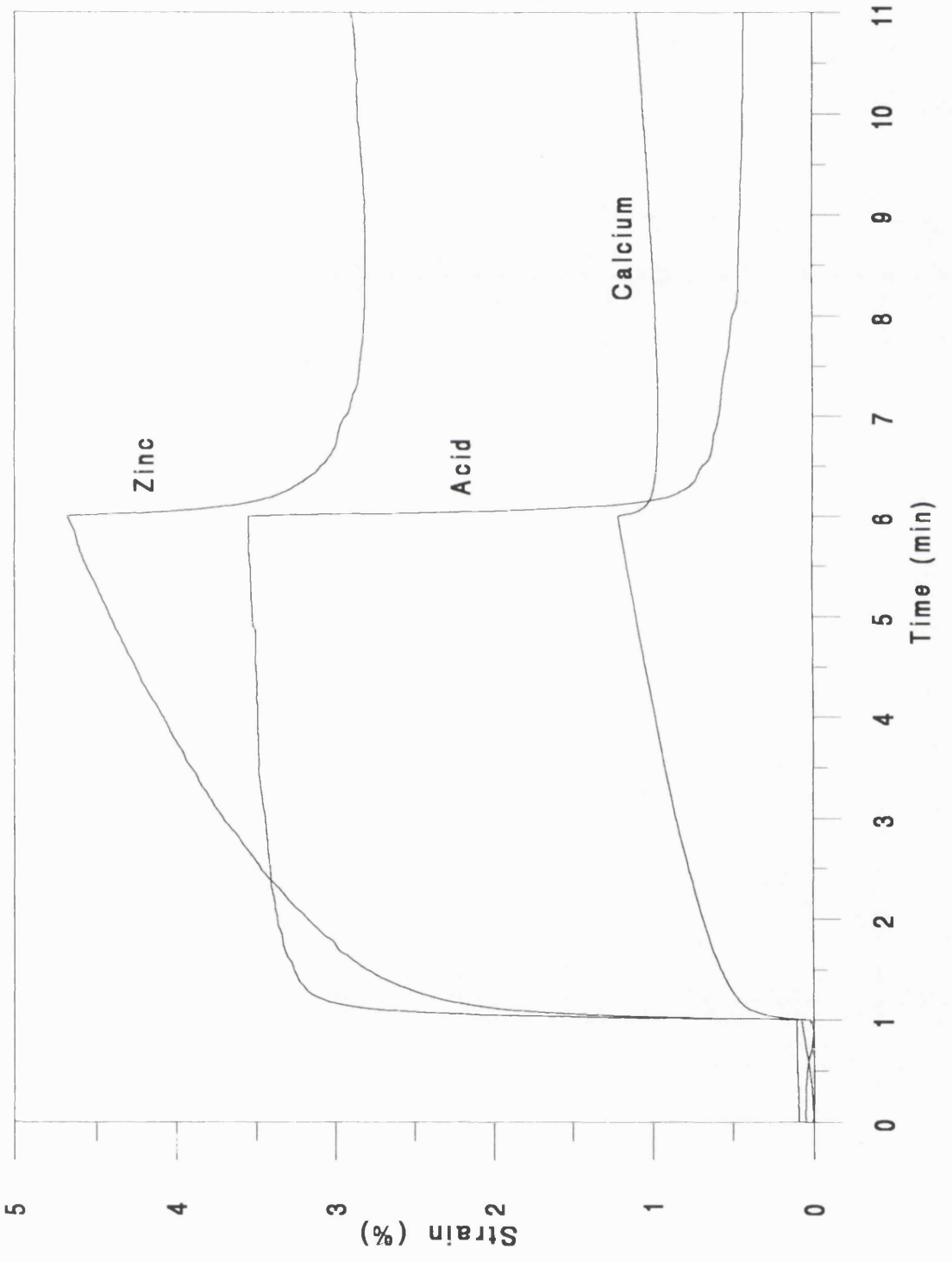

Figure 4.8(b) : Creep-recovery curves for LF 120M gels

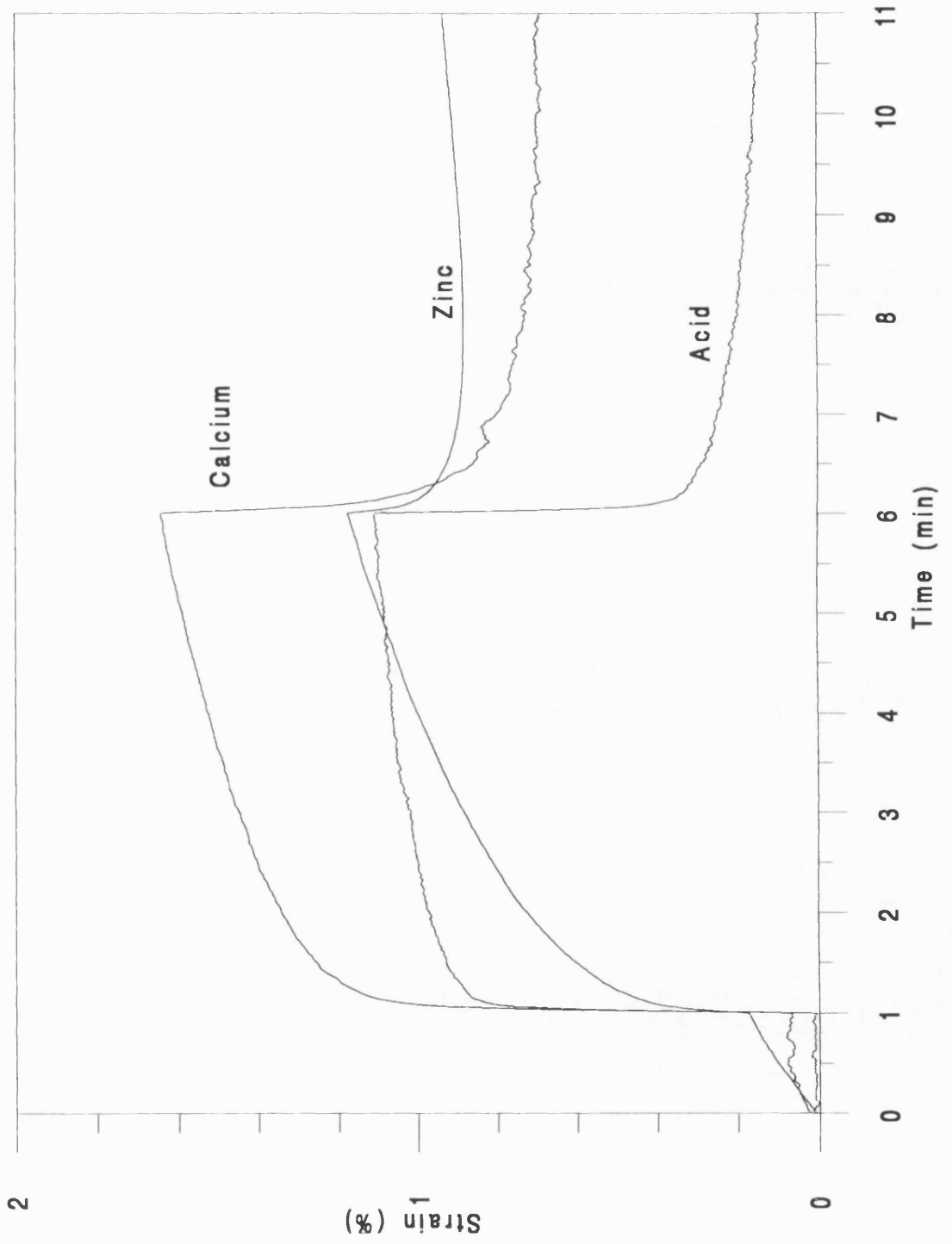

Figure 4.8(c) : Creep-recovery curves for LF 10/40RB gels

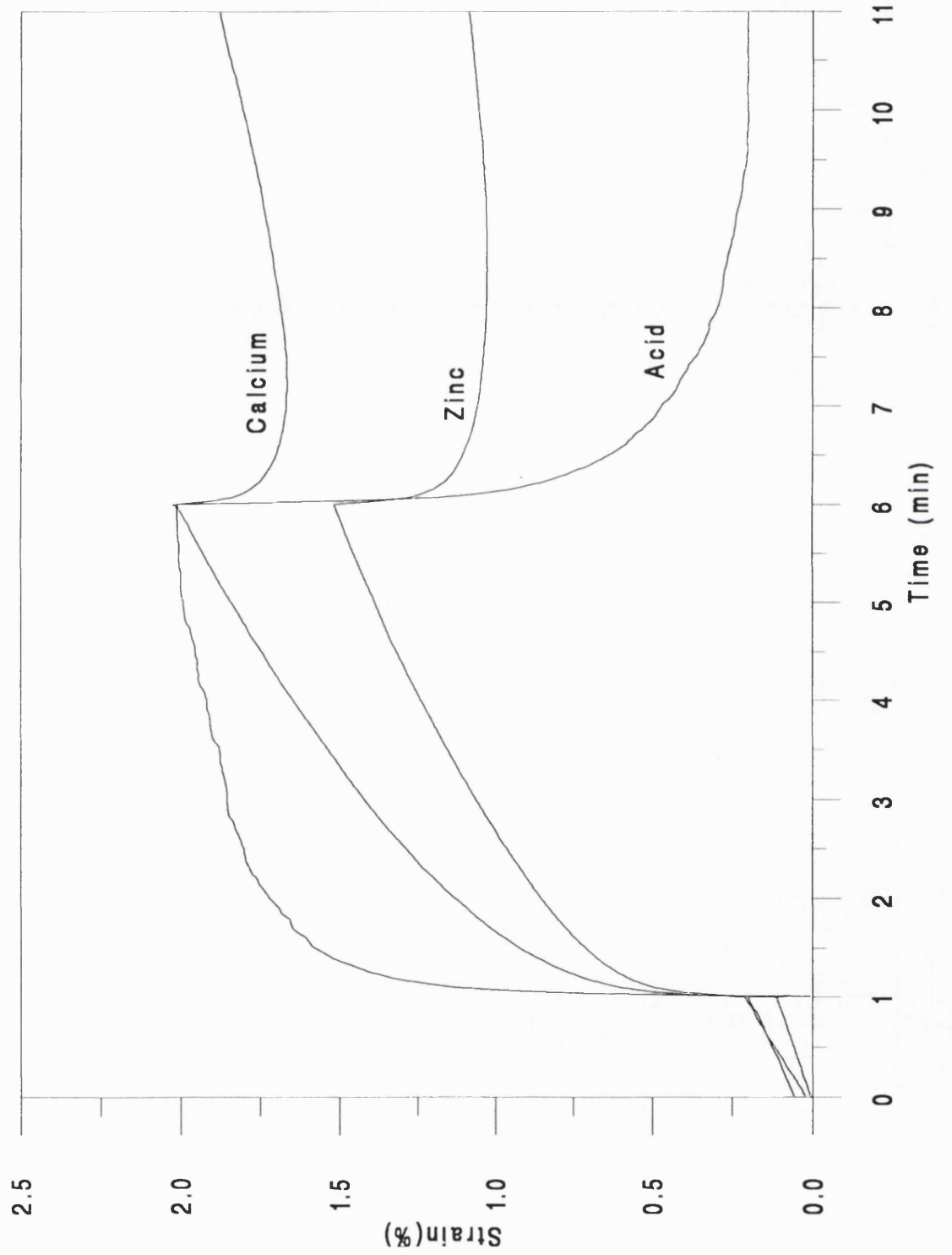

Figure 4.8(d) : Creep-recovery curves for LFR 5/60 + pectin gels

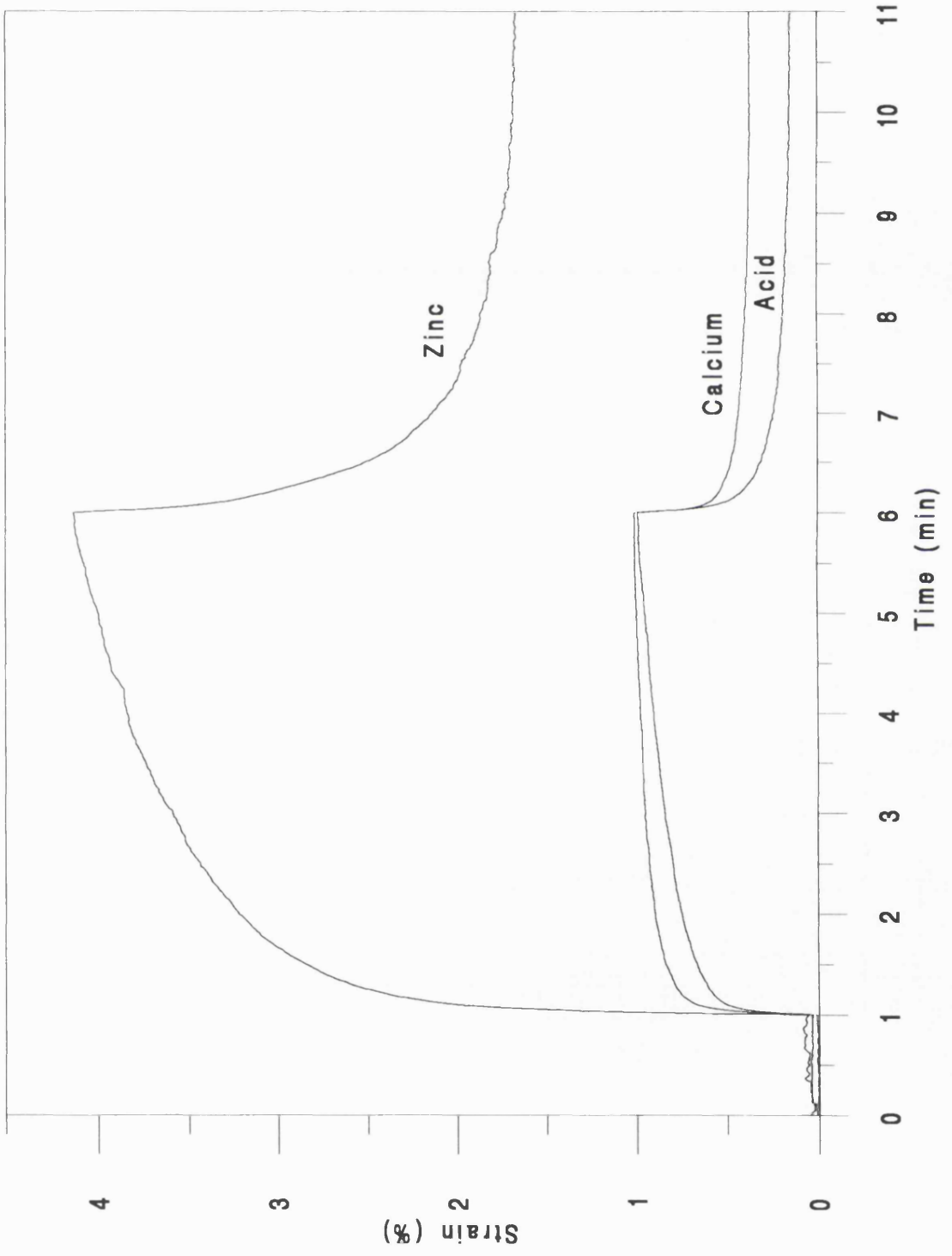

Table 4.7 : Creep-recovery results for calcium gels

Alginate	%G (NMR)	Compliance parameters (mPa^{-1}) ± s.d.					
		J_O	J_R	J_N	J_O'	J_R'	J_N'
LFR 5/60	67.2	2.64 ± 1.4	9.25 ± 2.2	9.21 ± 0.57	2.09 ± 1.4	4.05 ± 2.4	14.9 ± 0.69
LF 120M	42.4	4.25 ± 0.51	13.4 ± 0.75	5.65 ± 1.6	2.62 ± 0.37	10.7 ± 0.82	9.93 ± 0.30
LF 10/40RB	50.9	2.18 ± 0.28	13.3 ± 0.041	14.5 ± 0.99	1.68 ± 0.54	5.78 ± 4.0	22.6 ± 5.4
LFR 5/60 + Pectin	-	3.51 ± 0.045	8.14 ± 1.1	3.80 ± 0.65	3.06 ± 0.49	6.78 ± 1.6	5.61 ± 0.39
Pectin	-	16.4 ± 6.4	31.7 ± 6.7	17.6 ± 3.3	9.22 ± 2.2	27.5 ± 9.1	29.1 ± 10.1

Table 4.8 : Creep-recovery results for zinc gels

Alginate	%G (NMR)	Compliance parameters (mPa^{-1}) ± s.d.					
		J_O	J_R	J_N	J_O'	J_R'	J_N'
LFR 5/60	67.2	15.2 ± 5.2	32.7 ± 5.3	26.56 ± 10.0	6.46 ± 2.6	25.9 ± 13.5	42.1 ± 1.3
LF 120M	42.4	1.62 ± 0.41	9.54 ± 1.2	5.54 ± 0.93	0.78 ± 0.15	4.94 ± 1.1	11.0 ± 0.12
LF 10/40RB	50.9	2.67 ± 0.59	11.0 ± 4.8	8.37 ± 1.2	1.87 ± 0.55	7.45 ± 1.5	12.74 ± 6.4
LFR 5/60 + Pectin	-	16.3 ± 2.3	21.5 ± 7.7	13.9 ± 7.0	6.17 ± 0.87	35.3 ± 4.6	19.6 ± 4.7
Pectin	-	13.2 ± 3.7	35.4 ± 3.9	5.94 ± 0.66	5.85 ± 1.6	34.77 ± 9.4	13.9 ± 5.0

Table 4.9 : Creep-recovery results for acid gels

Alginate	%G (NMR)	Compliance parameters (mPa^{-1}) ± s.d.					
		J_O	J_R	J_N	J_O'	J_R'	J_N'
LFR 5/60	67.2	22.3 ± 1.6	38.6 ± 12.1	3.19 ± 0.78	12.2 ± 1.4	43.1 ± 11.2	8.74 ± 2.2
LF 120M	42.4	8.59 ± 0.77	8.70 ± 2.4	1.85 ± 0.18	6.09 ± 1.4	11.0 ± 2.9	2.07 ± 1.1
LF 10/40RB	50.9	7.19 ± 0.34	17.6 ± 3.4	3.44 ± 0.47	4.73 ± 0.64	21.96 ± 3.4	1.28 ± 0.13
LFR 5/60 + Pectin	-	4.69 ± 0.36	10.2 ± 1.7	1.93 ± 0.60	3.54 ± 0.93	9.69 ± 2.3	3.54 ± 1.2

recovery compared to the ionic gels. Comparison between the alginates can be made by reference to Tables 4.7, 4.8 and 4.9. In the calcium gels LF 120M shows the greatest elastic and the least viscous deformation. The recovery of LF 120M is also greater than that of LFR 5/60 or LF 10/40RB showing it to have a more elastic nature. The gels formed with pectin show greater elastic and viscous deformation than the other gels suggesting a weaker gel. The pectin and LFR 5/60 mixture gel show evidence for synergy between the components in that it is more elastic compared to viscous and it shows a lower viscous deformation than either of the components alone.

The zinc gels show larger differences than the calcium. The instantaneous elastic deformation (J_0) is much smaller for both LF 120M and LF 10/40RB than it is for LFR 5/60, as is the viscous deformation, suggesting that the latter is a weaker gel in comparison. There is less evidence for synergy between the alginate and pectin in this case. The differences between the calcium and zinc gels seem to suggest that the two cations do not act in exactly the same manner to produce gelation of the alginates.

In the acid gels as already noted the elastic behaviour is much greater than the viscous. The LFR 5/60 acid gels show the greatest deformation, with the other two alginates showing similar values. The inclusion of pectin with LFR 5/60 increases the modulus of the gel compared to LFR 5/60 alone. It is not possible to attribute this to a synergistic effect as there are no values for gels composed of pectin and acid alone.

The creep-recovery measurements enable the demonstration of the elastic properties of the gels as well as the viscous nature. The results show that the acid gels tend to show the greatest deformation and also the greatest degree of elastic behaviour compared with the ionic gels. It also shows that the LF 120M shows the least deformation of the three alginates, and LFR 5/60 the most. There is evidence for synergy between pectin and LFR 5/60; this occurs only when calcium is the gelating agent.

4.4.3 Frequency scan results

The transitions which occur within the gel samples with changes in the frequency of the applied stress can be seen by looking at the way the tan δ value varies with frequency. The tan δ typically shows a peak and the frequency at which this occurs, together with the values of the storage and loss moduli and tan δ at a frequency of 4Hz, are given in Table 4.10 for the calcium gels. Figure 4.9 shows the way in which the storage moduli of the gels varies with frequency and the corresponding frequency scans of the loss moduli are shown in Figure 4.10. The numerical data is given in Table 4.11 for the zinc gels and Table 4.12 for the gels formed by the action of acid.

The plots of the frequency scans given in Figures 4.9 and 4.10 show that the storage modulus of the acid gels is lower than that of the ionic gels in all cases. The calcium gels formed from LFR 5/60 alone or in combination with pectin showed a greater storage modulus compared with the zinc gels, whereas in the other alginates zinc produced a larger storage modulus than calcium. The loss modulus for the alginate gels is also found to be lowest with the acid gels than the ionic gels. Again with LFR 5/60 and the mixture of LFR 5/60 and pectin the calcium gels have a higher loss modulus than the zinc; this is reversed with the other alginates.

The calcium gels show a great difference between the gels containing alginate and the pectin gel. The pectin gel has a tan δ maximum much lower than any of the other gels while the parameters measured at 4Hz are also very different for the pectin gel. The gels formed either with an alginate alone or the mixture with LFR 5/60 and pectin show similar values of both moduli and tan δ. This pattern is repeated in the zinc gels where the tan δ maximum for the pectin is lower than that for the other gels. In the case of the zinc gels, however, the storage and loss moduli for LF 120M and LF 10/40RB are higher than those for the other gels. When considering the acid gels the LFR 5/60 and pectin mixture shows different characteristics to the gels formed with an alginate

Figure 4.9(a) : Variation of storage modulus with frequency for LFR 5/60 gels

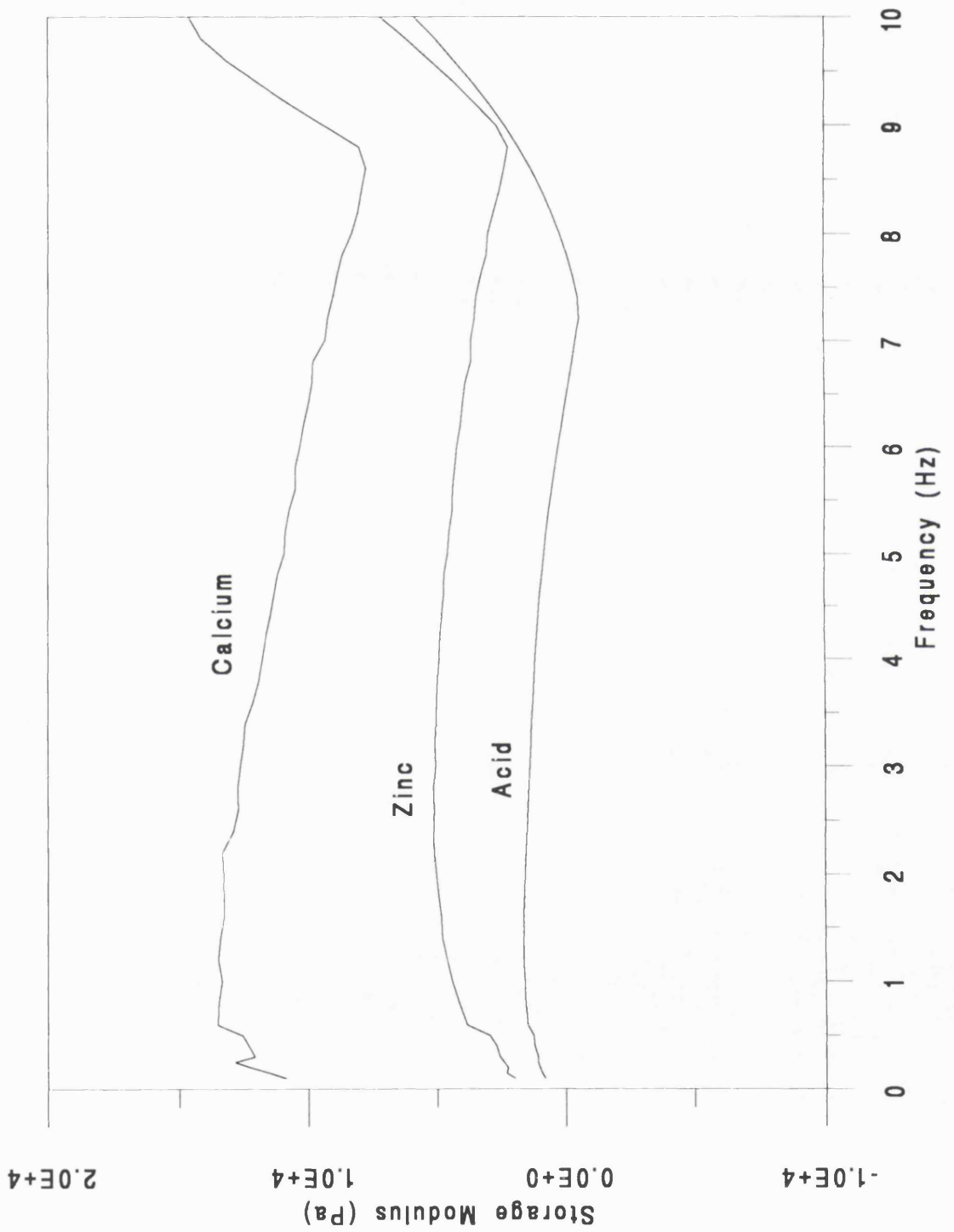

Figure 4.9(b) : Variation of storage modulus with frequency for LF 120M gels

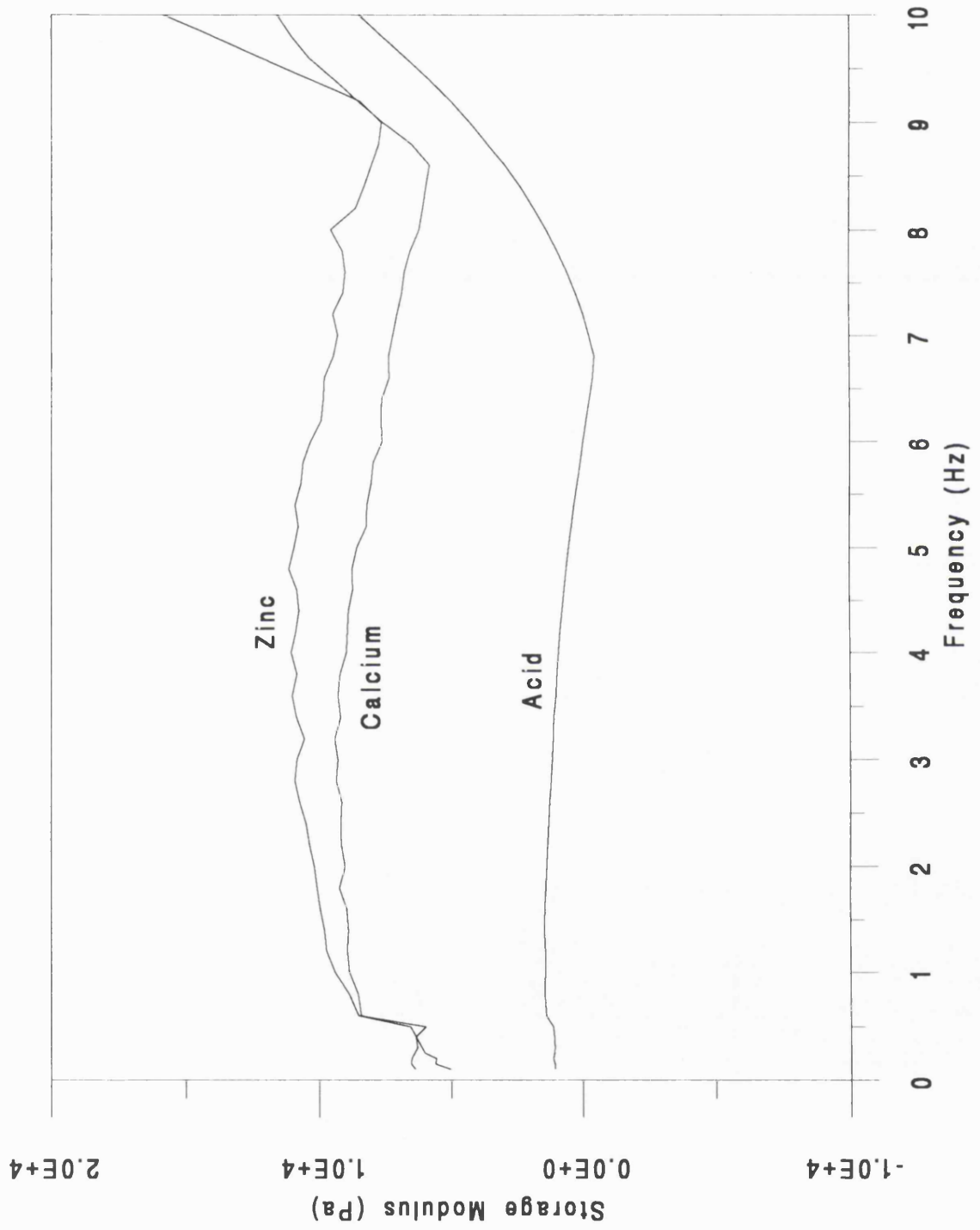

Figure 4.9(c) : Variation of storage modulus with frequency for LF 10/40RB gels

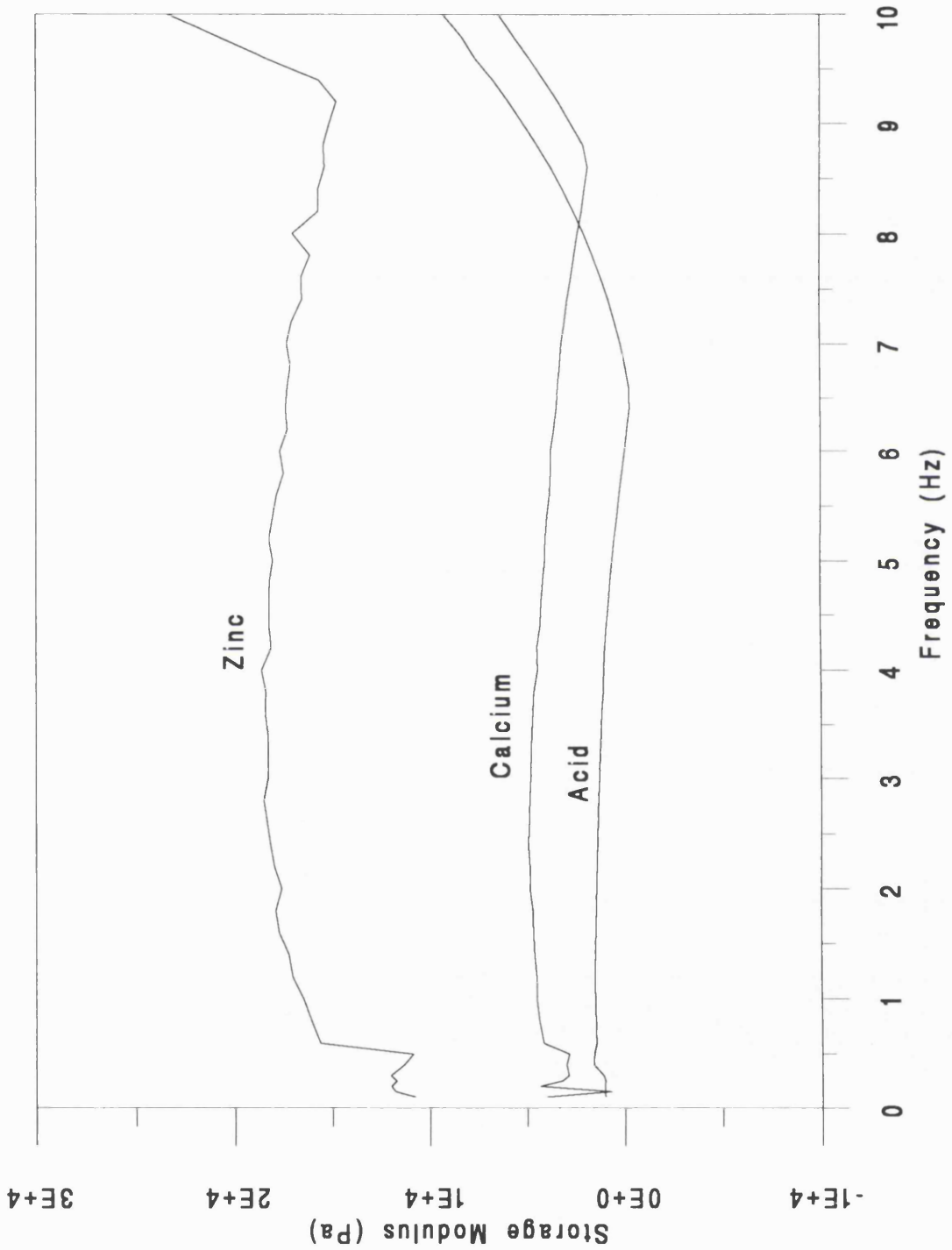

Figure 4.9(d) : Variation of storage modulus with frequency for LFR 5/60 + pectin gels

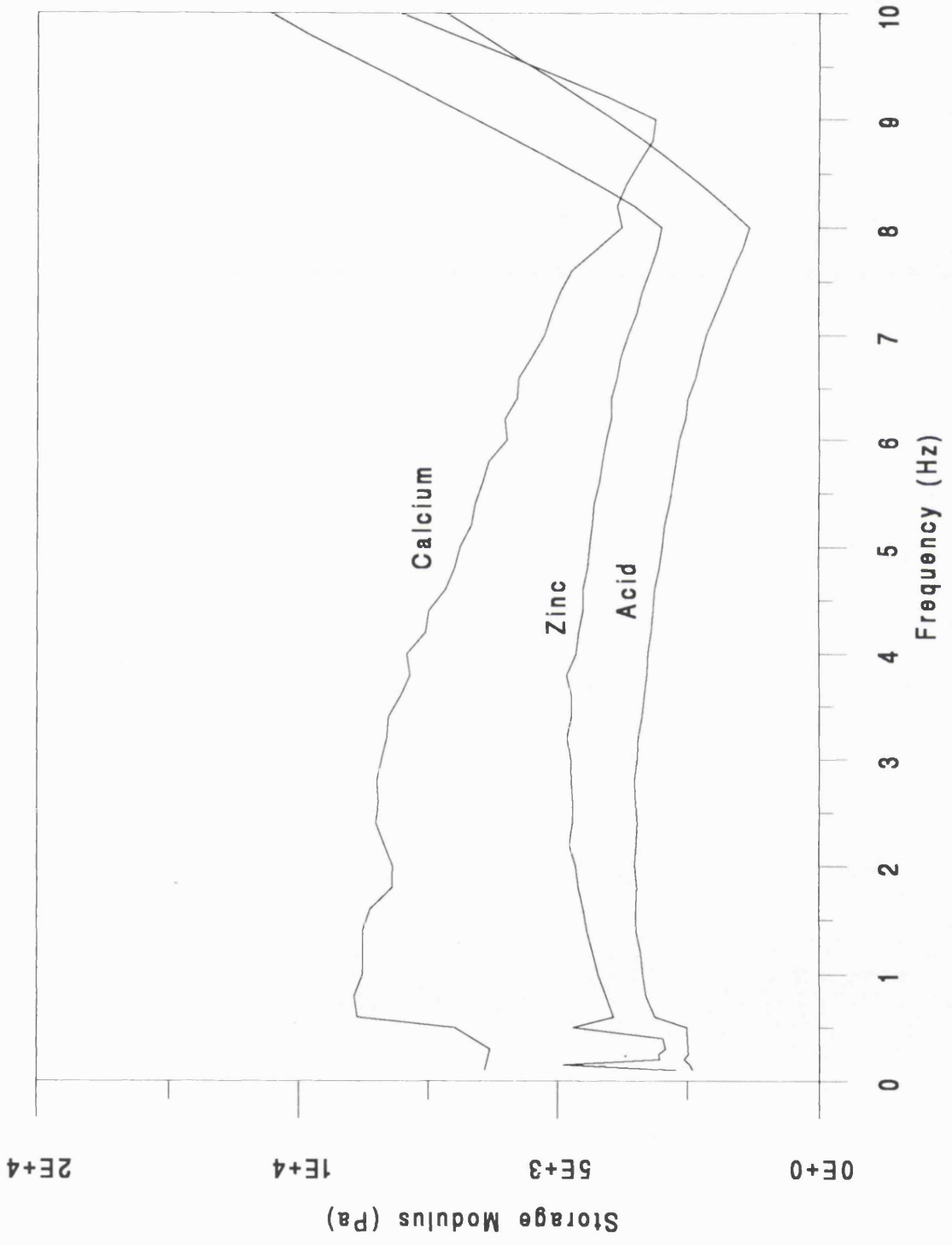

Figure 4.10(a) : Variation of loss modulus with frequency for LFR 5/60 gels

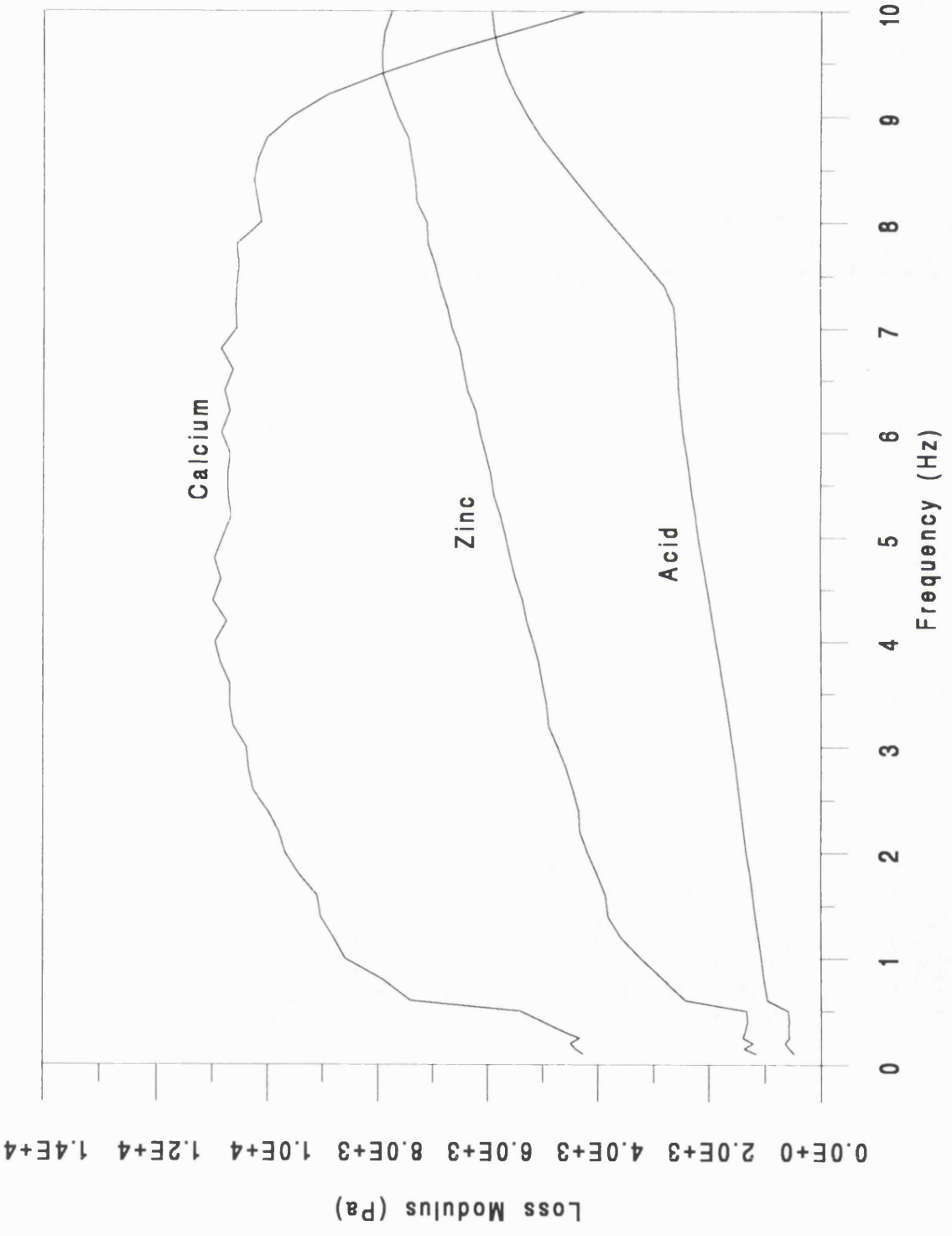

Figure 4.10(b) : Variation of loss modulus with frequency for LF 120M gels

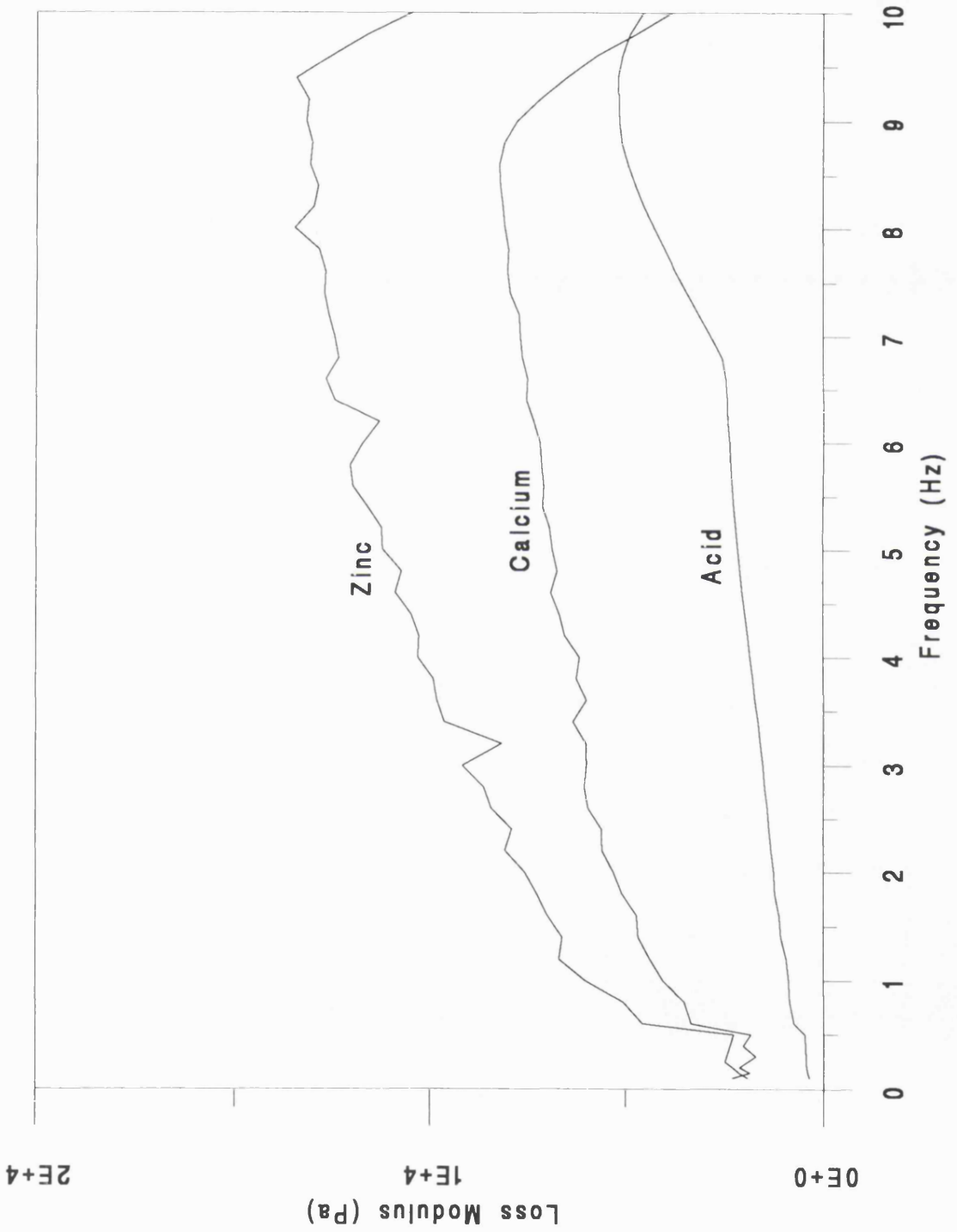

Figure 4.10(c) : Variation of loss modulus with frequency for LF 10/40RB gels

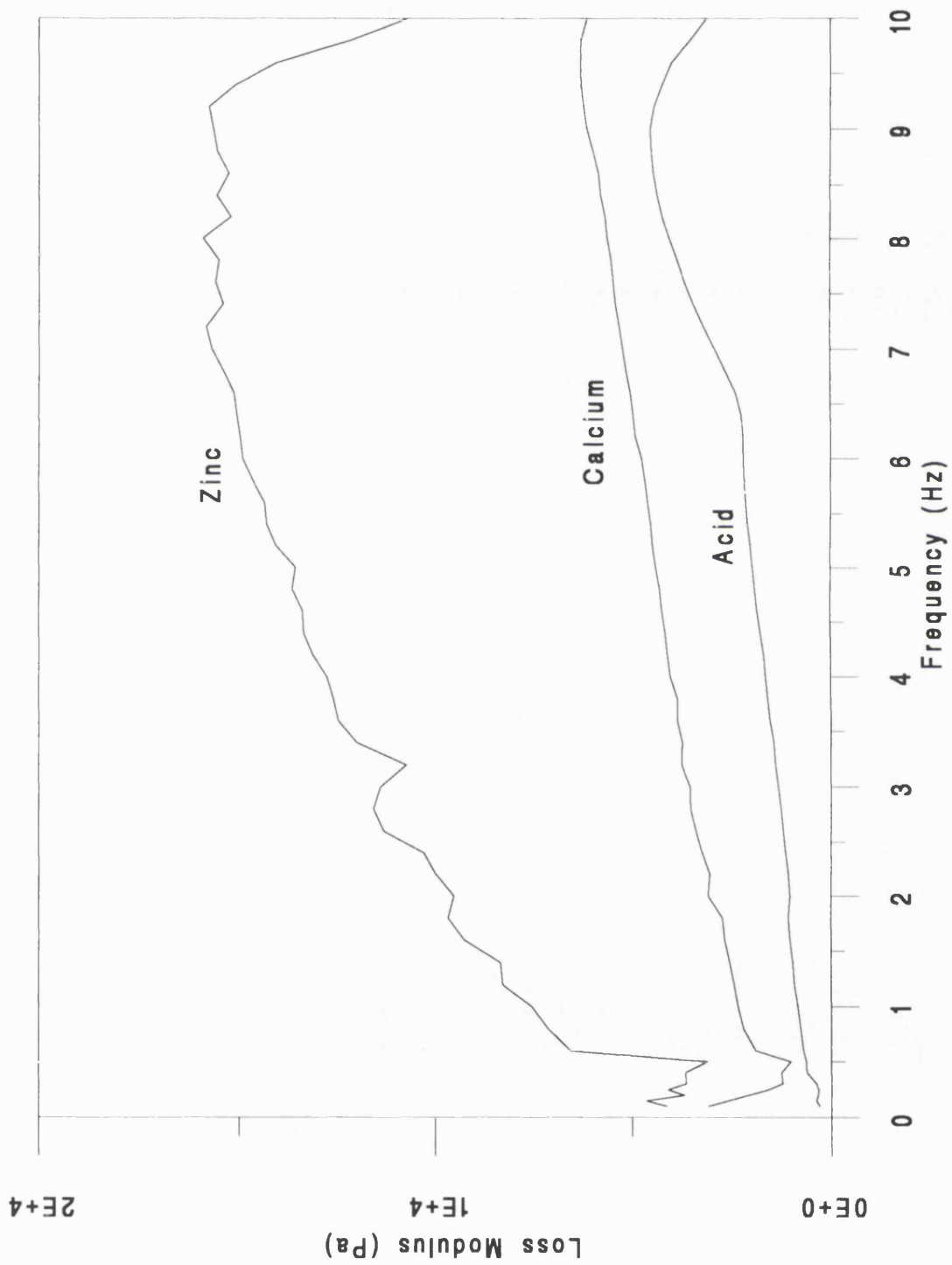

Figure 4.10(d) : Variation of loss modulus with frequency for LFR 5/60 + pectin gels

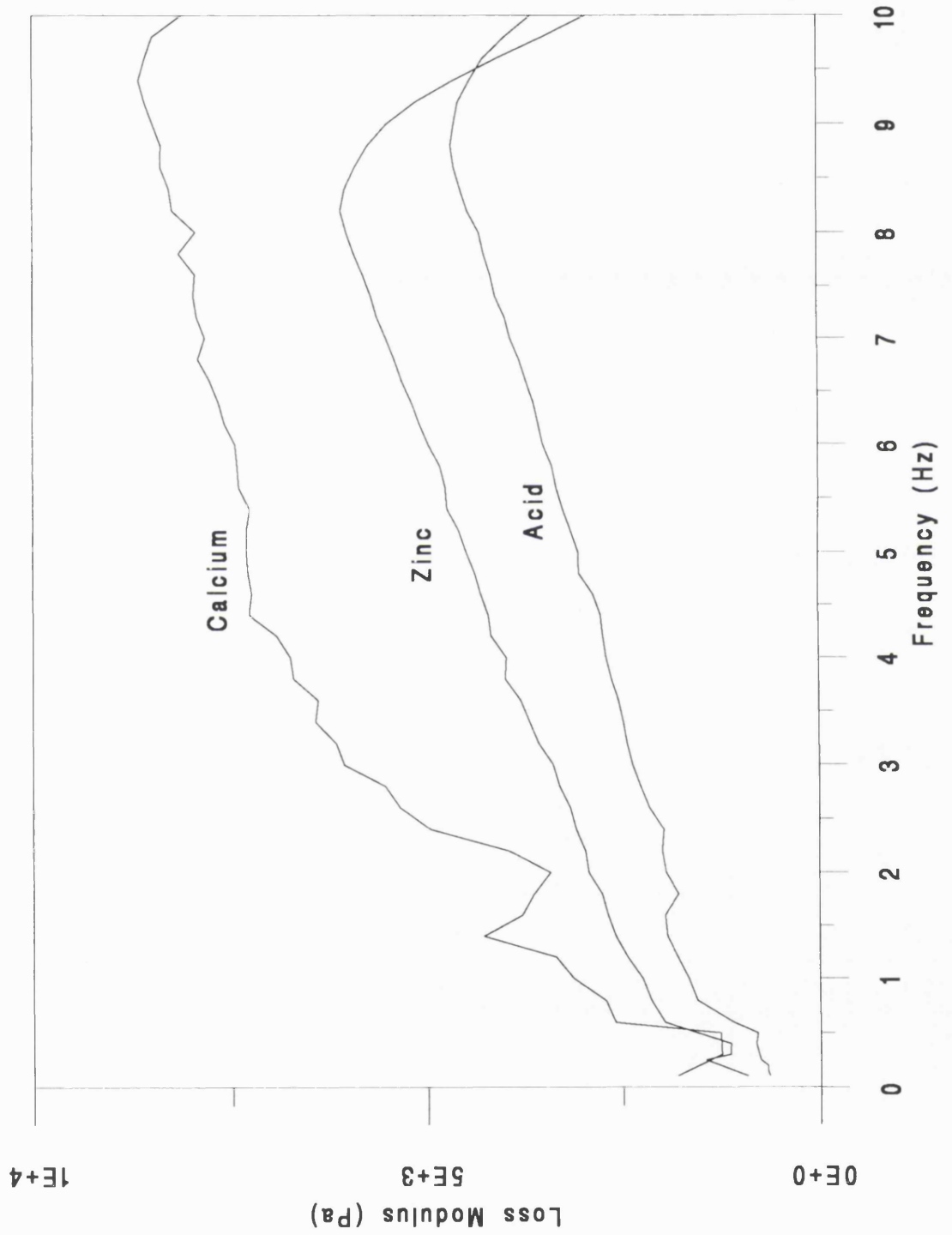

Table 4.10 : Frequency scan data for calcium gels.

Alginate	%G (NMR)	Mean storage modulus ($Pa \times 10^4$) ± sd at 4Hz	Mean loss modulus ($Pa \times 10^4$) ± sd at 4Hz	Tan δ at 4Hz	Frequency of tan δ maximum
LFR 5/60	67.2	5.89 ± 1.9	5.37 ± 2.2	0.87	8.5 ± 0.23
LF 120M	42.4	4.63 ± 0.48	3.28 ± 0.52	0.71	8.5 ± 0.06
LF 10/40RB	50.9	4.18 ± 1.5	3.51 ± 1.5	0.83	8.9 ± 0.38
LFR 5/60 + Pectin	-	4.76 ± 0.55	3.88 ± 0.69	0.82	8.6 ± 0.25
Pectin	-	1.31 ± 0.87	1.04 ± 0.46	0.91	6.4 ± 0.54

Table 4.11 : Frequency scan data for zinc gels.

Alginate	%G (NMR)	Mean storage modulus (Pa x10^4) ± sd at 4Hz	Mean loss modulus (Pa x10^4) ± sd at 4Hz	Tan δ at 4Hz	Frequency of tan δ maximum
LFR 5/60	67.2	2.60 ± 0.66	2.10 ± 0.43	0.81	8.4 ± 0.55
LF 120M	42.4	6.15 ± 2.1	5.14 ± 1.1	0.84	8.8 ± 0.42
LF 10/40RB	50.9	8.94 ± 1.2	6.16 ± 1.2	0.69	9.3 ± 0.10
LFR 5/60 + Pectin	-	2.57 ± 0.14	2.47 ± 0.69	0.96	8.0 ± 0.01
Pectin	-	2.14 ± 0.84	1.70 ± 0.36	0.84	7.2 ± 0.16

Table 4.12 : Frequency scan data for acid gels.

Alginate	%G (NMR)	Mean storage modulus ($Pa \times 10^4$) ± sd at 4Hz	Mean loss modulus ($Pa \times 10^4$) ± sd at 4Hz	Tan δ at 4Hz	Frequency of tan δ maximum
LFR 5/60	67.2	0.797 ± 0.14	0.725 ± 0.10	0.91	6.9 ± 0.35
LF 120M	42.4	0.84 ± 0.07	0.92 ± 0.02	1.10	6.6 ± 0.08
LF 10/40RB	50.9	1.00 ± 0.13	0.89 ± 0.09	0.89	6.7 ± 0.27
LFR 5/60 + Pectin	-	3.03 ± 0.64	1.94 ± 0.37	0.64	8.2 ± 0.21

alone. Firstly the tan δ maximum of the mixture is at a higher frequency than the other gels and secondly at 4Hz the tan δ of the mixture is considerably lower than that of the other gels.

Generally the frequency scans do not show large differences in tan δ or in the storage and loss moduli for calcium gels. In the zinc gels a drop in tan δ was seen for the alginate LF 10/40RB, but in general this method seems less discriminatory than the creep-recovery and clear trends are difficult to discern. It is not clear what causes the tan δ maximum which can be determined by this method.

4.5 DISCUSSION

The results from the stress scan experiments show that the gels under investigation behave in a manner typical of many viscoelastic materials. The values of the viscoelastic limit obtained allowed a value of 5mN to be chosen as a useful working limit for the creep-recovery and frequency scan experiments. The stress scan results also give an insight into the rank order of gel rigidity; the acid gels showed a greater deformation than the ionic gels, whilst the gels formed with LF 120M showed a greater resistance to deformation than the LFR 5/60 or LF 10/40RB gels.

The creep-recovery data provided a useful means of characterising the alginate gels, allowing an insight into the elastic and viscous behaviour of the systems. This was probably the most informative of the tests used showing that the acid gels produced a larger deformation but with a greater degree of elastic behaviour than the ionic gels and hence showed greater recovery. The alginate LF 120M again showed a lower deformation than either LFR 5/60 or LF 10/40RB. The addition of pectin to LFR 5/60 increases the instantaneous compliance and the Newtonian viscosity of the ionic gels. However, in the acidic gels the instantaneous compliance is decreased by the addition of pectin to LFR 5/60 whereas the Newtonian viscosity is again increased. In all cases

the Newtonian viscosity of the gels formed by the action of a divalent cation is greater than that of the gels formed by the action of acid.

From the frequency scan data it is more difficult to ascertain definite trends. A tan δ maximum was detected which has not previously been described in alginate gels, however, more work is necessary in order to interpret this feature. In general there is some evidence for synergy between LFR 5/60 and pectin, this is mostly in the gels with calcium and the data is often contradictory.

Little information is available on the viscosity of this type of gel because of the difficulties in measurement. The use of dynamic mechanical analysis in this study therefore represents a novel approach to the characterisation of rigid alginate gels.

CHAPTER 5

CHAPTER 5: CHARACTERISATION OF ALGINATE RAFTS.

5.1 INTRODUCTION

The *in vitro* testing of anti-reflux agents can be approached in one of two ways. The first method of testing involves measuring the neutralising capacity of the antacid preparation. This method was described by Rossett and Rice (1954) and is the standard for all types of antacid preparations, as described in Chapter 1.5.2. The limitation with this method is that the test involves vigorous agitation of the test mixture which does not allow raft formation in the alginate preparations under investigation. A modification of this method was used by Washington et al (1985) although this method, like the Rossett and Rice (1954) test, only measures the neutralising capacity of the antacid, whereas the effectiveness of alginate raft preparations is due to the physical presence of the foam floating on the stomach contents (Malmud et al, 1979; May et al, 1984). The other method for assessing antacid products, particularly applicable to alginate preparations, is the measurement of the physical parameters relating to the strength of the rafts formed. It is more appropriate in this case to investigate the strengths of the rafts formed as this information will be of more direct relevance in the assessment of various raft forming preparations.

In the previous two chapters the ways in which the components of alginate rafts can be characterised have been investigated. To be able to use this information to gain an insight into the ways in which changing the formulation will affect the raft structure, it is important to be able to measure certain properties of the rafts themselves. Three different properties of the raft have been investigated and the results of these techniques will be presented here.

The first property to be studied is the thickness of the rafts formed. Raft thickness was investigated by Patel (1991); it was shown that raft thickness tended to decrease with increasing acid strength in rafts formed from two commercial preparations. The other product tested, a commercial preparation

containing magnesium carbonate, showed no significant variation over the pH range investigated.

The second property of the rafts to be studied was the strength of the rafts. Washington et al (1986) described the measurement of the breaking strength of alginate rafts using a piece of apparatus designed for this purpose, as described in Chapter 5.3.1. The equipment used in the present study of raft strength was the Stable Microsystems TA.XT2 texture analyser, which constitutes a new approach to the problem of measuring the properties of such systems. This equipment has many advantages over the apparatus described by Washington et al (1986), particularly in terms of the reproducibility of results and the increased amount of data available from each experiment, as well as advantages in data handling provided by the Xtra Dimension software.

The final characteristic of the rafts which was studied was the nature of the bubbles entrapped by the gel. An alginate raft consists of the insoluble alginate material, which has been investigated in the previous sections, and the bubbles which are formed by the action of the acid on the bicarbonate. It is these entrapped bubbles which give the raft buoyancy and hence cause the raft to float on the stomach contents. However, the bubbles in rafts have not in themselves been previously studied. To this end various raft formulations were studied using image analysis to facilitate the counting and measurement of the bubbles.

5.2 RAFT THICKNESS

5.2.1 Theory

When observing various alginate rafts formed *in vitro* it can be seen that the rafts vary in thickness depending on the formulation used and the conditions under which the rafts are formed. Patel (1991) showed the way in which the thickness of rafts generated by some commercial preparations varied with the strength of the acid in which they were formed. The rafts produced by Algitec

and Gaviscon suspensions were found to produce rafts of decreasing thickness with an increase in acid strength. This trend was not seen in rafts produced from Algicon suspension, a magnesium containing preparation, which showed no significant variation in raft thickness over the pH range under investigation.

An alginate raft formed on top of hydrochloric acid will tend to cover the surface of the acid if there is sufficient raft forming mixture present. It is therefore important when measuring raft thickness to standardise the conditions under which the rafts are formed. It was noticed that as well as variations in the thickness of the raft there are also differences in the height of the contents of the cylinder after raft formation, thus in the present study the volume of the cylinder contents was recorded along with the thickness of the rafts. The volume of acid and that of the raft forming mixture were constant therefore differences in the total volume of the cylinder contents must be due to differences in the rafts.

Both gel formation and carbon dioxide entrapment cause an increase in the total volume of the contents of the cylinder, however these two processes are linked since the ability of the raft to trap carbon dioxide is dependent on the relative speeds of gas generation and gelation. If the gas is produced too quickly it will not be contained by the gel and hence a larger proportion will be lost. However, if gas production is too slow relative to the speed of gelation the alginate gel will be too viscous to entrap the carbon dioxide as it is formed. It is therefore reasonable to assume that both the raft thickness and the total volume of the cylinder will be affected by the processes of gelation and carbon dioxide production.

5.2.2 Method

A standard method of measuring the thickness of the rafts was needed as preliminary qualitative experiments showed that the thickness of a raft is dependent on the surface area of the acid, and hence the size and shape of

the container in which the raft forms. Measurement of raft thickness during the texture analysis experiments would have proved difficult and less accurate than making separate measurements due to the presence of the probe. All the rafts for thickness measurement were formed in the same 25ml pyrex measuring cylinder. Two ml of the raft forming mixture, prepared as described in Chapter 2.2.4, was added to 10ml HCl at 37°C. The raft was allowed to form for 10 minutes without agitation. The thickness of the raft was measured at three places around the cylinder with a 30cm perspex ruler and the total height of the cylinder contents was also noted. Three measurements were made for each of the formulations, and the mean of the three samples is given. The parameters recorded in the results section are the raft thickness and the increase in volume of the contents of the cylinder. The increase in volume was determined by measuring the volume of the contents of the cylinder after raft formation and subtracting the volume of acid and raft forming mixture from this value.

5.2.3 Results

5.2.3.1 The effect of time on the formation of LFR 5/60 rafts

The effect of time on the formation of alginate rafts was investigated. The rafts were formed in 0.1M HCl with LFR 5/60 mixtures as previously described. Measurements were taken 1,5,10,15 and 20 minutes after addition of the raft forming mixture to the acid. The way in which the thickness of the various rafts varies with time is shown in Figure 5.1.

The graph of raft thickness with time shows a general decrease in thickness over the time period investigated. The thickest rafts were those containing calcium carbonate, with the potassium bicarbonate raft showing a greater decrease in thickness with time than the sodium bicarbonate raft. The zinc containing rafts are the next thickest, however, the sodium and zinc raft falls to a similar size to that with sodium bicarbonate alone. The rafts formed with the addition of magnesium carbonate to the mixture are the thinnest and show the

Figure 5.1 : Graph of raft thickness against time for various LFR 5/60 formulations

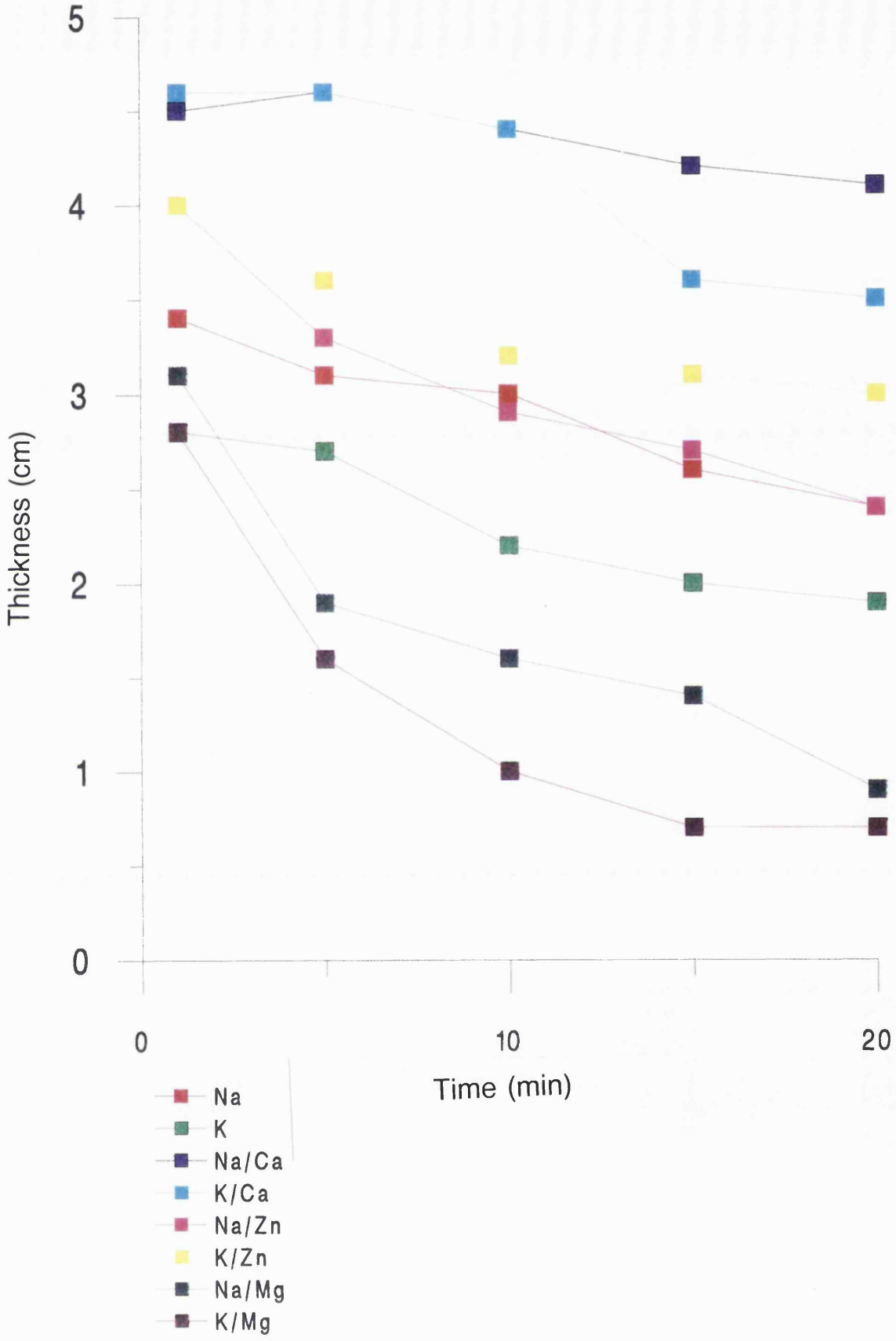

most rapid decrease in thickness with time. From the results shown in Figure 5.1 it can be seen that the most rapid changes in raft thickness occur shortly after the raft forming mixture has been added to the acid. Alginate raft system are dynamic systems, hence it is important to make measurements at a specified time after the raft formation begins. In order to standardise the measurement conditions a formation time of 10 minutes was chosen for the subsequent raft thickness and raft strength experiments.

5.2.3.2 The effect of raft forming mixture composition

The way in which the thickness of the raft and the resulting increase in volume is affected by the alginate used in the mixture was investigated. The alginates used are described in Chapter 2.1.1. The raft forming mixtures were prepared as described in Chapter 2.2.4, and the acid used for raft formation was 0.1M HCl. Table 5.1 shows the thickness of the rafts formed from the various formulations of the five alginate samples under investigation. The corresponding data for the increase in volume of the rafts are given in Table 5.2.

There are some general trends which can be seen in both the thickness data and the increase in volume data. All rafts have a greater increase in volume and thickness with the addition of either calcium or zinc carbonate compared to the rafts formed with the alginate and bicarbonate alone. When comparing rafts formed without the addition of a carbonate the rafts are thicker with sodium than potassium bicarbonate, except in the rafts formed from a mixture of pectin and an alginate where the potassium rafts are thicker than the sodium. The data for the increase in volume does not show the same trend, which suggests that there is no simple link between the thickness of the raft and the increase in volume it produces.

The addition of calcium carbonate to the raft forming mixtures causes the rafts to be thicker and promote a larger increase in volume compared with those

Table 5.1 : The thickness of rafts formed with various alginates

Alginate	%G (NMR)	Thickness (cm) ± s.d.					
		$NaHCO_3$	$KHCO_3$	$NaHCO_3$ + $CaCO_3$	$KHCO_3$ + $CaCO_3$	$NaHCO_3$ + $ZnCO_3$	$KHCO_3$ + $ZnCO_3$
LFR 5/60	67.2	3.0 ± 0.12	2.2 ± 0.17	4.4 ± 0.05	4.4 ± 0.12	2.9 ± 0.14	3.2 ± 0.17
LF 20/200	67.0	2.0 ± 0.09	1.7 ± 0.05	2.2 ± 0.12	2.4 ± 0.12	2.8 ± 0.17	2.6 ± 0.10
LF 200DL	55.1	1.6 ± 0.04	1.5 ± 0.05	1.9 ± 0.10	2.3 ± 0.07	1.5 ± 0.10	2.2 ± 0.07
LF 10/40RB	50.9	3.0 ± 0.07	2.1 ± 0.10	3.5 ± 0.16	2.4 ± 0.10	3.3 ± 0.12	2.6 ± 0.12
LF 120M	42.4	2.0 ± 0.10	1.9 ± 0.09	3.1 ± 0.06	1.9 ± 0.10	2.6 ± 0.04	2.4 ± 0.14
LFR 5/60 + Pectin	-	3.9 ± 0.12	4.6 ± 0.05	4.6 ± 0.05	5.1 ± 0.12	3.1 ± 0.17	3.2 ± 0.07
LF 120M + Pectin	-	3.3 ± 0.12	3.5 ± 0.10	4.4 ± 0.10	3.4 ± 0.17	3.6 ± 0.12	3.1 ± 0.10

Table 5.2 : The increase in volume of rafts formed with various alginates

Alginate	%G (NMR)	Increase in volume (ml)					
		$NaHCO_3$	$KHCO_3$	$NaHCO_3$ + $CaCO_3$	$KHCO_3$ + $CaCO_3$	$NaHCO_3$ + $ZnCO_3$	$KHCO_3$ + $ZnCO_3$
LFR 5/60	67.2	2.5	2.5	6.0	5.5	4.0	4.5
LF 20/200	67.0	1.0	1.5	2.0	2.5	2.5	2.5
LF 200DL	55.1	2.0	1.0	2.0	3.0	2.0	3.0
LF 10/40RB	50.9	2.5	1.5	3.5	3.0	3.5	3.5
LF 120M	42.4	1.0	1.5	4.0	2.5	2.5	3.0
LFR 5/60 + Pectin	-	2.5	3.0	6.5	4.5	4.0	4.0
LF 120M + Pectin	-	2.0	1.5	6.0	4.0	4.5	4.0

rafts formed without an additional carbonate in all cases. The bicarbonate used has an effect on both the thickness and the increase in volume, although the trends seem to suggest that potassium bicarbonate gives a thicker raft whilst sodium bicarbonate tends to have a greater effect on the increase in volume.

Zinc carbonate has a similar effect to that of calcium carbonate, although not so marked. The difference between the rafts formed with the two bicarbonates shows the thickness to follow the same trend as with calcium carbonate, that is the rafts are thicker with potassium bicarbonate except for LF 10/40RB, and LF 120M both with and without pectin. The increase in volume data shows little difference between the raft formed with either of the bicarbonates.

The addition of pectin to both LFR 5/60 and LF 120M produces an increase in thickness for all formulations except one which is unaltered. The increase in volume data shows that the LF 120M and pectin mixture gives a greater increase in volume compared to the LF 120M alone. However, the rafts formed with LFR 5/60 and pectin show no marked difference form those rafts formed from LFR 5/60 without pectin.

The alginate used in the raft forming mixture affects the thickness seen in the rafts. In the majority of the formulations used in this study the thickness of the alginate rafts formed falls into the rank order: LFR 5/60 > LF 10/40RB > LF 20/200 > LF 120M > LF 200DL.

5.2.3.3 The effect of acid strength on LFR 5/60 rafts

The way in which the thickness and increase in volume of rafts formed from LFR 5/60 mixtures vary with acid strength was investigated. The mixtures used contained either sodium or potassium bicarbonate, and where indicated calcium, zinc or magnesium carbonate. Table 5.3 shows the effect of acid strength on the thickness of rafts formed with LFR 5/60, an alginate with 67% guluronic acid residues. The corresponding increase in volume data are given

Table 5.3 : The effect of acid strength on raft thickness for LFR 5/60 mixtures

Additions to LFR 5/60 solution	Raft Thickness (cm)		
	0.1M HCl	0.07M HCl	0.05M HCl
$NaHCO_3$	3.0 ± 0.12	1.6 ± 0.08	1.0 ± 0.05
$KHCO_3$	2.2 ± 0.17	2.0 ± 0.05	1.5 ± 0.05
$NaHCO_3$+ $CaCO_3$	4.4 ± 0.05	2.4 ± 0.05	1.3 ± 0.04
$KHCO_3$ + $CaCO_3$	4.4 ± 0.12	2.5 ± 0.10	1.3 ± 0.07
$NaHCO_3$+ $ZnCO_3$	2.9 ± 0.14	1.5 ± 0.07	0.8 ± 0.05
$KHCO_3$ + $ZnCO_3$	3.2 ± 0.17	1.9 ± 0.10	1.1 ± 0.06
$NaHCO_3$ + $MgCO_3$	1.6 ± 0.05	1.1 ± 0.10	0.4 ± 0.05
$KHCO_3$ + $MgCO_3$	1.0 ± 0.04	1.2 ± 0.12	0.9 ± 0.05

Table 5.4 : The effect of acid strength on the increase in volume for LFR 5/60 mixtures

Additions to LFR 5/60 solution	Increase in volume (ml)		
	0.1M HCl	0.07M HCl	0.05M HCl
$NaHCO_3$	2.5	2.0	1.5
$KHCO_3$	2.5	1.5	1.0
$NaHCO_3 + CaCO_3$	6.0	3.0	1.5
$KHCO_3 + CaCO_3$	5.5	3.5	1.5
$NaHCO_3 + ZnCO_3$	4.0	2.0	1.0
$KHCO_3 + ZnCO_3$	4.5	2.0	1.0
$NaHCO_3 + MgCO_3$	2.5	1.5	1.0
$KHCO_3 + MgCO_3$	1.5	2.5	1.5

in Table 5.4. The data given are the means of three measurements for each of the variables ± the standard deviation. The thickness results show that in general thickness decreases with a decrease in the molarity of the HCl; this trend is repeated in the data given in Table 5.4 for the increase in volume of the contents of the cylinder on raft formation. This is not the same as the effect shown by Patel (1991) who found that the thickness of the rafts formed by two of the commercial preparations investigated, Gaviscon and Algitec, tended to decrease with an increase in molarity of HCl and the third product investigated, Algicon, was not significantly affected by the strength of the acid. It is difficult to compare these measurements directly with those shown here as the formation conditions are different. Patel (1991) used a 250ml pyrex beaker containing 125ml of HCl in which to form the rafts and 10ml of each of the commercial products. The formation time used by Patel (1991) was 20 minutes which is twice that used in the present study and the formation time has been shown to affect raft thickness, as described in Chapter 5.2.3.1.

It is interesting to note that the formulations are not equally affected by the change in the pH of the acid medium. The rafts containing either calcium or zinc carbonate show a greater decrease in raft thickness with acid strength than the rafts formed without the addition of a carbonate. No clear trend can be seen in the rafts formed with the addition of magnesium carbonate as they are affected by varying amounts and they are the thinnest rafts, producing the smallest increase in volume of those studied.

The variation in the thickness of the rafts formed in different acid strengths shows that the experimental conditions are important in the formation of alginate rafts and that a known acid strength should be used for experimentation.

Table 5.5 : The effect of acid strength on raft thickness for LFR 5/60 and Pectin mixtures

Additions to LFR 5/60 + pectin solution	Raft Thickness (cm)		
	0.1M HCl	0.07M HCl	0.05M HCl
$NaHCO_3$	3.9 ± 0.12	3.6 ± 0.13	2.9 ± 0.09
$KHCO_3$	4.6 ± 0.05	4.4 ± 0.09	4.0 ± 0.10
$NaHCO_3 + CaCO_3$	4.6 ± 0.10	3.6 ± 0.10	2.4 ± 0.10
$KHCO_3 + CaCO_3$	5.1 ± 0.12	4.1 ± 0.10	3.5 ± 0.11
$NaHCO_3 + ZnCO_3$	3.1 ± 0.17	2.8 ± 0.12	1.8 ± 0.12
$KHCO_3 + ZnCO_3$	3.2 ± 0.07	2.8 ± 0.07	2.0 ± 0.07
$NaHCO_3 + MgCO_3$	3.3 ± 0.12	2.3 ± 0.05	1.8 ± 0.05
$KHCO_3 + MgCO_3$	4.7 ± 0.10	3.6 ± 0.04	2.5 ± 0.10

Table 5.6 : The effect of acid strength on the increase in volume for LFR 5/60 and Pectin mixtures

Additions to LFR 5/60 + pectin solution	Increase in volume (ml)		
	0.1M HCl	0.07M HCl	0.05M HCl
$NaHCO_3$	2.5	2.0	1.0
$KHCO_3$	3.0	2.0	1.0
$NaHCO_3 + CaCO_3$	6.5	3.5	1.5
$KHCO_3 + CaCO_3$	4.5	3.0	1.0
$NaHCO_3 + ZnCO_3$	4.0	2.5	1.0
$KHCO_3 + ZnCO_3$	4.0	2.0	1.0
$NaHCO_3 + MgCO_3$	3.5	2.5	1.5
$KHCO_3 + MgCO_3$	3.0	2.0	1.0

The same measurements of raft thickness and increase in volume were made for raft forming mixtures containing the alginate LFR 5/60 and pectin. Table 5.5 shows the thickness data for the various alginate/pectin raft formulations and the effect of acid strength on these formulations. The increase in volume has been calculated for each of the rafts and is shown in Table 5.6.

These results show that as with the alginate formulations without pectin, the thickness of the rafts decreases with a decrease in acid strength. The rafts formed with pectin are thicker than those containing alginate alone. The addition of calcium and zinc carbonates to the formulations tends to increase the thickness, and gives a greater increase in volume compared with the mixtures with no added carbonate. The addition of magnesium carbonate to the alginate/pectin rafts does not seem to have such a deleterious effect as on the rafts formed with alginate alone. It would also appear that the alginate/pectin rafts formed with potassium bicarbonate as opposed to sodium bicarbonate gave thicker rafts; this was more marked than in the rafts not containing pectin.

The rafts formed with the addition of pectin again showed that the acid strength had a greater effect on those rafts containing either calcium or zinc carbonate compared to those without an added carbonate. However, this effect was less pronounced in the rafts including pectin than was seen in those composed of LFR 5/60 alone.

5.3 TEXTURE ANALYSIS

5.3.1 Theory

The second method of testing is more directly relevant to raft forming preparations, as it involves measuring the strength of a raft formed under a range of conditions. The measurement of raft strength has been carried out using a piece of equipment described by Washington et al (1986). This equipment comprises of a modified beam balance with a probe suspended from

Figure 5.2 : Apparatus for measuring raft strength (Patel, 1991)

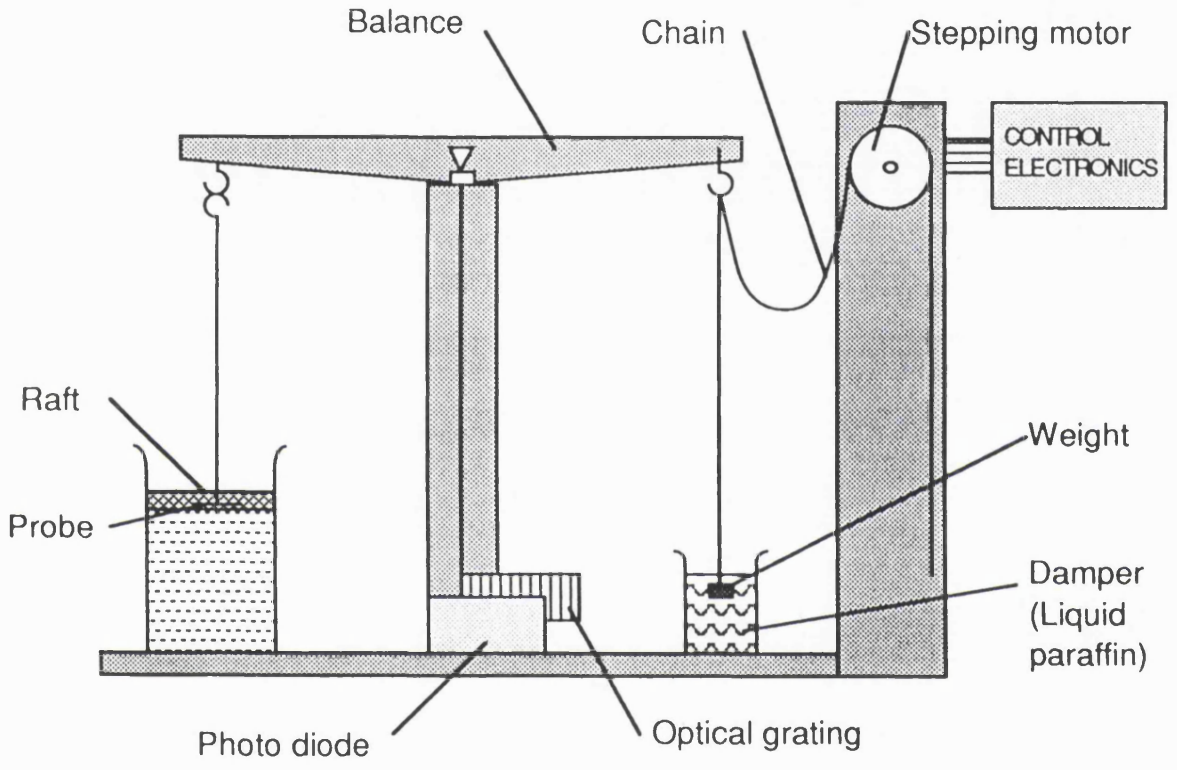

one arm and a length of chain attached to the other arm as shown in Figure 5.2. The load on the probe is determined by the length of the chain which is controlled by a stepping motor. The stepping motor is driven by a microcomputer which also collects information on the deflection of the beam from an optical grating and light beam arrangement. With this equipment it is possible to measure the force required to cause the raft to rupture. This force value is termed the raft strength and is dependent on the size and shape on the probe used. The apparatus designed by Washington et al (1986) has been used in the investigation of different formulations of Gaviscon (Washington, 1986), who showed that the inclusion of calcium into the formulation increased the raft strength while antacids such as aluminium hydroxide reduced it. The same experimental set up was used by Patel (1991) in an investigation into the effect of acid strength on raft formation. The author showed that raft strength increases with increasing acid strength and that calcium containing rafts were stronger than those with added magnesium. The alginate used in the basic raft formulation, containing sodium bicarbonate and no additional ions, was shown to have little effect on the strength of the raft formed.

In the present investigation the Stable Microsystems TA.XT2 Texture Analyser, as shown in Figure 5.3, was used to move a probe through the alginate raft. The TA.XT2 has been used in various applications in the food and pharmaceutical industries for the routine testing of a variety of products with a range of characteristics. There is no published data to suggest that the texture analyser has been used in the characterisation of alginate rafts. It has been used in the food industry to perform similar tests and within pharmaceutical field it has been used in mucoadhesive research (Tobyn et al, 1993). The TA.XT2 has advantages over the apparatus described by Washington et al (1986), particularly in the ease of calibration. The calibration of the Washington apparatus involves plotting the number of optic counts against the number of motor pulses under various conditions. The mass of the chain displaced by the sprocket wheel must also be calculated in order to determine the weight applied per motor pulse. The method for calibration of equipment of this type is

Figure 5.3 : The Stable Microsystems TA.XT2 texture analyser

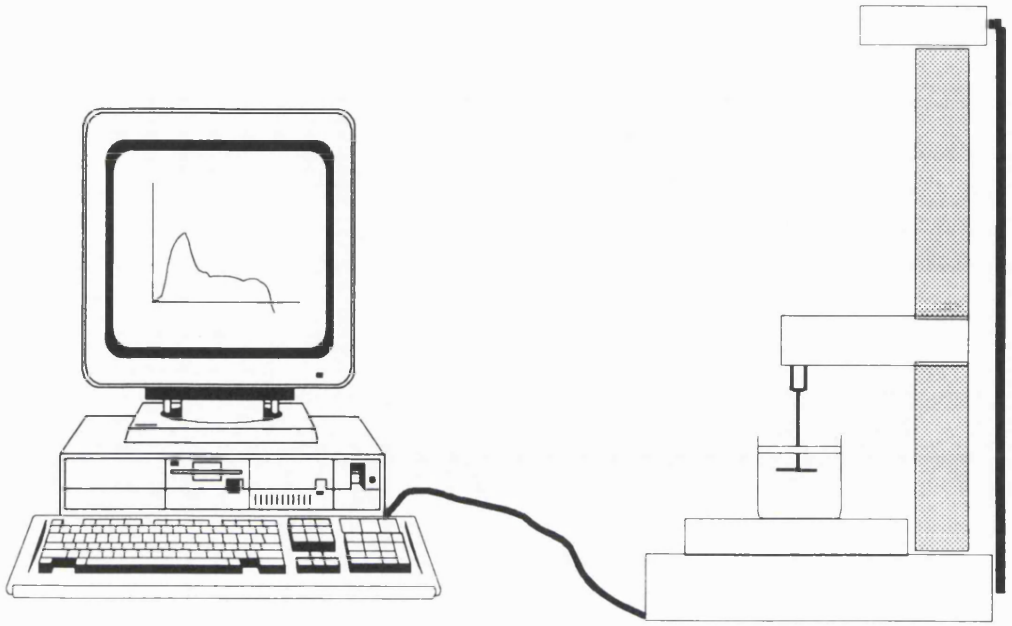

Figure 5.4 : The probe used in the texture analysis experiments

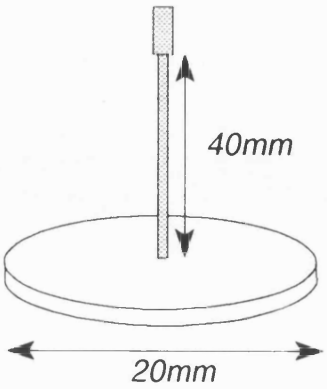

described by Patel (1991). Calibration of the Stable Microsystems TA.XT2 texture analyser is by means of an external standard weight and internal software checks. The use of an external standard weight for calibration purposes ensures that results from different machines will be comparable providing that the experiments are carried out using the same method.

The TA.XT2 texture analyser records and plots the force on the probe against time for the whole of the cycle. This provides not only the maximum force exerted on the raft before it begins to rupture, but also it gives the potential to determine the work done in breaking the raft; this is a parameter which was not previously determined.

Control of the TA.XT2 texture analyser is via the Xtra Dimension software which also collects and analyses the data. The sample is placed on the test platform and the probe is attached to the arm positioned above the sample. The probe is moved a pre-determined distance, at a pre-determined speed, either in tension or compression. The method, once decided on, can be entered onto the computer attached to the texture analyser, allowing the same test to be run repeatedly.

5.3.2 Method

The rafts to be tested were formed in 100ml pyrex beakers containing 20ml hydrochloric acid, which had been kept in a water bath at 37°C until immediately before the addition of the raft forming mixture. The acid used was 0.1M HCl except in the experiments where the effect of acid strength was under investigation in which case the strength of the acid used is quoted. The raft forming mixtures were prepared freshly on the day of use as described in Chapter 2.2.4. The Stable Microsystems TA.XT2 texture analyser was used in the tension mode, thus the rafts were formed with the probe *in situ* at the start position, just above the bottom of the beaker. The rafts were formed by the addition of 4ml of the raft forming mixture to the acid from a 5ml BD syringe.

The mixture was expelled from the syringe onto the surface of the acid surrounding the probe. The beaker was allowed to stand for 10 minutes without agitation to permit raft formation.

A variety of probe types were considered during the preliminary investigations of alginate rafts using the TA.XT2 texture analyser. It was decided that the best probe arrangement would be the one which gave the best resolution between a raft sample and the acid alone. The maximum force exerted on each probe was determined with an alginate raft formed with LFR 5/60 and sodium bicarbonate, and in a beaker containing acid alone. The maximum force recorded in the blank sample (acid alone) is due to the surface tension of the liquid and the way in which the material of the probe affects that surface. The metal probes used in the comparison of probe type were all stainless steel. The shape of the probe also affects the way in which it breaks the surface of the liquid. The maximum forces for the blank and the raft sample with each probe are given in Table 5.7. The blank maximum is also expressed as a percentage of the sample maximum.

Table 5.7 : Comparison of breaking strengths recorded with different probes.

Probe type	Blank max (mN)	Raft max (mN)	Percentage
Large metal ball (10mm diameter)	16.9	23.1	73.2%
Small metal ball (5mm diameter)	5.3	7.1	74.6%
Plastic flat end (10mm diameter)	21.3	29.3	72.7%
Plastic round end (10mm diameter)	14.2	17.8	79.8%
Metal disc (20mm diameter)	26.7	44.6	59.8%

It can be seen from these results that the blank is the smallest proportion of the sample response with the metal disc probe. This was, therefore, chosen for all subsequent investigations of raft characteristics. The texture analyser was set up in tension mode to travel a distance of 30mm at a constant speed of 1mm/s and then return to the start at the same speed. The probe used was a flat circular disc probe, diameter 20mm (see Figure 5.4) as this was found to give the most reproducible results. Data were collected at a rate of 50 points per second via the Xtra dimension software onto a computer.

5.3.3 Results

The parameter measured by the apparatus designed by Washington et al (1986) was the breaking strength of the raft. This can also be measured by the TA.XT2 texture analyser; however, the values of breaking strength obtained by the two methods can not be directly compared since the probes used are different in size and shape. A typical texture analysis force-time profile for an alginate raft is shown in Figure 5.5. The force increases form point A to a maximum recorded at point B which is the force required to disrupt the raft; at this point the raft is deformed to the greatest extent and the raft begins to rupture. A force-distance profile can also be produced which will be the same basic shape as the force-time profile as the probe moves at a fixed speed. The area under this can be used to determine the work done in breaking the raft. The area used is calculated from the point where the raft produces an increasing resistance on the probe, point A in Figure 5.5, to point C, where the raft is completely ruptured. A correction is made for the differences in the initial force at which the probe comes into contact with the raft. These differences are probably due to unreacted raft forming mixture remaining on the probe. The correction is made by subtracting the rectangular area under the curve. The profile contains a great deal more information than has been analysed here, however in order to relate other parameters to raft characteristics further experimental work would be necessary.

Figure 5.5 : A typical force-time profile for an alginate raft

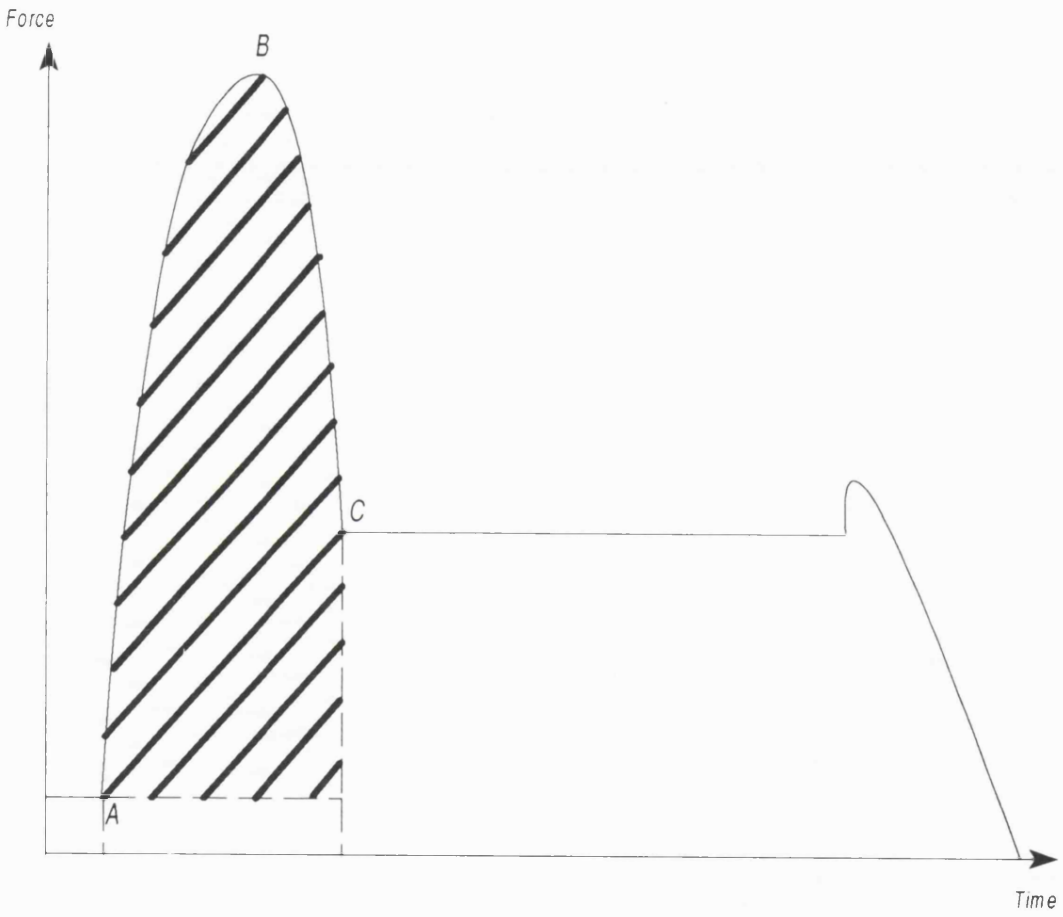

5.3.2.1 The effect of time on raft formation

Raft formation is a dynamic process, and as shown in Chapter 5.3.1.1 the thickness of the rafts is dependent on the time allowed for raft formation. In this section the breaking strength and work done in breaking rafts was investigated over a period of 20 minutes. Measurements were made after 1, 5, 10, 15 and 20 minutes. Freshly prepared rafts were used for each measurement as the process involved disrupts the raft. Three measurements were made for each condition. The rafts were formed from a range of formulations of LFR 5/60 raft forming mixtures, hence any variations in time effects on the different formulations may also be seen. Figure 5.6 shows the variation in breaking strength of LFR 5/60 rafts with time and Figure 5.7 is the corresponding graph of work done in breaking the rafts with time.

The graphs show that there is a general increase in raft strength with time in those rafts containing calcium or zinc. In the rafts which contain either magnesium or no added carbonate the raft strength tends to decrease with time, within the period of this investigation. The rate at which these changes in raft strength occur varies between formulations. The rafts formed with either sodium or potassium bicarbonate and no added carbonate appear to be least affected by the time allowed for raft formation. The rafts formed with calcium or zinc carbonate and potassium bicarbonate show a greater increase in raft strength with time than those with sodium bicarbonate. These results show an opposite tendency to that shown by the raft thickness studies, where the raft thickness tends to decrease with time over the period studied.

It seems that at a formation time of 10 minutes the raft strength parameters for each of the formulations begin to show differences due to the effects of the ingredients of the mixtures. These differences are not so easily distinguishable before this time. This shows, as with the thickness results in Chapter 5.3.1.1, that the earliest time suitable for making routine measurements on alginate rafts is 10 minutes after the addition of the raft forming mixture to the acid.

Figure 5.6 : Graph of breaking strength with time for LFR 5/60 rafts

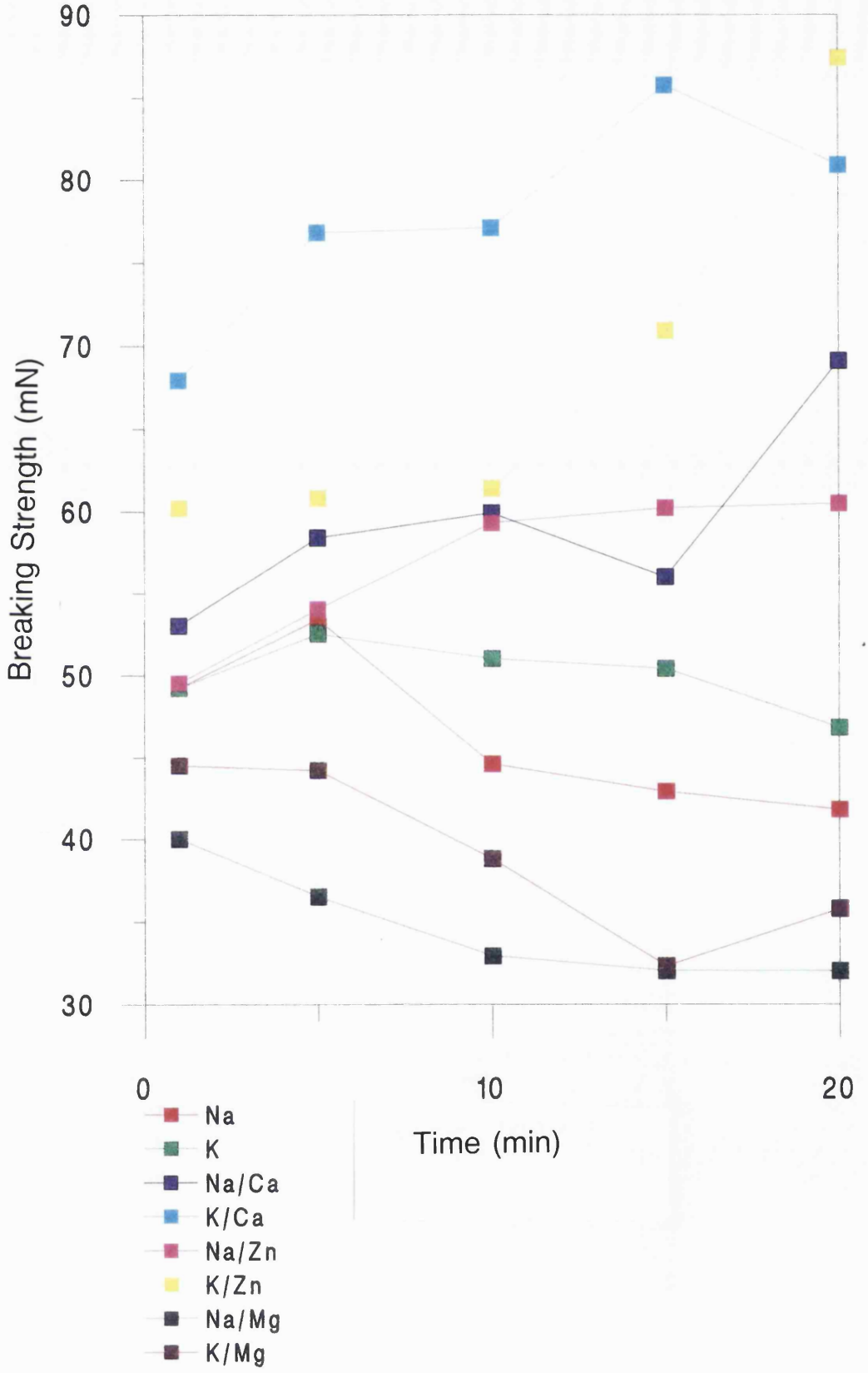

Figure 5.7 : Graph of work done with time for LFR 5/60 rafts

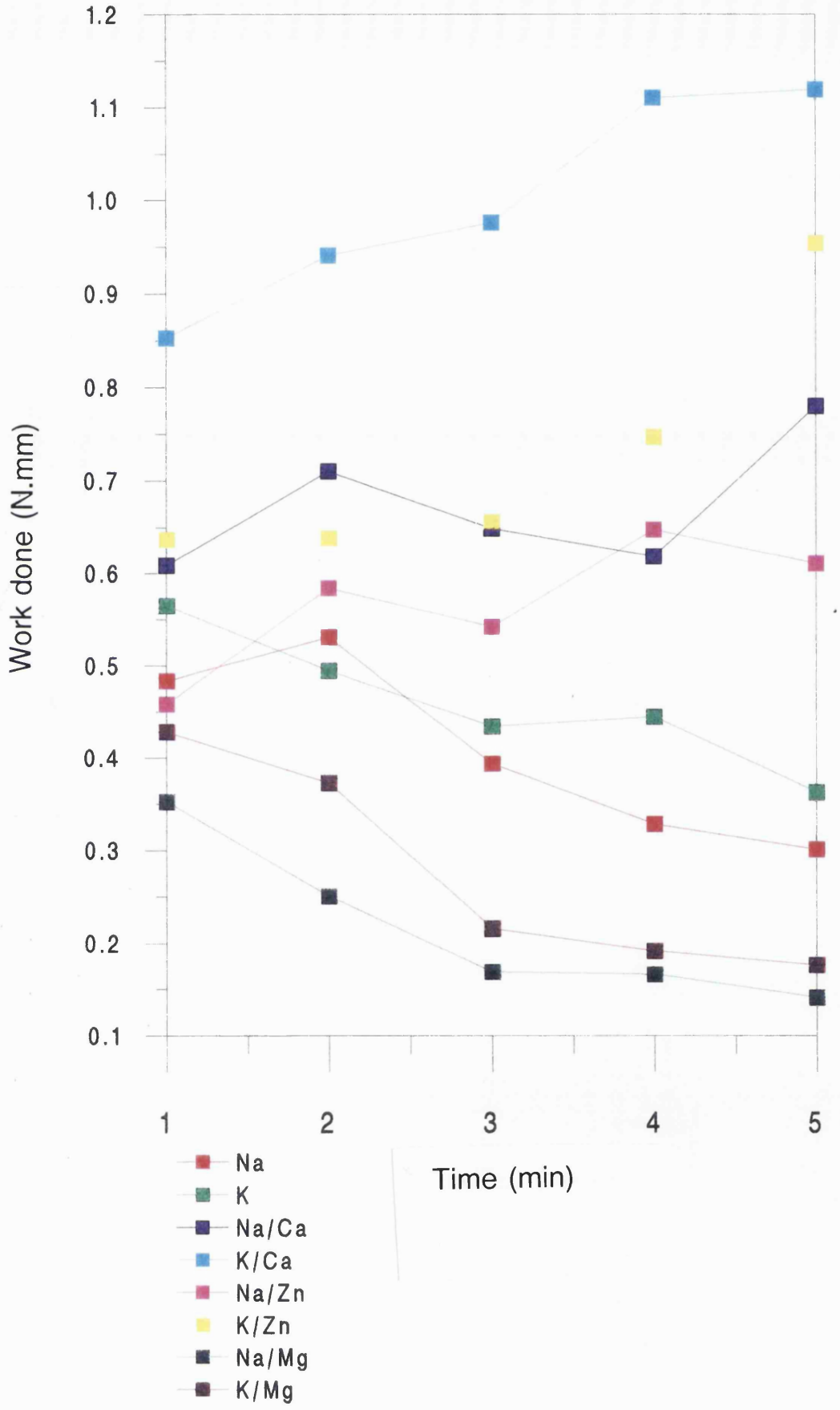

5.3.2.2 The effect of raft forming mixture composition

It has been shown in Chapter 4.4 that the different alginates investigated have different properties in the gel state. It is also known from the literature that the composition of the alginate will have an effect on how it interacts with cations (see Chapter 1.1.2.3). A part of raft formation is the gelation of the alginate, and the interaction with any cations present. It is therefore possible that the composition of the alginate used will affect the characteristics of the rafts produced.

Table 5.8 shows the breaking strength of rafts formed with the five alginates under investigation and also pectin/alginate mixtures for the highest and lowest guluronic acid content alginates. The mean work done in breaking these rafts is given in Table 5.9. These results relate to an acid strength of 0.1M HCl throughout.

The results show that there is a generally good correlation between the breaking strength and the work performed in breaking the rafts. The majority of raft forming mixtures, except those containing potassium bicarbonate and zinc carbonate, can be described in the rank order LF 20/200 > LF 10/40RB > LF 120M > LF 200DL ≥ LFR 5/60. This ranking, as shown in Figure 5.8, seems to correspond reasonably to the M/G ratio of the alginates with the higher guluronic acid content alginate giving higher values for breaking strength and work done in breaking the rafts. The exception to this is LFR 5/60 which is the highest guluronic acid content alginate but shows values similar to those of the lowest guluronic acid content alginate. This may be a reflection of the degree of polymerisation (D.P.) of the samples. Chapter 3.4.3.1 gives the D.P. for each of the samples and it shows the D.P. for LFR 5/60 to be 17.7 whereas the D.P. for the other samples is between about 200 to 300.

Figure 5.8 : Force-time profiles for five alginate rafts formed with $KHCO_3$

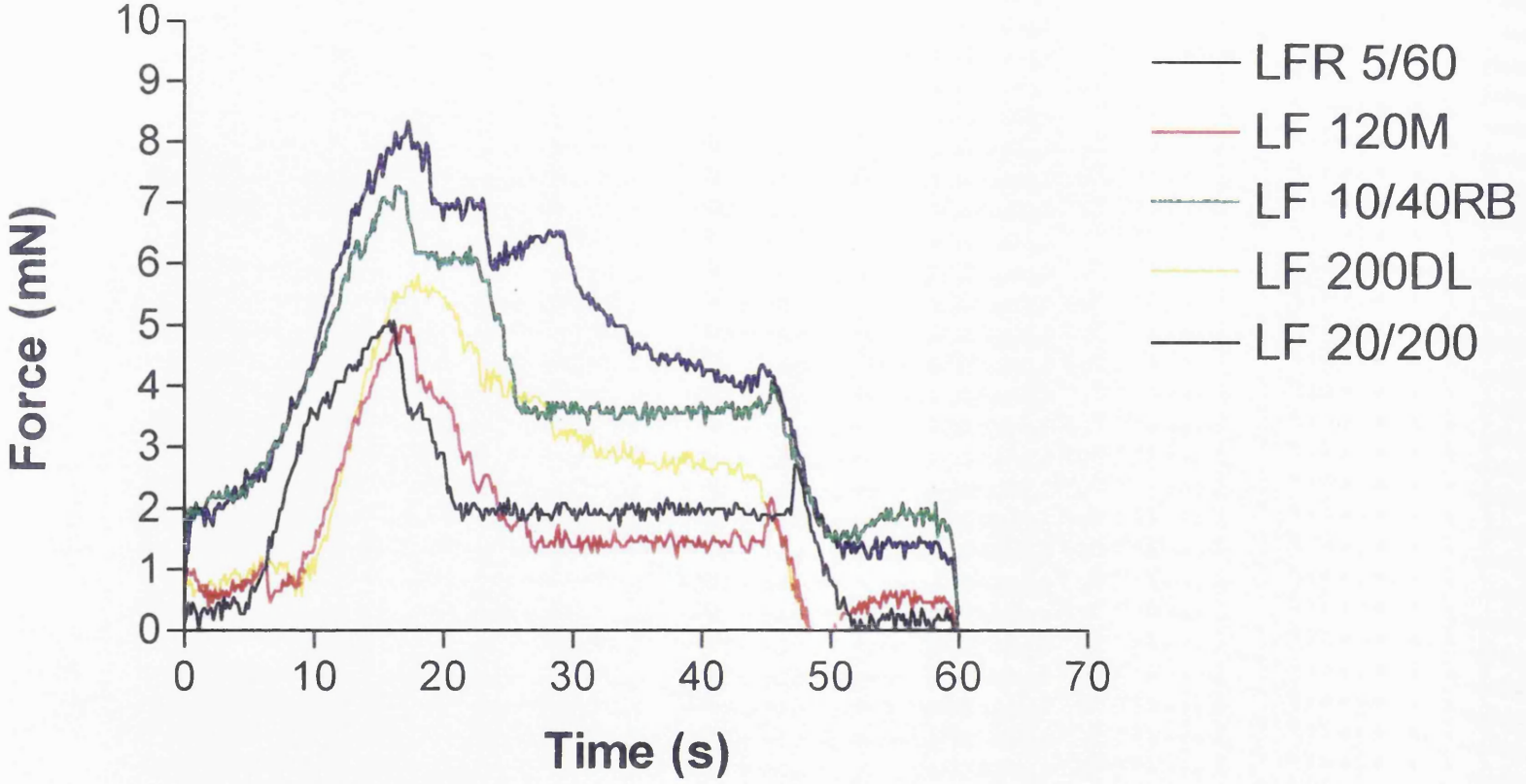

Figure 5.9 : Force-time profiles for six formulations of LF 10/40RB rafts

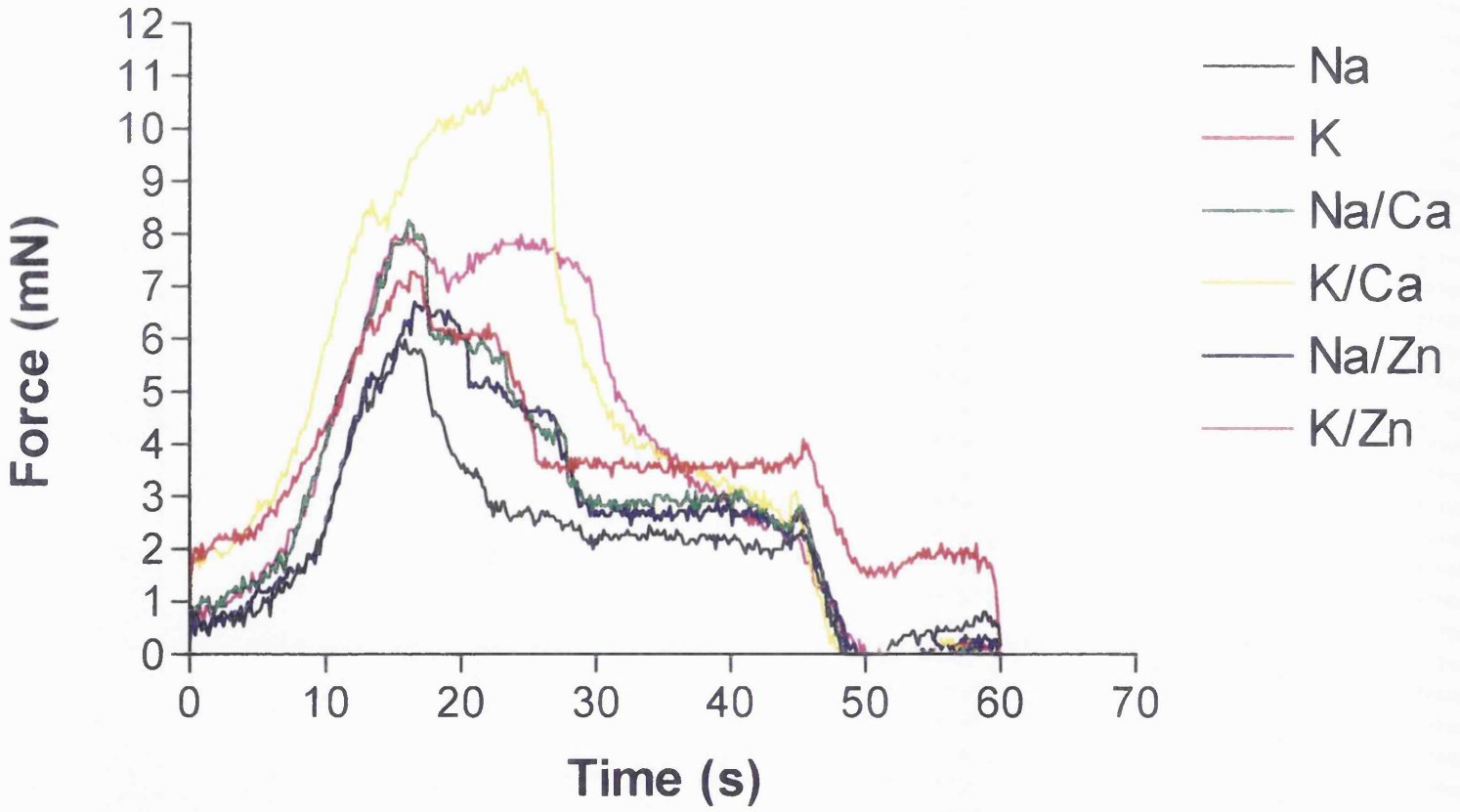

Table 5.8 : Mean breaking strength of rafts formed with five different alginates

Additions to alginate solutions	Breaking Strength (mN) ± s.d.						
	LFR 5/60	LF 20/200	LF 200DL	LF 10/40RB	LF 120M	LFR 5/60 + Pectin	LF 120M + Pectin
$NaHCO_3$	44.6 ± 1.2	63.0 ± 5.1	50.0 ± 2.2	57.1 ± 7.1	41.6 ± 3.4	81.6 ± 4.9	51.0 ± 1.7
$KHCO_3$	45.5 ± 3.5	79.8 ± 6.1	56.7 ± 2.4	75.6 ± 4.1	51.6 ± 3.5	97.3 ± 5.5	73.1 ± 4.2
$NaHCO_3$ + $CaCO_3$	58.9 ± 1.6	90.5 ± 3.7	63.5 ± 3.4	80.1 ± 9.6	74.4 ± 2.5	90.6 ± 4.5	52.4 ± 4.5
$KHCO_3$ + $CaCO_3$	62.8 ± 5.4	87.7 ± 2.9	78.4 ± 3.9	109.9 ± 3.4	89.8 ± 3.9	111.1 ± 4.8	61.0 ± 2.3
$NaHCO_3$ + $ZnCO_3$	56.5 ± 3.2	85.2 ± 4.8	54.1 ± 2.0	66.9 ± 2.3	58.0 ± 2.2	80.4 ± 4.7	46.1 ± 2.8
$KHCO_3$ + $ZnCO_3$	67.1 ± 2.3	91.2 ± 7.2	72.2 ± 3.3	82.5 ± 5.2	75.7 ± 3.1	76.1 ± 4.3	59.4 ± 3.9

Table 5.9 : Mean work done in breaking rafts formed with five different alginates.

Additions to alginate solutions	Mean work done in breaking rafts (N.mm) ± s.d.						
	LFR 5/60	LF 20/200	LF 200DL	LF 10/40RB	LF 120M	LFR 5/60 + Pectin	LF 120M + Pectin
$NaHCO_3$	0.4057± 0.070	0.8041± 0.20	0.6515± 0.18	0.5580± 0.11	0.3520± 0.045	0.9408 ± 0.099	0.5141± 0.037
$KHCO_3$	0.5000 ± 0.013	1.032 ± .024	0.8492 ± 0.10	0.8303 ± 0.16	0.5042 ± 0.054	1.242 ± 0.073	0.8630± 0.135
$NaHCO_3$ + $CaCO_3$	0.7080 ± 0.040	1.496 ± 0.15	1.210 ± 0.075	0.9573 ± 0.22	0.7043 ± 0.12	1.102 ± 0.086	0.4306± 0.034
$KHCO_3$ + $CaCO_3$	0.9390 ± 0.089	0.9456 ± 0.23	1.981 ± 0.21	1.775 ± 0.15	1.092 ± 0.22	1.479 ± 0.039	0.5099± 0.059
$NaHCO_3$ + $ZnCO_3$	0.5093 ± 0.026	1.138 ± 0.28	1.007 ± 0.11	0.6843 ± 0.085	0.5226 ± 0.035	1.004 ± 0.065	0.4840± 0.026
$KHCO_3$ + $ZnCO_3$	0.8018 ± 0.031	0.7169 ± 0.071	1.669 ± 0.21	1.319 ± 0.29	0.6829 ± 0.061	0.9981 ± 0.051	0.5174± 0.039

The inclusion of pectin into the raft forming mixtures of LFR 5/60 increases both the breaking strength and the work done in breaking the rafts of all formulations. This is not the case for raft forming mixtures of LF 120M containing pectin, which show an increase in the raft strength parameters only for those rafts without the addition of a carbonate. The addition of pectin to LF 120M rafts with calcium or zinc carbonate caused a decrease in both the breaking strength and work done in breaking the rafts compared with the LF 120M rafts without the addition of pectin.

There is a general trend between the samples which shows an overall ranking for the formulations in both the work done and breaking strength of the rafts as shown:

K/Ca > K/Zn > Na/Ca > Na/Zn > K > Na

This can be seen in Figure 5.9 where the force-time profiles for LF 10/40RB rafts are shown. This ranking does not apply to the rafts formed with the addition of pectin to either LFR 5/60 or LF 120M. The results from the rafts formed with LF 20/200 also fit less well into the ranking than the other alginate samples.

5.3.2.3 The effect of acid strength

The way in which the breaking strength of commercial alginate rafts varies with the strength of the acid in which the raft forms was investigated by Patel (1991) using apparatus similar to that used by Washington (1986). Patel (1991) showed that raft strength increases with increasing acid strength. Table 5.10 shows the effect of acid strength on the breaking strength of LFR 5/60 rafts of various compositions. The results for the work done in breaking these rafts is shown in Table 5.11. The results contained in Tables 5.12 and 5.13 show the effect of acid strength on the breaking strength and work done in breaking rafts formed from LFR /50 and pectin mixtures. The raft forming mixtures used were made as described in Chapter 2.2.4.

Table 5.10 : The effect of acid strength on the breaking strength of LFR 5/60 rafts

Additions to alginate solution	Breaking Strength (mN) ± s.d.		
	0.1M HCl	0.07M HCl	0.05M HCl
$NaHCO_3$	44.6 ± 1.2	40.3 ± 1.3	33.2 ± 1.0
$KHCO_3$	45.5 ± 3.5	43.5 ± 1.9	36.4 ± 1.9
$NaHCO_3 + CaCO_3$	58.9 ± 1.6	49.7 ± 2.6	45.2 ± 2.5
$KHCO_3 + CaCO_3$	62.8 ± 5.4	59.4 ± 2.0	46.5 ± 3.2
$NaHCO_3 + ZnCO_3$	56.5 ± 3.2	43.3 ± 1.8	35.3 ± 1.5
$KHCO_3 + ZnCO_3$	67.1 ± 2.3	52.6 ± 4.1	37.5 ± 0.6
$NaHCO_3 + MgCO_3$	38.2 ± 3.3	32.2 ± 1.3	33.3 ± 1.9
$KHCO_3 + MgCO_3$	37.9 ± 1.2	33.5 ± 1.3	33.6 ± 1.4

Table 5.11 : The effect of acid strength on the work done in breaking rafts formed from LFR 5/60 raft forming mixtures

Additions to alginate solution	Mean work done in breaking raft (N.mm) ± s.d		
	0.1M HCl	0.07M HCl	0.05M HCl
$NaHCO_3$	0.4057 ± 0.070	0.3130 ± 0.024	0.1841 ± 0.013
$KHCO_3$	0.5000 ± 0.013	0.4024 ± 0.013	0.2200 ± 0.003
$NaHCO_3 + CaCO_3$	0.7080 ± 0.040	0.5562 ± 0.054	0.2836 ± 0.024
$KHCO_3 + CaCO_3$	0.9390 ± 0.089	0.5930 ± 0.009	0.2813 ± 0.024
$NaHCO_3 + ZnCO_3$	0.5093 ± 0.026	0.2983 ± 0.022	0.1580 ± 0.008
$KHCO_3 + ZnCO_3$	0.8018 ± 0.031	0.4685 ± 0.027	0.1817 ± 0.005
$NaHCO_3 + MgCO_3$	0.2669 ± 0.045	0.1319 ± 0.014	0.1349 ± 0.008
$KHCO_3 + MgCO_3$	0.2667 ± 0.016	0.1787 ± 0.003	0.1341 ± 0.010

Table 5.12 : The effect of acid strength on the breaking strength of LFR 5/60 and pectin mixture rafts

Additions to alginate solution	Mean Breaking Strength (mN) ± s.d.		
	0.1M HCl	0.07M HCl	0.05M HCl
$NaHCO_3$	81.6 ± 4.9	60.8 ± 6.7	48.2 ± 3.3
$KHCO_3$	97.3 ± 5.5	74.6 ± 8.2	74.6 ± 2.7
$NaHCO_3 + CaCO_3$	90.6 ± 4.5	76.2 ± 2.4	68.4 ± 3.1
$KHCO_3 + CaCO_3$	111.1 ± 4.8	87.8 ± 11.1	68.5 ± 4.3
$NaHCO_3 + ZnCO_3$	80.4 ± 4.7	73.6 ± 4.1	55.3 ± 3.5
$KHCO_3 + ZnCO_3$	76.1 ± 4.3	79.7 ± 5.4	64.7 ± 6.8
$NaHCO_3 + MgCO_3$	54.7 ± 2.6	46.1 ± 1.9	44.9 ± 3.1
$KHCO_3 + MgCO_3$	66.1 ± 1.9	50.6 ± 4.8	53.5 ± 3.2

Table 5.13 : The effect of acid strength on the work done in breaking rafts formed from LFR 5/60 and pectin mixture rafts

Additions to alginate solution	Mean work done in breaking raft (N.mm) ± s.d.		
	0.1M HCl	0.07M HCl	0.05M HCl
$NaHCO_3$	0.9408 ± 0.099	0.7574 ± 0.058	0.3907 ± 0.019
$KHCO_3$	1.242 ± 0.073	0.8911 ± 0.102	0.7715 ± 0.036
$NaHCO_3 + CaCO_3$	1.102 ± 0.086	1.036 ± 0.020	0.6478 ± 0.041
$KHCO_3 + CaCO_3$	1.479 ± 0.039	1.158 ± 0.067	0.6440 ± 0.047
$NaHCO_3 + ZnCO_3$	1.004 ± 0.065	0.8743 ± 0.030	0.4441 ± 0.029
$KHCO_3 + ZnCO_3$	0.9981 ± 0.051	1.043 ± 0.072	0.6637 ± 0.088
$NaHCO_3 + MgCO_3$	0.6250 ± 0.042	0.4525 ± 0.042	0.3411 ± 0.042
$KHCO_3 + MgCO_3$	0.7210 ± 0.061	0.4707 ± 0.047	0.3998 ± 0.014

The breaking strength, and work done in breaking rafts generally decreases with a decrease in acid strength. This applies not only to the LFR 5/60 rafts, but also to those formed with the inclusion of pectin into the raft forming mixture. It is interesting to note that the rafts containing pectin seem to be affected more by acid strength than those formed with alginate alone. The different formulations are not equally affected by the strength of the acid in which the raft forms. In the LFR 5/60 rafts those containing magnesium carbonate seem to be least affected by acid strength whereas those rafts including calcium carbonate the pH of the acid medium. This is also seen in the rafts containing pectin where the addition of magnesium carbonate gives rafts with lower breaking strengths which are less affected by the acid strength.

5.4 IMAGE ANALYSIS

5.4.1 Theory

The property of the alginate raft which makes it unique in the way it acts as an antacid is the buoyancy. The buoyancy of the raft is due to the carbon dioxide bubbles trapped within the alginate gel. Preliminary observation of various rafts suggested that the size of the bubbles trapped by the gels varies depending on the ionic content of the gel and possibly depending on the bicarbonate used as the source of the carbon dioxide. There is no published data on the size of bubbles in alginate rafts, thus there is no established method which could be followed. There are a range of methods which have been used in the measurement of bubble size in other applications; one described by Ronteltap and Prins (1989) involves the use of an opto-electronic fibre which can be moved at a known rate through a foam. The tip of the fibre monitors the refractive index of the medium and the probe is connected to an analogue-digital converter to aid data acquisition. Other methods for measuring bubble size involve either direct manual measurement from a photograph (Hilton et al 1993) or counting of a photomicrograph performed by a particle size analyser (Bee et al, 1989). This method shares the same principle as image analysis technique used in this investigation in that an image is obtained from the

sample. This image can then be measured and counted without the problems of the bubbles changing size and coalescing with time. The image analyser provides a convenient means of capturing the desired image and storing it, as well as measuring the desired parameters and counting the number of bubbles present.

Since this method has not been reported for use in the measurement of the size of bubbles contained within alginate rafts there is no established method for data analysis. The data presented here has therefore been shown in order to assess whether a similar method could be used in the future to give more detailed information about the nature of the bubbles within alginate rafts.

5.4.2 Method

The raft forming mixture was prepared as described in Chapter 2.2.4. A clear plastic petri dish containing 5ml 0.1M HCl (kept at 37°C) was placed on the light source and a single drop of the raft forming mixture was introduced onto the surface of the acid using a 5ml BD plastic syringe. This quantity of the raft forming mixture was used in order to produce a single layer of bubbles as the image analyser does not take the depth of field into account. Multiple bubble layers also make it difficult for the image analyser to distinguish individual bubbles. The bubbles were allowed to form for 30 seconds before the image was captured.

The SeeScan image analyser was set up with suitable lenses attached to the closed circuit television camera; the focus was adjusted to give a clear image on the screen. Once the focus had been set the system was calibrated via the software. After calibration the petri dish containing the acid was placed on a light source under the camera and lens assembly as shown in Figure 5.10 and the image was captured after the specified time. The captured image was then thresholded, to give the optimum resolution of the objects. The image could then be manipulated before the objects were counted. "Kill small" was used to

Figure 5.10 : Schematic representation of the image analysis system used

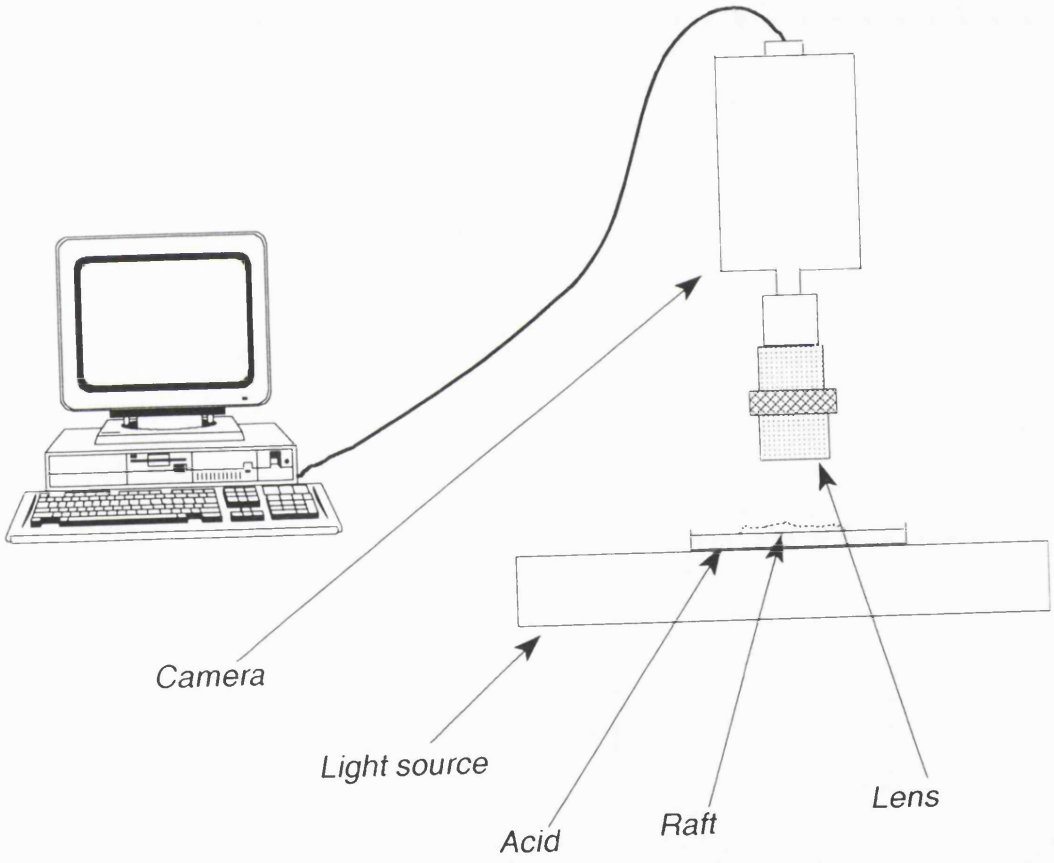

remove single pixels which did not have neighbouring pixels. Certain objects were discarded where, for example, two bubbles were so close that the image analyser could not resolve them into discreet objects, or where portions of the raft forming mixture had not reacted with the acid.

The image analyser interprets the perimeter layer around the bubble as the object, as shown in Figure 5.11. However, in order to measure the area of the bubble itself it is necessary for the whole of the bubble to be recognised as the object. The command "fill holes" was therefore used in order to produce objects which appeared to be coloured circles rather then rings of colour as seen in Figure 5.12. The objects were then automatically counted and measured, the parameters chosen for measurement were the area and the perimeter of the bubbles. It is possible to measure other parameters of the objects captured in the image. However as the purpose of this investigation was to carry out a preliminary study of the bubbles by this technique it was felt that these two basic parameters would be sufficient.

Three alginates were chosen for investigation, LFR 5/60, LF 10/40RB and LF 120M which represents a range of uronic acid compositions found to be 67.2%, 50.9% and 42.4% guluronic acid by NMR (Chapter 3.2.3). The raft forming mixtures for each of the alginates were produced in six formulations containing either sodium or potassium bicarbonate with or without the addition of calcium carbonate or zinc carbonate.

5.4.3 Results

The two parameters measured were the bubble area and the perimeter of the bubbles. This enables both the size of the bubbles to be investigated and also the deviation of the shape of the bubbles from spherical to be estimated. It should be noted that the measurements made are two dimensional, when in reality the raft and the bubbles trapped within it are three dimensional. The shape of the bubbles is therefore seen as circular and deviation from circularity

Figure 5.11 : A thresholded image of an alginate raft before using the "fill holes" command

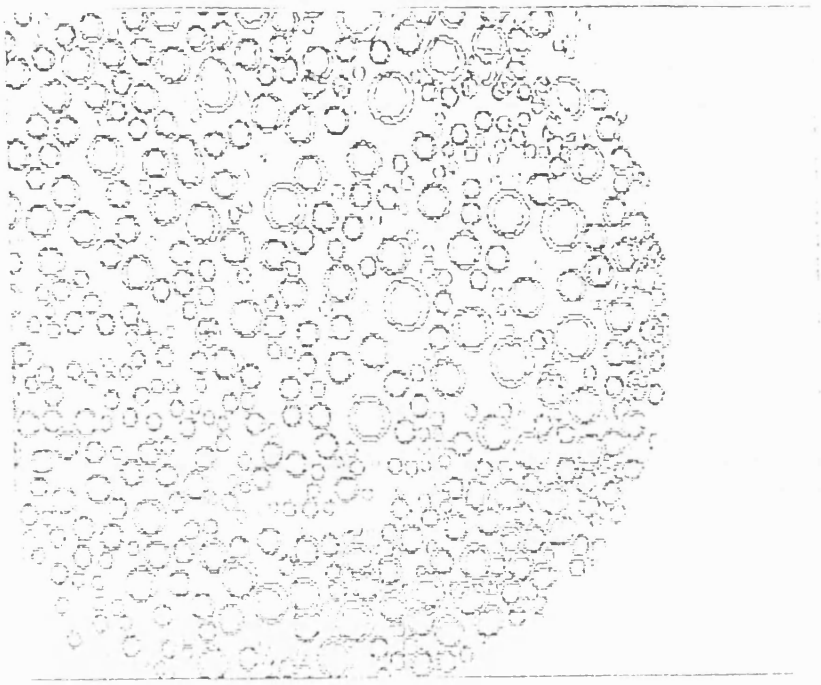

Figure 5.12 : A thresholded image of an alginate raft after using the "fill holes" command

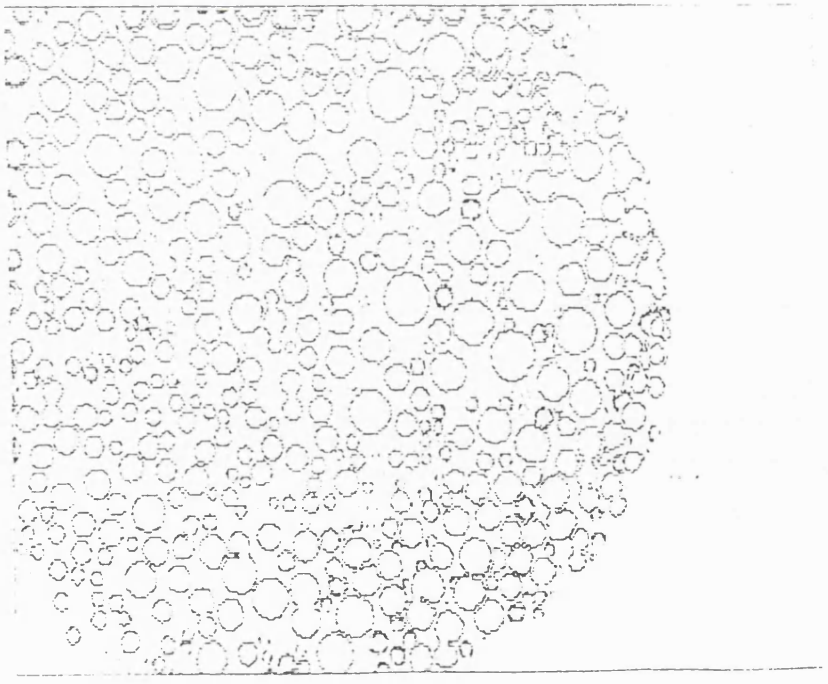

Table 5.14 : The effect of formulation on the mean bubble area of alginate rafts

Additions to alginate solution	Mean bubble area (mm^2) ± s.d.		
	LFR 5/60	LF 10/40RB	LF 120M
$NaHCO_3$	0.1479 ± 0.1970	0.0692 ± 0.0261	0.0425 ± 0.0201
$KHCO_3$	0.0562 ± 0.0801	0.0503 ± 0.0251	0.0532 ± 0.0167
$NaHCO_3$ + $CaCO_3$	0.2569 ± 0.1486	0.0183 ± 0.067	0.0395 ± 0.0143
$KHCO_3$ + $CaCO_3$	0.1371 ± 0.0947	0.0729 ± 0.0272	0.0646 ± 0.0271
$NaHCO_3$ + $ZNCO_3$	0.1180 ± 0.1351	0.0331 ± 0.0248	0.0520 ± 0.0181
$KHCO_3$ + $ZNCO_3$	0.2417 ± 0.1912	0.0618 ± 0.0234	0.0448 ± 0.0115

Table 5.15 : The effect of formulation on the mean perimeter of bubbles in alginate rafts

Additions to alginate solution	Mean bubble perimeter (mm) ± s.d.		
	LFR 5/60	LF 10/40RB	LF 120M
$NaHCO_3$	1.2446 ± 0.7629	0.9935 ± 0.1802	0.7392 ± 0.1807
$KHCO_3$	0.7995 ± 0.5015	0.8254 ± 0.2139	0.8404 ± 0.1338
$NaHCO_3 + CaCO_3$	1.8603 ± 0.5536	0.4895 ± 0.0912	0.7611 ± 0.1487
$KHCO_3 + CaCO_3$	1.3017 ± 0.4388	1.0192 ± 0.2061	0.9427 ± 0.1952
$NaHCO_3 + ZnCO_3$	1.1404 ± 0.6062	0.6456 ± 0.2166	0.8424 ± 0.1465
$KHCO_3 + ZnCO_3$	1.7382 ± 0.6953	0.9247 ± 0.1886	0.7886 ± 0.1104

can be shown by plotting the perimeter squared (P^2) against the area (A). For perfect circles plotting P^2 against A gives a straight line, the scatter of experimental points will show how far the bubbles vary from perfect circles. Table 5.14 shows the mean bubble areas for each of the samples and the standard deviation. The data for the mean bubble perimeters and the standard deviation is given for each of the samples in Table 5.15. The area and perimeter values show a wide range of bubble sizes. The rafts formed with LFR 5/60 show the greatest standard deviation of bubble size in all formulations.

The bubbles produced by the raft forming mixtures containing LFR 5/60 and sodium bicarbonate are much larger than those of the other alginates. Although there seems to be a general trend for the bubble size to increase with increasing guluronic acid content of the alginate this does not hold for all formulations.

Figure 5.13 shows scatter plots of P^2 against A for the formulations of each of the alginates without added carbonates. Plotting P^2 against A for perfect circle gives a straight line with a gradient of 4π (= 12.566); this line is also included on the plots in Figure 5.13 for reference. Using the line of best fit through the experimental points the gradient can be calculated, and hence the deviation from circularity can be quantified. Table 5.16 shows the gradients for each of the formulations and the gradient divided by 4π which gives an idea of deviation from a perfect circle. Table 5.17 gives an idea of the diameter of the bubbles calculated from the mean bubble area for each of the formulations.

All the bubbles show a close correlation with circularity. Those produced in the LF 120M +$NaHCO_3$ raft show the greatest degree of circularity whilst the least circular are those formed by the LFR 5/60 +$KHCO_3$ raft. As with the bubble areas, there are no definite patterns which can be seen in the circularity of the bubbles.

Figure 5.13(a) : P^2 against area for LFR 5/60 rafts

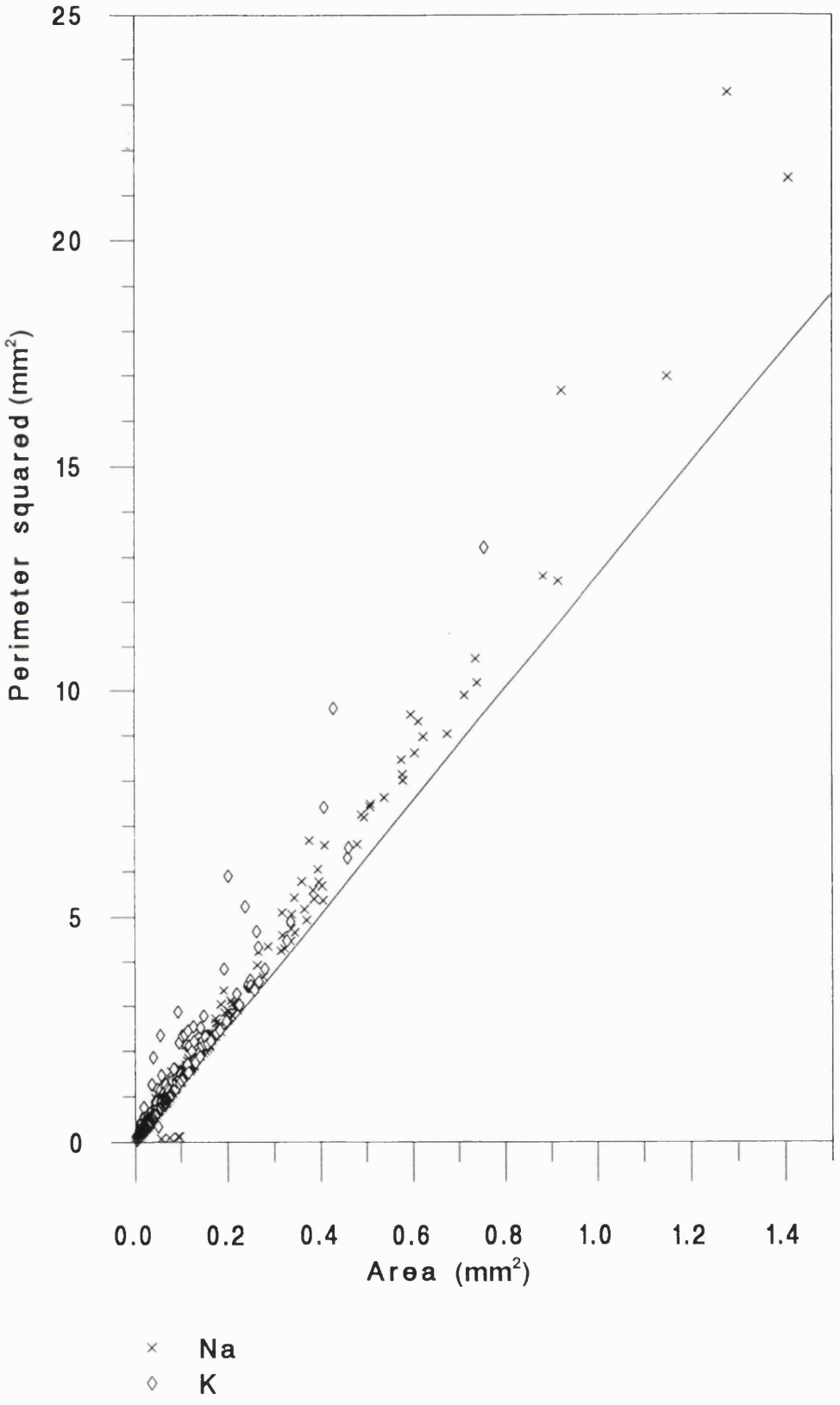

Figure 5.13(b) : P^2 against area for LF 10/40RB rafts

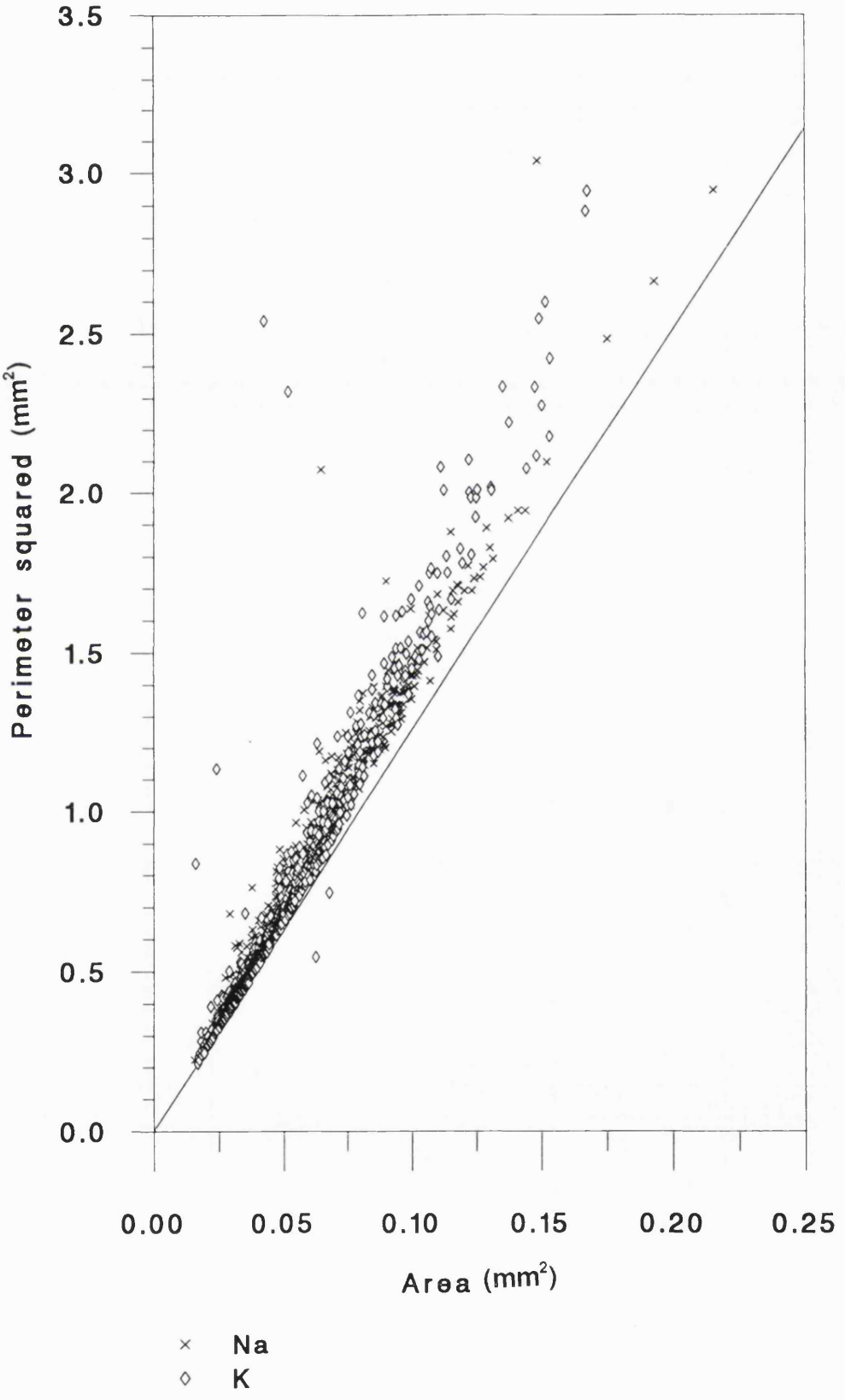

Figure 5.13(c) : P^2 against area for LF 120M rafts

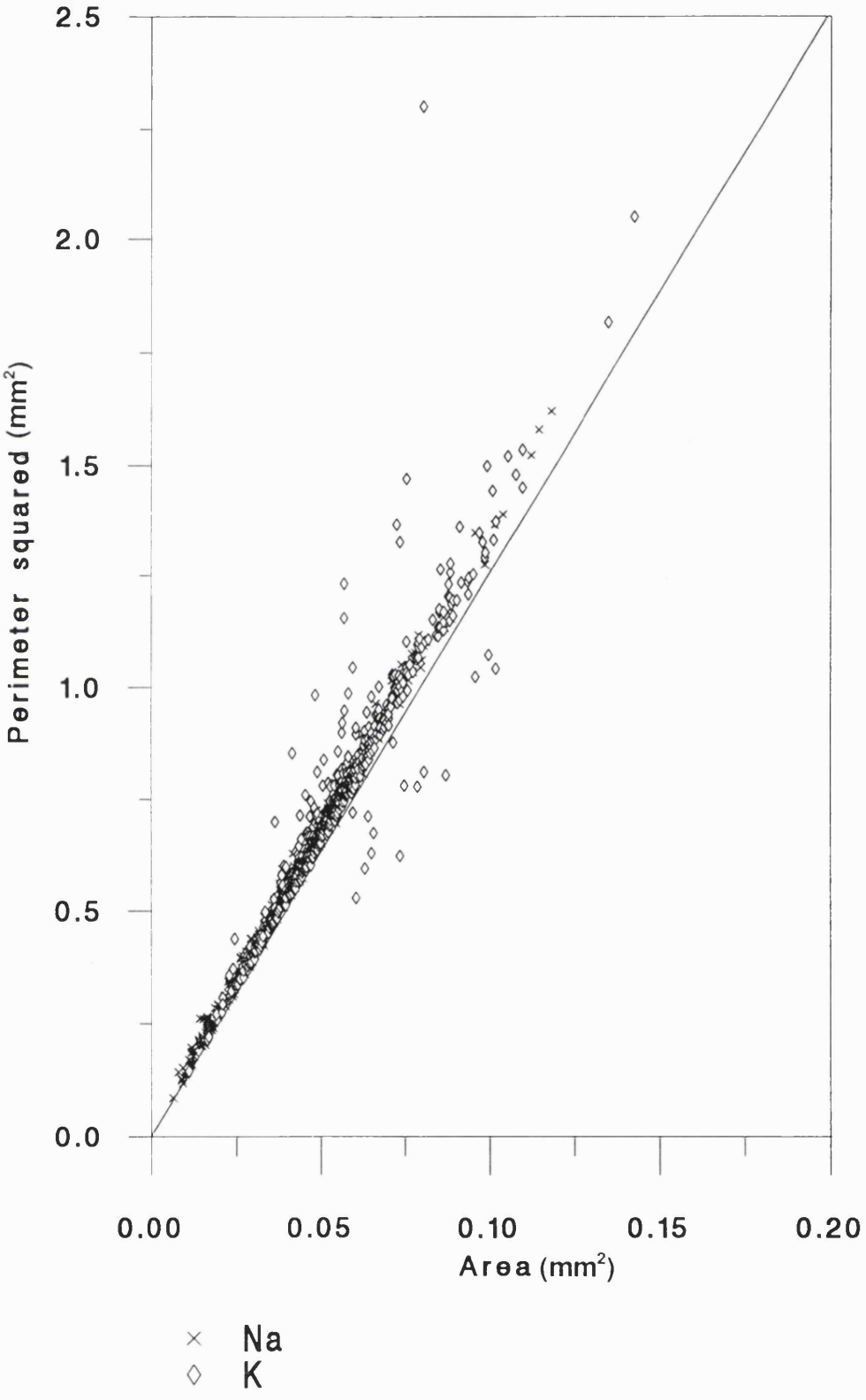

Table 5.16 : The gradients of P^2 against A for each of the samples.

Additions to alginate solution	Gradient			Gradient/4π		
	LFR 5/60	LF 10/40RB	LF 120M	LFR 5/60	LF 10/40RB	LF 120M
$NaHCO_3$	15.195	13.986	13.278	1.209	1.113	1.057
$KHCO_3$	16.130	15.952	13.459	1.284	1.269	1.071
$NaHCO_3$ + $CaCO_3$	14.047	13.392	15.285	1.118	1.066	1.216
$KHCO_3$ + $CaCO_3$	13.925	15.479	14.011	1.110	1.232	1.115
$NaHCO_3$ + $ZnCO_3$	14.328	14.291	14.110	1.140	1.137	1.123
$KHCO_3$ + $ZnCO_3$	14.701	14.970	14.511	1.170	1.191	1.155

Table 5.17 : The effect of formulation on mean bubble diameter (calculated from mean bubble area)

Additions to alginate solution	Mean diameter (mm)		
	LFR 5/60	LF 10/40RB	LF 120M
$NaHCO_3$	0.434	0.297	0.233
$KHCO_3$	0.267	0.253	0.260
$NaHCO_3 + CaCO_3$	0.572	0.153	0.224
$KHCO_3 + CaCO_3$	0.418	0.305	0.287
$NaHCO_3 + ZnCO_3$	0.388	0.205	0.257
$KHCO_3 + ZnCO_3$	0.555	0.281	0.239

5.5 DISCUSSION

The results from the raft thickness studies show that the thickness of the rafts tends to decrease over the period of the present investigation. The texture analysis data shows that the breaking strength of the rafts with calcium and zinc tends to decrease with time over the same time whereas the rafts without any additional carbonate tend to slightly decrease in breaking strength with time. It would seem that there is no simple correlation between raft thickness and breaking strength.

The data from the experiments to investigate the effect of acid strength on the thickness and breaking strength of the rafts show that both raft strength and thickness tend to decrease as the molarity of the HCl decreases.

The addition of the carbonates to the raft has the effect of increasing both the thickness and the strength of the rafts compared with those containing alginate

and bicarbonate alone. The effect in both cases is larger with calcium than zinc carbonate and there is a tendency for the rafts containing potassium bicarbonate to be thicker and stronger than those with sodium bicarbonate.

The lack of clear trends from the bubble size measurements means that any correlation with the other raft data is difficult. The results show that there is no simple relationship between bubble size and raft strength, although this does not mean that the raft characteristics are not affected by the properties of the bubbles trapped within the raft.

CHAPTER 6

CHAPTER 6: CONCLUSIONS

The overall objective of the project was to investigate the way in which each component of an alginate raft affects the raft performance. This is necessary in order to be able to optimise the formulation. Although at present there are a range of raft forming products with a variety of ingredients as well as the alginate and the bicarbonate, the effect of the ingredients on the rafts has not been fully investigated. The performance of alginate rafts has only been studied using commercial preparations, hence it was felt important to investigate ways of characterising rafts with a wider variety of components. The objective was approached in a combination of two ways. Firstly the individual components of the rafts were characterised and secondly the effect of formulation variables on the rafts themselves were investigated.

The characterisation of the components of the raft took the form of the determination of the chemical structure of the alginate and the measurement of the rheological properties of the alginate solutions and gels. Analysis of alginate structure is important because of the links between the chemical structure and the physical properties of the polysaccharide. The analysis of the chemical structure was carried out by two methods, nuclear magnetic resonance (NMR) and circular dichroism (CD). The results of the analysis of the five alginate samples used are given in Chapter 3, and show a good agreement between the values found with NMR and CD. The two methods of structural analysis for alginate are both useful since the CD can be used as a quick method for the determination of the M/G ratio whilst NMR gives a larger amount of structural data, although it is by far a more time consuming method.

The measurement of the rheological properties of the alginate solutions allowed calculation of the intrinsic viscosity for the alginate samples used. This is not only a useful parameter in the comparison of the alginate, but also enables the calculation of an approximate molecular weight for each of the samples. The molecular weight of alginate samples is highly dependent on the method

of preparation and the processing of the sample, thus the molecular weight can vary widely.

The rheological characterisation of the alginate gels was performed in order to assess the effect the method of gelation had on the rheological properties of the gels. A new method of dynamic mechanical analysis was used with the alginate gels which showed creep-recovery to be the most useful experimental method with these systems. The data given in Chapter 4 showed that there are large differences between the characteristics of the gels formed with acid and those formed by the action of a divalent cation. The results suggest that the gels formed with either calcium or zinc have a similar structure, whereas those formed by the action of acid involve a different mechanism of gelation.

The evaluation of the effect of formulation variables on the rafts required the development of a novel method for measuring the breaking strength of the rafts. The Stable Microsystems TA.XT2 texture analyser provided a simple and reproducible method for the characterisation of these systems. An image analysis method was also investigated for measuring the size of the bubbles trapped within the alginate raft, although as the results in Chapter 5 show, this approach is not as useful in the characterisation of the rafts as the other methods used.

Using a combination of the techniques mentioned above four main variables were investigated. These were the choice of bicarbonate used, the effect of additional cations, the choice of alginate sample used and the effect of acid strength on the rafts. The effect that each of these variables had on the raft properties will be considered separately.

The effect that the bicarbonate chosen has on the rafts will be considered first. In the majority of commercial preparations sodium bicarbonate is used to produce the carbon dioxide necessary for the raft to float, however potassium bicarbonate could be used as an alternative. This could be beneficial to some

patients where sodium intake is restricted. The viscosity of the alginate solutions containing the bicarbonates was measured and the results given in Chapter 3 show that whilst sodium bicarbonate generally increases the viscosity of the solutions, compared to those without a bicarbonate added, the potassium has little effect on the viscosity of the solutions.

The raft thickness and increase in volume results given in Chapter 5 show that in rafts containing alginate and bicarbonate alone the sodium bicarbonate rafts are thicker than the potassium. This is reversed in the mixtures containing alginate and pectin where the potassium bicarbonate rafts are thicker. The addition of the carbonate of a divalent cation to the alginate rafts causes some of the rafts, notably those formed with the higher guluronic acid content alginate, to be thicker with potassium whilst the lower guluronic acid content alginate rafts remain thicker with sodium bicarbonate.

The breaking strengths of all the rafts containing potassium bicarbonate are higher than the corresponding sodium rafts. A better understanding of the way in which the bicarbonate affects the raft may be gained by further DMA studies of the alginate gels formed by dialysis against a solution containing sodium or potassium ions in addition to the divalent cation under investigation.

The second formulation variable studied was the addition of a divalent cation to the raft forming mixture on the basis that certain divalent cations promote gelation of alginate, and may therefore have an effect on the properties of an alginate raft. Calcium salts are most often used to provide the divalent ions necessary for alginate gelation, therefore calcium carbonate was chosen with zinc carbonate as an alternative.

The thickness studies in Chapter 5 show that both calcium and zinc cause an increase in the thickness of the raft and the volume occupied, compared to those rafts formed without the addition of a divalent cation. In general zinc carbonate has a lesser or equal effect to that of calcium carbonate.

The breaking strength investigations show the same general trend in that both calcium and zinc increase the breaking strength of the rafts with the exception of the alginate/pectin mixture rafts where the increase is only seen with calcium. In all rafts formed with sodium bicarbonate, calcium had a greater effect than zinc, however, the difference between calcium and zinc was less marked in the rafts containing potassium bicarbonate.

The rheology studies in Chapter 4 show the similarity between the gels formed with zinc and calcium. As previously mentioned additional rheological measurements of the gels formed with the addition of sodium or potassium ions would aid in the interpretation of these results. It is interesting to note that the synergy suggested by the creep results between the alginate and pectin in the presence of calcium can also be seen in the increased breaking strength of the alginate pectin rafts with calcium which is not seen with the zinc carbonate.

The effect of the acid strength on the rafts was the third variable considered. This is not because the pH of the patients stomach could be altered to suit the raft forming product, but rather to investigate the behaviour of the rafts to the variation in pH which may occur within and between patients. Increasing the pH of the formation medium, i.e. reducing the acid strength, has the effect of reducing both the thickness and the strength of the rafts. This general trend did not occur to the same extent with all formulations; those containing zinc carbonate, for example, showed greater variation in breaking strength with pH. This suggests that formulations containing calcium carbonate will form rafts which are less affected by the pH of the stomach contents, and thus have a more reproducible therapeutic effect.

The final formulation variable considered was the alginate itself. Chapter 3 shows the differences between the sample used. The chemical structure is shown by the M/G ratio and the NMR data also gives an idea of the block structure of the alginate. The intrinsic viscosity data shows that the alginate LFR 5/60 has a very low intrinsic viscosity which may be accounted for by the

lower molecular weight of the sample. Hence although LFR 5/60 has a similar M/G ratio the intrinsic viscosity is much lower.

The creep-recovery data on three of the samples shows that LF 120M has a greater degree of elastic behaviour than the other two alginate, which have higher guluronic acid contents. The calcium gels show that LFR 5/60, the highest guluronic acid content alginate studied, has a much lower bulk modulus than the other samples. The zinc and acid gels show that LFR 5/60 has a higher bulk modulus than the other samples which were quite similar.

The raft thickness studies show a rank order for the rafts which covers most formulations which is:

LFR 5/60 > LF 10/40RB > LF 20/200 > LF 120M > LF 200DL.

This ranking approximates to the inverse ranking of the alginate by degree of polymerisation, suggesting that an alginate with a lower degree of polymerisation will produce a thicker raft. The breaking strength data does not fit into this pattern quite so well although the results suggest that alginates containing lower proportions of guluronic acid tend to form rafts with lower breaking strengths and show less deformation under creep testing. However, the alginate composition should not be considered alone since the degree of polymerisation must also be taken into account. This again suggests the need for further information on the rheological properties of the gels for all the alginate studied.

The project has shown that the properties of an alginate raft are not solely due to the combination of components within the raft forming mixture, but that the interaction between these components also affects the characteristics of the rafts formed. It would seem that zinc carbonate could provide a useful alternative to calcium carbonate in the formulation of these products and that the use of potassium bicarbonate may have some benefits over sodium bicarbonate. The current work has shown texture analysis to be a useful and convenient measure of raft properties and the application of dynamic

mechanical analysis, particularly the creep-recovery test, to alginates has been demonstrated.

Further work would be useful in the rheology of the alginate gels, particularly in extending the range of alginate sampled and the gel dialysis solutions used. It would also be helpful to investigate the rheological properties of gels formed by a combination of acid and cations. The texture analysis of the rafts could be extended by using the enhanced abilities of the equipment it should be possible to establish parameters of study other than just the breaking strength and work done in breaking the rafts. In order to be able to establish which characteristics of an alginate raft should be considered optimal it would be useful to perform gamma scintigraphic studies using human volunteers to assess the effectiveness of various formulations.

REFERENCES

REFERENCES

Bao, Q.-B. and C.S. Bagga. "Dynamic mechanical analysis of hydrogel elastomers". 1993. Unpublished results

Beckloff, G.L., J.H. Chapman, and P. Shiverdecker. "Objective evaluation of an antacid with unusual properties." *J. Clin. Pharmacol.* 12(1972):11-21.

Bee, R.D., A. Clement, and A. Prins. "Behaviour of an aerated food model." In: *Food Emulsions and Foams.* Edited by Dickinson, E. London: R. Soc. Chem., 1989, p.128.

Bennett, C.E., J.G. Hardy, and C.G. Wilson. "The influence of posture on the gastric emptying of antacids." *Int. J. Pharm.* 21(1984):341-347.

Braconnot, H. " Research on a novel acid universally found in all vegetables" *Ann. Chim. Phys. Ser.* 28(1825):173-178

Brown, A.H. "Determination of pentose in the presence of large quantities of glucose." *Arch.Biochem.* 11(1946):269-278.

Connell, A.M. and T.E. Waters. "Assessment of gastric function by pH telemetry capsule." *Lancet* ii(1964):227-230.

Craig, D.Q.M. and F.A. Johnson. "Pharmaceutical applications of dynamic mechanical thermal analysis." *Thermochim.Acta* 248(1995):97-115.

Dodds, W.J., W.J. Hogan, J.F. Helm, and J. Dent. "Pathogenesis of reflux esophagitis." *Gastroenterol.* 81(1981):376-394.

Donnan, F.G. and R.C. Rose. "Osmotic pressure, molecular weight and viscosity of sodium alginate." *Can. J. Res.* 28 (B)(1950):105-113.

Drummond, D.W., E.L. Hirst, and E. Percival. "The constitution of alginic acid." *J.Chem.Soc.* (1962):1208-1216.

Durand, D., C. Bertrand, A.H. Clark, and A. Lips. "Calcium-induced gelation of low methoxy pectin solutions - thermodynamic and rheological considerations." *Int. J. Biol. Macromol.* 12 (1)(1990):14-18.

Evans, D.F., G. Pye, R. Bramley, A.G. Clark, T.J. Dyson, and J.D. Hardcastle. "Measurement of gastrointestinal pH profiles in normal ambulant subjects." *Gut* 29(1988):1035-1041.

Ferry, J.D. *Viscoelastic properties of polymers.* London: John Wiley & Sons, 1961.

Fischer, F.G. and H. Dorfel. "Die polyuronsauren der braunalgen (kohlenhydrate der algen I)." *Z.Physiol.Chem.* 302(1955):186-203.

Gacesa, P. "Alginates." *Carbohydr.Polym.* 8(1988):161-182.

Glicksman, M. "Seaweed Extracts." In: *Gum Technology in the Food Industry.* Edited by Anonymous. New York / London: Academic Press, 1969, p.239.

Grant, G.T., E.R. Morris, D.A. Rees, P.J.C. Smith, and D. Thom. "Biological interactions between polysaccharides and divalent cations: The egg-box model." *FEBS Lett.* 32 [1] (1973):195-198.

Grasdalen, H., B. Larsen, and O. Smidsrød. "^{13}C-nmr studies of alginate." *Carb. Res.* 56(1977):C-11-C-15.

Grasdalen, H., B. Larsen, and O. Smidsrød. "A pmr study of the composition and sequence of uronate residues in alginates." *Carb. Res.* 68(1979):23-31.

Grasdalen, H., B. Larsen, and O. Smidsrød. "^{13}C-NMR studies of monomeric composition and sequence in alginate." *Carb. Res.* 89(1981):179-191.

Harkness, M.L.R. and A. Wassermann. "The intrinsic viscosity of sodium alginate." *J.Chem.Soc.* (1952):497-499.

Haug, A. "Viscosity of alginate solutions." *Norwegian Inst. Seaweed Res.* 20(1958):20-24.

Haug, A. "Fractionation of alginic acid." *Acta Chem.Scand.* 13(1959):601-603.

Haug, A. "Ion exchange properties of alginate fractions." *Acta Chem.Scand.* 13(1959):1250-1251.

Haug, A. "Dissociation of alginic acid." *Acta Chem.Scand.* 15(1961):950-952.

Haug, A. *Composition and properties of alginates.* Norwegian Institute of Seaweed Research. Report No. 30, 1964.

Haug, A. and B. Larsen. "Quantitative determination of the uronic acid composition of alginates." *Acta Chem.Scand.* 16(1962):1908-1918.

Haug, A. and B. Larsen. "The solubility of alginate at low pH." *Acta Chem.Scand.* 17(1963):1653-1662.

Haug, A., B. Larsen, and O. Smidsrød. "A study of the constitution of alginic acid by partial acid hydrolysis." *Acta Chem.Scand.* 20(1966):183-190.

Haug, A., B. Larsen, and O. Smidsrød. "Studies on the sequence of uronic acid residues in alginic acid." *Acta Chem.Scand.* 21(1967a):691-704.

Haug, A., S. Myklestad, B. Larsen, and O. Smidsrød. "Correlation between chemical structure and physical properties of alginates." *Acta Chem.Scand.* 21(1967b):768-778.

Haug, A. and O. Smidsrød. "Determination of intrinsic viscosity of alginates." *Acta Chem.Scand.* 16(1962):1569-1578.

Haug, A. and O. Smidsrød. "The effect of divalent metals on the properties of alginate solutions. II: Comparison of different metal ions." *Acta Chem.Scand.* 19(1965):341-351.

Haug, A. and O. Smidsrød. "Fractionation of alginates by precipitation with calcium and magnesium ions." *Acta Chem.Scand.* 19(1965):1221-1226.

Haug, A. and O. Smidsrød. "Strontium-calcium selectivity of alginates." *Nature* 215(1967):757.

Haug, A. and O. Smidsrød. "The solubility of polysaccharides in salt solutions." In: *Solution properties of natural polymers.* London: The Chemical Society, 1968, p.273.

Hilton, A.M., M.J. Hey, and R.D. Bee. "Nucleation and growth of carbon dioxide gas bubbles." (1993) Unpublished results.

Hirst, E.L., E. Percival, and J.K. Wold. "The structure of alginic acid . Part IV. Partial hydrolysis of the reduced polysaccharide." *J.Chem.Soc.* (1964):1493-1499.

Hirst, E.L. and D.A. Rees. "The structure of alginic acid: Part V. Isolation and unambiguous characterisation of some hydrolysis products of the methylated polysaccharide." *J.Chem.Soc.* (1965):1182-1187.

Jenkins, J.R.F., J.G. Hardy, and C.G. Wilson. "Monitoring antacid preparations in the stomach using gamma scintigraphy." *Int. J. Pharm.* 14(1983):143-148.

Knight, L.C., A.H. Maurer, I.A. Ammar, J.A. Siegel, B. Krevsky, R.S. Fisher, and L.S. Malmud. "pH dependence of In-111 alginic acid anti-gastroesophageal reflux barrier." *J.Nucl.Med.* 27 (6)(1986):1011-1012.

Kohn, R., I. Furda, A. Haug, and O. Smidsrod. "Binding of calcium and potassium ions to some polyuronides and monouronates." *Acta Chem.Scand.* 22(1968):3098-3102.

Larsen, B. and A. Haug. "Separation of uronic acids on anion exchange columns." *Acta Chem.Scand.* 15(1961):1397-1398.

Lin, L.P. and H.L. Sadoff. "Production of alginate by *A. vinelandii.*" *J.Bacteriol.* 95(1968):2336-2343.

Linker, A. and R.S. Jones. "A new polysaccharide resembling alginic acid isolated from *Pseudomonads.*" *J.Biol.Chem.* 241(1966):3845-3851.

Malmud, L.S., N.D. Charkes, J. Littlefield, J. Reilley, H. Stern, R. Rosenberg, and R.S. Fisher. "The mode of action of alginic acid compound in the reduction of gastroesophageal reflux." *J.Nucl.Med.* 20(1979):1023-1028.

May, H.A., C.G. Wilson, and J.G. Hardy. "Monitoring radiolabelled antacid preparations in the stomach." *Int. J. Pharm.* 19(1984):169-176.

McDowell, R.H. *Properties of Alginates.* 5th ed. London: Kelco International, 1986.

Morris, E.R., D.A. Rees, and D. Thom. "Characterisation of polysaccharide structure and interactions by circular dichroism: order-disorder transition in the calcium alginate system." *J. C. S. Chem. Comm.* (1973):245-246.

Morris, E.R., D.A. Rees, G.R. Sanderson, and D. Thom. "Conformation and circular dichroism of uronic acid residues in glycosides and polysaccharides." *J.C.S.Perkin Trans* II(1975):1418-1425.

Nelson, W.L. and L.H. Cretcher. "The alginic acid from *Macrocystis pyrifera.*" *J.Am.Chem.Soc.* 51(1929):1914-1922.

Patel, P. "Alginate raft studies." M.Sc. thesis. London: University of London, 1991.

Penman, A. and G.R. Sanderson. "A method for the determination of uronic acid sequence in alginates." *Carb. Res.* 25(1972):273-282.

Rees, D.A. "Structure, conformation and mechanism in the formation of polysaccharide gels and networks." *Adv.Carbohydrate Chem.Biochem.* 24(1969):267-332.

Rees, D.A. "Shapely polysaccharides." *Biochem.J.* 126(1972):257-273.

Rees, D.A. and J.W.B. Samuel. "The structure of alginic acid: Part VI. Minor features and structural variations." *J.Chem.Soc.* (1967):2295-2298.

Ronteltap, A.D. and A. Prins. "Contribution of drainage, coalescence and disproportionation of the stability of aerated foodstuffs and the consequences for the bubble size distribution as measured by a newly developed glass-fibre technique." In: *Food Colloids.* Edited by Bee, R.D., P. Richmond, and J. Mingins. London: R. Soc. Chem., 1989, p.39.

Ross-Murphy, S.B. "Physical gelation of synthetic and biological macromolecules." In: *Polymer gels, fundamentals and biomedical applications.* Edited by DeRossi, D. New York: Plenum Press, 1991, p.21.

Rossett, N.E. and M.L. Rice. "An in vitro evaluation of the efficacy of the more frequently used antacids with particular attention to tablets." *Gastroenterol.* 26(3)(1954):490-495.

Sandmark, S. and L. Zenk. "New principles in the treatment of reflux oesophagitis in hiatus hernia." *Svenska Lakart* 61(1964):1940-1943.

Scandola, M., G. Ceccorulli, and M. Pizzoli. "Molecular motions of polysaccharides in the solid state: dextran, pullulan and amylose." *Int. J. Biol. Macromol.* 13(4)(1991):254-260.

Skjak-Bræk, G., H. Grasdalen, and B. Larsen. "Monomer sequence and acetylation pattern in some bacterial alginates." *Carb. Res.* 154 (1986a): 239-250.

Skjak-Bræk, G., H. Grasdalen, and O. Smidsrød. "Inhomogeneous polysaccharide ionic gels." *Carbohydr.Polym.* 10(1989)

Skjak-Bræk, G. and B. Larsen. "Biosynthesis of alginate: Purification of mannuronan c-5-epimerase from *Azotobacter vinelandii.*" *Carb. Res.* 139 (1985):273-283.

Skjak-Bræk, G., O. Smidsrød, and B. Larsen. "Tailoring of alginates by enzymatic modification *in vitro*." *Int.J.Macromol.* 8 (Dec)(1986b):330-336.

Smidsrød, O. "Molecular basis for some physical properties of alginates in the gel state." *Faraday Disc. Chem. Soc.* 54(1974):263-274.

Smidsrød, O., R.M. Glover, and S.G. Whittington. "The relative extension of alginates having different chemical composition." *Carb. Res.* 27(1973):107-118.

Smidsrød, O. and A. Haug. "The effect of divalent metals on the properties of alginate solutions. I: Calcium ions." *Acta Chem.Scand.* 19(1965):329-340.

Smidsrød, O. and A. Haug. "A light scattering study of alginate." *Acta Chem.Scand.* 22(1968b):797-810.

Smidsrød, O. and A. Haug. "Dependence upon uronic acid composition of some ion-exchange properties of alginates." *Acta Chem.Scand.* 22(1968a):1989-1997.

Smidsrød, O. and A. Haug. "Properties of poly(1,4 hexuronates) in the gel state. II. Comparison of gels of different chemical composition." *Acta Chem.Scand.* 26(1972):79-88.

Smidsrød, O., A. Haug, and B. Larsen. "The influence of pH on the rate of hydrolysis of acidic polysaccharides." *Acta Chem.Scand.* 20(1966):1026-1034.

Smidsrød, O., A. Haug, and B. Lian. "Properties of poly(1,4-hexuronates) in the gel state. I. Evaluation of a method for the determination of stiffness." *Acta Chem.Scand.* 26(1972):71-78.

Smith and Montgomery. "The structure of polysaccharides from seaweed." In: *Chemistry of plant gums and mucilages.* Edited by Smith and Montgomery. American Chemical Society, 1959, p.402.

Spoehr, H.A. "The hydrolysis of alginic acid with formic acid." *Arch.Biochem.* 14(1947):153-155.

Stanford, E.C.C. "On Algin: A new substance obtained from some of the commoner species of marine algae." *Chem. News* 47(1883):254-269.

Tobyn, M., J. Johnson, and S. Gibson, "Use of TA.XT2 texture analyser in mucoadhesive research." *International Labmate* (1993):35-37.

Washington, N. "Investigation into the barrier action of an alginate gastric reflux suppressant, liquid gaviscon." *Drug Investigation.* 2(1990):23-30.

Washington, N. "Gastro-oesophageal reflux and anti-reflux agents." In: *Antacids and anti-reflux agents.* London: CRC Press, 1991, p.187.

Washington, N., C. Washington, S.S. Davis, and C.G. Wilson. "Effect of aluminium hydroxide on raft-forming antacids." *J. Pharm. Pharmacol.* suppl 37(1985):13p

Washington, N., C. Washington, and C.G. Wilson. "Gastric distribution and residence time of two anti-reflux formulations." *Int. J. Pharm.* 39(1987):163-171.

Washington, N., C. Washington, C.G. Wilson, and S.S. Davis. "The effect of inclusion of aluminium hydroxide in alginate-containing raft-forming antacids." *Int. J. Pharm.* 28(1986a):139-143.

Washington, N., C. Washington, C.G. Wilson, and S.S. Davis. "What is "Liquid Gaviscon"? A comparison of four international formulations." *Int. J. Pharm.* 34(1986b):105-109.

Washington, N., C.G. Wilson, and S.S. Davis. "Evaluation of 'raft forming' antacid neutralising capacity: *in vitro* and *in vivo* correlations." *Int. J. Pharm.* 27(1985):279-286.

Watase, M. and K. Nishinari. "Effects of pH and DMSO content on the thermal and rheological properties of high methoxyl pectin-water gels." *Carbohydr.Polym* 20(1993):175-181.